Control Design Using Energy-Shaping Methods

Jacques Arno Naudé

A dissertation submitted to the Faculty of Engineering and the Built Environment, University of the Witwatersrand, in fulfillment of the requirements for the degree of Master of Science in Engineering.

Johannesburg, 2012

The financial assistance of the National Research Foundation (NRF) towards this research is hereby acknowledged . Opinions expressed and conclusions arrived at, are those of the author and are not necessarily to be attributed to the NRF.

Contents

Declaration

I declare that this dissertation is my own unaided work. It is being submitted to the Degree of Master of Science in Engineering at the University of the Witwatersrand, Johannesburg. It has not been submitted before for any degree or examination to any other University.

_____

(Signature of Candidate)

_____ day of _____ year _____

Abstract

The aim of this research project was to investigate the benefits and shortfalls of Energy-Shaping controllers and use them to gain insight into industry standard control methods. Energy is a fundamental quantity in nature and is conserved due to the first law of thermodynamics. Actuators, necessarily, add energy into the system or remove energy from the system. Sensors remove (in some cases, negligible amounts of) energy from the system in order to measure some variable of interest. All control algorithms employing feedback, must measure at least one physical variable of the system to be controlled. Furthermore, all control algorithms must have at least one actuator in order to control the system. Hence, by proxy, all control algorithms affect the energy of the system. Two key ideas in energy shaping are: Energy Balancing and Power Shaping. Other control algorithms, ultimately, can be classed under these two ideas. Three constructive energy shaping algorithms were investigated, these were: Controller Interpolation via a common Lyapunov function, Energy-Shaping Robot control and Interconnection and Damping Assignment Passivity Based Control (IDAPBC). In this dissertation, a modelling paradigm has been proposed which is a multi-dimensional extension of *The Energy Method.* It is also shown that dissipation acts as a constant disturbance in the power of the system. A non-linear PI-like controller has been proposed to compensate for it. A clear link between the phase portrait and the system's energy is shown. By shaping the system energy, the phase portrait is altered and by shaping the phase portrait, the time domain performance is altered. In this dissertation, the various techniques used to shape a system's energy and power are all applied to the same non-linear control problem i.e. the simple pendulum. With hindsight, popular existing control strategies are reinterpreted via energy and power shaping. A notable example is that PID is shown to affect the potential and dissipation functions of the closed loop system. A pattern that emerged during the research was that: in order to fully control the system, it appears that the controller must be at least as computationally complicated as the plant. This is dubbed, the Controller Complexity Principle. A formal proof of it is a recommended research direction. The main conclusion of this work is that energy and power are concepts of tremendous value in control engineering. In this dissertation, energy and power are used to tie seemingly disparate work in control together. It is this re-interpretation of existing techniques in terms of energy and power which demonstrates the value of physical reasoning in control.

Acknowledgments

I would like to wholeheartedly thank my supervisor, Professor Brian Wigdorowitz, for his guidance, sense of humor and enthusiasm during this work. It has been a pleasure to get to know him and I have learned a tremendous amount from him, both about the world and about control engineering.

A massive thank-you to Professor Ivan Hofsajer for his fruitful discussions, his guidance and motivation during this work.

A big thank-you to Doctor Fabio Frescura for sharing his insight into Lagrangian mechanics and his reminder to always check dimensional consistency.

Thank-you to Mister Craig Sinclair for his invaluable discussions, proof reading and assistance with the editing of this dissertation.

Lastly, I would like to thank Misters Shamil Morars and Steven Dinger for their stimulating conversations about energy, and for their assistance in validating some of the proofs in this dissertation.

For my family, both here and gone, veteran and new.

List of Figures

List of Tables

List of Symbols

δx	Virtual displacement (total derivative of x, with $\mathrm{d}t = 0$)
E_d	Desired (closed-loop) energy
E_s	System energy
$[h]_y$	Partial derivative of h with respect to y i.e. $(\frac{\partial}{\partial y}h)$
μ	Membership function
χ	Generalised state or virtual co-ordinate
ν	Generalised velocity or virtual velocity = $\dot{\chi}$
x	Generalised co-ordinate or state
$\mathbf{x}$	Vector of states: $\in \mathbb{R}^N$
v	Generalised velocity = $\dot{x}$
$\mathbf{v}$	Vector of rates = $\dot{\mathbf{x}}$

$V(\mathbf{x})$	Lyapunov candidate function: $\mathbb{R}^N \rightarrow \mathbb{R}$
u	Control input
$\mathbf{u}$	Vector of control inputs
ζ	Integrator
x_d	Desired trajectory for x
x^*	Desired state for x
$\hat{x}$	Estimated state x
$\dot{x}$	Derivative of x with respect to time i.e. $(\frac{\mathrm{d}}{\mathrm{d}t}x)$
$\ddot{x}$	Second derivative of x with respect to time i.e. $(\frac{\mathrm{d}^2}{\mathrm{d}t^2}x)$
$\mathbb{I}$	The identity matrix
$\mathbb{O}$	The zero matrix or vector
note:	A capital-lettered function implies a matrix eg. $\mathbf{M}(\mathrm{x})$
	A bold-letter implies a vector eg. $\mathbf{x}$

1 Introduction

"*The journey of a thousand miles begins with a broken fan belt and a leaky tire.*"

- The Cynic's Guide to Life

Modelling of the dynamics of an engineering system using energy-based methods has been around since Maxwell wrote his celebrated paper, "On Governors" which is considered to be the birth of control engineering [1]. However, the idea of *designing* controllers using energy-based methods was first described in [2]. The aim of this research project was to investigate the benefits and shortfalls of Energy-Shaping control and use it to gain insight into the commonly used Proportional-Integral-Derivative (PID) control, amongst others. Linear control techniques are, by far, the main ones used in modern industrial control and PID control is used extensively, hence the reason for the comparison [3, 4], [5, pp. 293-313].

The conservation of energy is an unalterable, physical constraint. Actuators, necessarily, add energy into the system or remove energy from the system[1]. Sensors remove (in some cases, negligible amounts of) energy from the system in order to measure some variable of interest. All control algorithms employing feedback, must measure at least one physical variable of the system to be controlled. Furthermore, all control algorithms must have at least one actuator in order to control the system. Hence, by proxy, all control algorithms affect the energy of the system[2] under control. Therefore, by explicitly looking at the energy of the system and how it is affected by a closed loop control algorithm, additional insight not available using other analysis and design techniques is gained. In fact, as will be shown, Energy-Shaping Control methods employ a few simple ideas which lead to powerful and useful control laws. Furthermore, it is possible to analyse other control laws in terms of the effect on the system's energy. The energy domain, therefore, provides a domain for both analysis and design of control laws.

Energy Balancing [6, 7, 8, 9] and Power Shaping [10, 11] are the key techniques available for Energy-Shaping. Speaking generally, the Energy-Balancing design paradigm requires the engineer to select a closed-loop energy of the system. This would entail specifying: desired potential, kinetic and dissipation functions; a loss-less power transformation (similar to a gyrator) and finally *match* these with the actual system [7, 8, 6]. *How* to select these desired functions is left to the imagination of the engineer. Power shaping is essentially concerned with how the power of the system is affected by the control law [10, 11, 12]. As described in Chapter 5.2, power shaping considers all the possible trajectories which the system can take and if any one trajectory is desirable, then the control algorithm ensures that trajectory is followed [10, 11]. Constructive methods for assigning a desired closed-loop energy and/or power explored in this dissertation are: Controller Interpolation via a common Lyapunov function [13]; Energy-Shaping Robot control [2, 14],[15, Ch. 9] and Interconnection and Damping Assignment Passivity Based Control (IDAPBC) [6, 16, 17,

[1] If power was flowing into the actuator.

[2] Assuming the system is a physical system and not a mathematical one.

18, 19]. These control methods have all been grouped under the umbrella term *Energy-Shaping Control*.

This energy paradigm is fundamentally different from the classical control paradigm involving modes (in the Laplace domain) and frequencies (in the Fourier domain). A transfer function/matrix or input-output model can be called *black box* modelling, because the internal distribution of energy is never taken into account. Modelling in the energy framework is, necessarily, *white box* since one needs to know *how* the input energy is being distributed throughout the system. As will be shown this kind of white box modelling leads to elegant control laws since one may, for example, remove a potential energy function and replace it with another more suitable one. This would not be possible in the input/output framework since knowledge of how the system stores energy internally would, necessarily, be lost.

1.1 Research Questions and Scope

The types of systems considered are systems that can be modelled using energy-based methods. This modelling framework is appropriate since a very large class of practical problems can be modeled using energy-based methods and the modelling framework can easily incorporate non-linearities of practical interest [20, 16, 17, 21]. The control problems to be tackled will be the regulation problem and the trajectory tracking problem[3]. Systems with delays have been excluded from the scope of this project.

Question: "How does one design an energy based controller for both linear and nonlinear plants?"

The entire process of energy shaping rests on the solution of what are termed the *Matching Equations,* which, in general, require the solution of a set of partial differential equations [7, 8, 6]. The *Matching Equations* are a statement about the desired equivalence of the real physical system and the desired controlled system. Explicitly, if Σ is a physical system and Σ_d is the desired system, then the matching equation is $\Sigma = \Sigma_d$.

Question: "How does PID control affect the energy of a linear Second Order Single Input, Single Output system?"

A fundamental question in this research is how the PID control algorithm affects the energy stored in a system. Once this is known, a valid comparison with energy-shaping methods can be made, since both control methodologies will be in the same domain. The severe restriction to second order linear single input, single output (SISO) systems is because PID control algorithms, which require a model, typically use these system models [22]. This is because many practical problems can be modelled with second order differential equations [22]. This question is answered in Chapter 3.4 where the influences of the three terms have a clear interpretation in terms of the energy of the system. In summary, the proportional term affects the potential function, the derivative term affects the dissipation of the system and the integral term affects the instantaneous stationary point of the energy function.

[3] The regulation problem involves bringing a system to a state and keeping it there, while the tracking problem involves the system's state(s) following an arbitrary reference trajectory.

Question: "Can Energy-Shaping Control provide more insight into the design of controllers?"

Given that energy is of such fundamental importance in nature, it seems likely that the effect of a control law on the energy of the system would lead to new insight. This question is explored throughout the dissertation but is specifically tackled for various well-known control algorithms in Chapter 6.

The research questions are dealt with in the dissertation as follows: Chapter 2 presents the literature review, Chapter 3 explores a number of important concepts and Chapter 4 deals with modelling issues using energy. Chapter 5 presents energy-shaping methods for control and Chapter 6 presents the insights gained from this framework as well as constructive techniques for energy-shaping. Recommendations and conclusions are presented in Chapter 7.

1.2 Summary of Research

The key outcome of this research was the usefulness of viewing control action in terms of energy. It appears that energy manipulation is a unifying theme in control engineering. A number of classical and modern techniques for control can be reinterpreted in terms of their manipulation of the system's energy.

1.3 A Few Key Findings

The Energy Method is a well known method for determining the equations of motion for a scalar loss-less, "input-less" system [23, Ch. 7]. This method has been extended to the multi-dimensional case, which now includes dissipation, input forces and loss-less power transformations and is presented in Chapter 4. This methodology offers a simple alternative to Lagrangian and Hamiltonian mechanics for the modelling of complicated, multi-variable systems.

It is shown in Chapter 5.2 that dissipation acts as a constant disturbance in the power of the system. The dissipation is removed by including an integrator into the power shaping control law, analogous to the well-known disturbance rejection technique, using a PI-like controller.

Phase portrait analysis is a well known tool for non-linear system analysis [15, pp. 17-18]. For a second order system, the phase portrait is a plot of the system's state (position, charge etc.) against its rate (velocity, current etc.) for various initial conditions [15, pp. 17-18]. In Chapter 3.4 a clear link between the phase portrait and the system's energy is shown. Therefore, by shaping the system energy, the phase portrait is altered and by shaping the phase portrait, the time domain performance is altered. Hence, phase portraits are the link between the energy domain and the time domain.

A pattern that emerged during the research was that: in order to fully control the system, it appears that the controller must be at least as computationally complicated as the aspects of the plant to be controlled. For want of a better name, this phenomenon is referred to as the Controller Complexity principle. There is a strong analogy to this principle in the 1870 thought experiment by J.C Maxwell [24]. It is described in Chapter 6.1.

1.4 Conclusions

The principles related to energy have been shown to be an invaluable tool in both modelling and control algorithm design. Thus, by considering the effects of a control algorithm on the energy of a system, additional insight into the action of the controller on the system is gained.

The generalisation of *The Energy Method* has offered a viable alternative to Lagrangian and Hamiltonian mechanics. Furthermore, since it is founded on the conservation of energy, it adds insight into the understanding of systems that can be put into prototypical form. All physical systems can be put into this prototypical framework since it is founded on the first law of thermodynamics.

The link between phase portraits and the energy of a system was established. Hence, shaping the energy of a system shapes the phase portrait and shaping the phase portrait shapes the time domain performance. Phase portraits therefore represent the link between energy and time. Phase portraits also provide global information at a glance, information that is not available in time plots such as step responses and initial condition plots amongst others.

Energy Shaping controllers have far richer control structures and allow for greater performance (even in the presence of non-linearity and modelling errors) than linear PID techniques. Furthermore, the energy-shaping controllers are synthesised in a framework with which every engineer is familiar, namely energy. There is a tremendous advantage to using physical insight into control algorithm development, rather than the abstract mathematical techniques that appear to have dominated the control engineering field of late and which seem to lose track of both engineering insight and reality.

2 Literature Review

"*We have to know the past to understand the present.*"
- Carl Sagan

Modelling of the dynamics of an engineering system using energy-based methods has been around since Maxwell wrote his celebrated paper, "On Governors" which is considered to be the birth of control engineering [1]. However, the idea of *designing* controllers using energy based methods was first described in [2]. In [2], the idea of considering the *actuator* as a system that adds energy into the system to be controlled, via some *interconnection*, was described for the first time. This paper, [2], is considered to be the birth of Passivity Based Control [25, pp. 10-11].

Passivity Based Control's objective is to render a closed loop system *passive* which means simply that energy is conserved in the system i.e. that the energy stored in the closed loop system is equal to the initial energy stored plus the energy supplied via the input minus the energy lost via dissipation [25, Appendix A]. The restriction in Passivity Based Control is that for all inputs, $\mathbf{u}(t) \in \mathbb{R}^m$, there must exist some corresponding outputs, $\mathbf{y}(t) \in \mathbb{R}^m$ such that $\mathbf{u}^{\mathrm{T}}\mathbf{y}$ has units of power [25, Appendix A]. If these can be found then a (scalar) storage function $H(\mathbf{x})$ with states $\mathbf{x} \in \mathbb{R}^N$ exists which captures the notion of energy balancing i.e.

$$H(\mathbf{x}) - H(0) \quad \leq \quad \int_0^t \mathbf{u}^{\mathrm{T}}(s)\mathbf{y}(s)\mathrm{d}s - d,$$

where d is the dissipation of the system and the map $\mathbf{u} \to \mathbf{y}$ is defined as a *passive map* [6]. Now if the system's storage function $H(\mathbf{x})$ has a global minimum at $\mathbf{x}^*$ then, using the storage function $H(\mathbf{x})$ as a Lyapunov function, convergence of $\mathbf{x}$ to $\mathbf{x}^*$ can be proved [6].

The unique feature of energy-shaping methods is that this result is intuitive. This is further articulated: if a system has a potential function with a unique minimum and the system always dissipates energy away from the minimum, then the system will eventually settle to the minimum. Passivity Based Control was originally based on the Euler-Lagrange equations used to model a system [25] but evolved into using another model structure, namely the Port-Controlled Hamiltonian [19].

For the reader who is not familiar with Lagrangian mechanics, the idea is to take the energy of a system and use it to find the equations of motion [25, pp. 16-18, Appendix B]. For an N degree of freedom system described by generalised co-ordinates $\mathbf{q} \in \mathbb{R}^N$, the Lagrangian $\mathscr{L}(\mathbf{q}, \dot{\mathbf{q}}) = T(\dot{\mathbf{q}}, \mathbf{q}) - U(\mathbf{q})$ is formed, where T is the total kinetic energy and U is the total potential energy [25, pp. 16-18, Appendix B]. To get the equations of motion for the system, employ Hamilton's Principle to arrive at,

$$\frac{\mathrm{d}}{\mathrm{d}t}\left(\frac{\partial \mathscr{L}}{\partial \dot{\mathbf{q}}}\right) - \frac{\partial \mathscr{L}}{\partial \mathbf{q}} \quad = \quad \mathbf{Q},$$

where $\mathbf{Q}$ is defined as all the vector of generalised forces that act along each of the various degrees of freedom [25, pp. 16-18, Appendix B]. This will lead, in general, to N coupled

second order differential equations. The Controlled Lagrangian technique, which shapes the kinetic and potential energies via the available input forces is done completely in the Euler-Lagrange framework [7, 8, 26].

The Port-Controlled Hamiltonian framework is similar, but it leads to $2N$ coupled *first* order differential equations for an N degree of freedom system [19]. The model equations are given in terms of $2N$ states $\mathbf{x} \in \mathbb{R}^{2N}$, m inputs and outputs $\mathbf{u}, \mathbf{y} \in \mathbb{R}^m$ and an energy function $H(\mathbf{x}) = T(\mathbf{x}) + U(\mathbf{x})$ [19]. The Port-Controlled Hamiltonian for the system has the form

$$\begin{aligned} \dot{\mathbf{x}} &= [\mathbf{J}(\mathbf{x}) - \mathbf{R}(\mathbf{x})] \frac{\partial}{\partial \mathbf{x}} H(\mathbf{x}) + \mathbf{G}(\mathbf{x})\mathbf{u} \\ \mathbf{y} &= \mathbf{G}^T(\mathbf{x}) \frac{\partial}{\partial \mathbf{x}} H(\mathbf{x}) \end{aligned}$$

where $\mathbf{J}(\mathbf{x})$ is a skew-symmetric matrix which called the *interconnection matrix* (which captures the loss-less power transform between the various states), $\mathbf{R}(\mathbf{x})$ is the symmetric positive definite *damping matrix* (which captures how the system dissipates energy among the various degrees of freedom) and $\mathbf{G}(\mathbf{x})$ is the input coupling matrix (which models how the input couples to the various degrees of freedom) [19]. These equations are used in the celebrated Interconnection and Damping Assignment Passivity Based Control (IDAPBC) [19].

These two design methods (IDAPBC and Controlled Lagrangians) have been shown to be equivalent for simple mechanical systems, which can be expected given that the Lagrangian and Hamiltonian are related by the Legendre Transform [27]. What should be noted is that the IDAPBC framework appears to have had a wider adoption into practice, probably because the Controlled Lagrangian framework can be shown to be a subset of the general Port-Controlled Hamiltonian framework [19]. Moreover the Controlled Lagrangian method relies on extremely advanced mathematics such as group theory, and invokes strange notions such as "symmetry breaking potentials" and "vertical and horizontal decompositions of the configuration space" and has related problems with *how* to shape the kinetic and potential energy of the system to get the results desired [28]. Whereas it is clear in the Port-Controlled Hamiltonian framework that by shaping $H(\mathbf{x})$ one is shaping the equilibrium points, choosing $\mathbf{R}(\mathbf{x})$ shapes how the system tends to "slow down" (think of a resistor's role in a series RLC circuit) and $\mathbf{J}(\mathbf{x})$ shapes which states exchange energy with one another (think of the skew symmetry of the well known DC-motor, where the current in the armature and the angular speed of the load affect one another) [25].

A staple of non-linear control stability proofs is Lyapunov's Second Method and it is interesting to note that it is based on energy dissipation [15, Chapter 3]. It is used in the Controlled Lyapunov design techniques[29, 30, 31, 13, 32]. This is where an energy-like function, the Lyapunov candidate function, a scalar function dependent on all of the states of the system is shaped[1] [29]. The shaping of the first derivative of this function is necessary to prove stability and can be shaped for a guaranteed minimum performance of the closed loop system [15, Chapter 3]. Control design for fuzzy rules can be done in this framework directly and stability easily proved. This is a valuable tool, given the lack of stability proofs for fuzzy controllers in general [13, 32]. The main idea was presented in [13, 32] as a Heuristic Fuzzy Logic controller. The basic idea is first to define regions in the state space, $\mathbf{x} \in \mathbb{R}^N$ using fuzzy membership functions $\mu_i(\mathbf{x}) : \left\{\mathbb{R}^N \rightarrow [0,1]\right\}$ [13, 32]. Then using a Lyapunov function, $V(\mathbf{x})$, choose a control input $\mathbf{u}_i(\mathbf{x})$ which makes the derivative

[1] The Lyapunov function does not have to be the physical energy of the system.

of the Lyapunov function, $\dot{V}(\mathbf{x})$ negative definite *in that region* [13, 32]. Using the *same* Lyapunov function, look at each of the defined regions in turn and choose a control input function which makes each region's $\dot{V}(\mathbf{x})$ negative definite [13, 32]. Finally, each of the functions are interpolated using the weighted sum defuzzification method

$$\mathbf{u}(\mathbf{x}) = \frac{\sum_i \mu_i(\mathbf{x})\mathbf{u}_i(\mathbf{x})}{\sum_i \mu_i(\mathbf{x})},$$

where $\mathbf{u}(\mathbf{x})$ is the total input to the system [13, 32]. Since each controller stabilises each region of the state space, their interpolation via the weighted sum defuzzification method, stabilises the system over the entire state space [13, 32].

Moreover, Controlled Lagrangians and IDAPBC both use the Lyapunov direct method for stability proofs [7, 8, 9, 25, 17, 19].

Power shaping is another technique which is concerned with the rate of change of energy within a system. The idea of power shaping presented is originally presented as an "energy swing up" controller by [11], and further presented in [10]. See [12] for the idea of power shaping as applied to the process control problem of an unstable Continuously Stirred Tank Reactor. The basic idea is to add energy into the system until the system reaches the energy level which corresponds to a particular desired trajectory in the state space [10, 11].

Hence energy-shaping is at the heart of stability proofs for non-linear control, via the Lyapunov technique. Controlled Lagrangians and IDAPBC exploit energy-shaping directly. Some of the key features of these available methods for energy-shaping controllers are: the modelling of the system and the design of the controller are done in a single framework; stability analysis can be done simply by looking at the sign of the power of the closed loop system (i.e. the first derivative of the energy); the control design is physically motivated and hence does not require linearity. Some excellent resources for in depth reading on Energy-Shaping control are [15, 26, 33, 14, 34, 25].

Techniques from physical energy consideration, IDAPBC and Lyapunov based control will be presented in this dissertation under the umbrella term *Energy-Shaping Control*.

3 Introduction to Energy Concepts

"*One does not simply walk into Mordor.*"
- Boromir, JRR Tolkien's Lord of the Rings

3.1 Research Framework

It is reasonable to infer that no control methodology can be applied equally well to *all* possible systems, both mathematical and physical. Hence, it is important to limit the class of problems when investigating a control methodology. For the purposes of energy-shaping, the class of problems has been limited to physical systems that obey the conservation of energy. A prototypical system has been defined, which obeys the conservation of energy and is thoroughly investigated in Chapter 4. It is shown in Chapter 6 that a number of other modelling paradigms are a subset of this prototypical model. Hence, once the prototypical model is understood, if a given system can be represented as this prototypical model, physical insight into the system can be gained at once. The prototypical system is introduced next, followed by a simple example showing the value of energy-based reasoning.

Prototypical System

A second order non-linear ordinary differential equation used throughout this dissertation is equation (3.1.1) which is an amalgamation from various sources [7, 20, 26, 35, 36, 37, 21, 10, 38]. Clearly, a large class of practical, multi-variable problems can be modelled in this way and hence the reason for its adoption. Furthermore, once all of the terms in the model are understood, the effect of a control law on any one of the terms can be readily appreciated.

$$\mathbf{M}(\mathbf{x},t)\ddot{\mathbf{x}}+\mathbf{D}(\mathbf{x},\mathbf{v})\mathbf{v}+\mathbf{K}(\mathbf{x}) \quad = \quad \mathbf{G}(\mathbf{x})\mathbf{u} \tag{3.1.1}$$

where: $\mathbf{x}\in\mathbb{R}^N$ is the vector of states, $\mathbf{v}=\dot{\mathbf{x}}$ is the vector of rates, $\mathbf{M}(\mathbf{x},t)=\mathbf{M}(\mathbf{x},t)^{\mathrm{T}}>0$ is the mass matrix, $\mathbf{D}(\mathbf{x},\mathbf{v})$ is the dissipation, Coriolis/Centripetal forces and loss-less power transformation, $\mathbf{K}(\mathbf{x})$ is the spring-like force or potential-derived force, $\mathbf{G}(\mathbf{x})$ is the input coupling matrix, $\mathbf{u}$ is the vector of inputs and $\mathbf{G}(\mathbf{x})\mathbf{u}$ has units of generalised force.

To assist the understanding of energy flow in the prototypical system, it is necessary to expand the term linear in the velocity, v, into

$$\mathbf{D}(\mathbf{x},\mathbf{v}) \quad = \quad \mathbf{R}(\mathbf{x},\mathbf{v})+\mathbf{J}(\mathbf{x},\mathbf{v})+\frac{1}{2}\dot{\mathbf{M}}(\mathbf{x},t),$$

with $\mathbf{R}(\mathbf{x},\mathbf{v})=\mathbf{R}(\mathbf{x},\mathbf{v})^{\mathrm{T}}>0$ and $\mathbf{J}(\mathbf{x},\mathbf{v})=-\mathbf{J}(\mathbf{x},\mathbf{v})^{\mathrm{T}}$ skew symmetric. $\mathbf{J}(\mathbf{x},\mathbf{v})$ allows the model to account for Coriolis and Centripetal forces in the spirit of Robotics [15, pp. 393-403], $\mathbf{R}(\mathbf{x},\mathbf{v})$ accounts for dissipation as is done in IDAPBC [19, 18] and the $\frac{1}{2}\dot{\mathbf{M}}(\mathbf{x},t)$ term is an energy accounting term explained in Chapter 4 and adapted from [14].

It will be shown in Chapter 4 that the energy of the system, E_s is given by

$$E_s = \frac{1}{2}\mathbf{v}^{\mathrm{T}}\mathbf{M}(\mathbf{x},t)\mathbf{v} + \int \mathbf{K}(\mathbf{x})^{\mathrm{T}}\mathrm{d}\mathbf{x},$$

where $\frac{1}{2}\mathbf{v}^{\mathrm{T}}\mathbf{M}(\mathbf{x},t)\mathbf{v}$ is the kinetic energy of the system and $\int \mathbf{K}(\mathbf{x})^{\mathrm{T}}\mathrm{d}\mathbf{x}$ is the potential energy of the system.

The power of the system given by

$$\frac{\mathrm{d}}{\mathrm{d}t}E_s = -\mathbf{v}^{\mathrm{T}}\mathbf{R}(\mathbf{x},\mathbf{v})\mathbf{v} + \mathbf{v}^{\mathrm{T}}\mathbf{G}(\mathbf{x})\mathbf{u} - \mathbf{v}^{\mathrm{T}}\mathbf{J}(\mathbf{x},\mathbf{v})\mathbf{v}.$$

This power equation describes friction-like loss of power via $\mathbf{v}^{\mathrm{T}}\mathbf{R}(\mathbf{x},\mathbf{v})\mathbf{v}$, power gain via inputs $\mathbf{v}^{\mathrm{T}}\mathbf{G}(\mathbf{x})\mathbf{u}$ and power shuffling within the system via $\mathbf{v}^{\mathrm{T}}\mathbf{J}(\mathbf{x},\mathbf{v})\mathbf{v}$. Note that $\mathbf{v}^{\mathrm{T}}\mathbf{J}(\mathbf{x},\mathbf{v})\mathbf{v} = 0$ captures loss-less power transformations within the system itself and are referred to as Coriolis and Centripetal forces in the Robotics literature [15, pp. 393-403], [14] and as the interconnection in IDAPBC [19, 18]. The prototypical model eq (3.1.1) is recovered from the energy and power equations using the conservation of energy and is presented in detail in Chapter 4.

This modelling methodology is *a priori* using known physical principles and can be characterised as white box modelling. It is important to recognise that each term in the prototypical equation has intuitive physical meaning[1], meaning which is lost in the more abstract mathematical models such as the ubiquitous *input affine* non-linear state space model. The model's usefulness will be demonstrated throughout the dissertation. A further restriction in this dissertation is that $\mathbf{G}(\mathbf{x})\mathbf{u}$ is $N \times 1$ with N inputs u. This seemingly severe restriction is actually not unrealistic since it is a hardware design issue, namely if one wants to arbitrarily get all co-ordinates in the system to behave independently, then at least one input is required for each co-ordinate i.e. the system is fully actuated [39, Ch. 13]. This restriction implies that $\mathbf{G}(\mathbf{x})$ must have an inverse [18, 19]. Furthermore, the system is assumed to be controllable. For the under-actuated case i.e. for an N degree of freedom system with $m < N$ inputs, only m co-ordinates can be independently controlled [10].

Example of Energy-Based Reasoning

To demonstrate the insight and value of energy-based reasoning, the following special *scalar* case of the prototypical model is presented:

consider

$$\ddot{x} + b(v) + c(x) = 0,$$

where b and c are continuous functions [15, pp. 74-75]. In addition these functions satisfy the "first and third quadrant" non-linearity

$$\begin{aligned} vb(v) &> 0 \qquad v \neq 0 \\ xc(x) &> 0 \qquad x \neq 0, \end{aligned}$$

as in [15, pp. 74-75]. A typical "first and third quadrant" function is depicted in Figure 3.1.1. This system can be shown to be globally asymptotically convergent to $x = 0$ [15, pp.

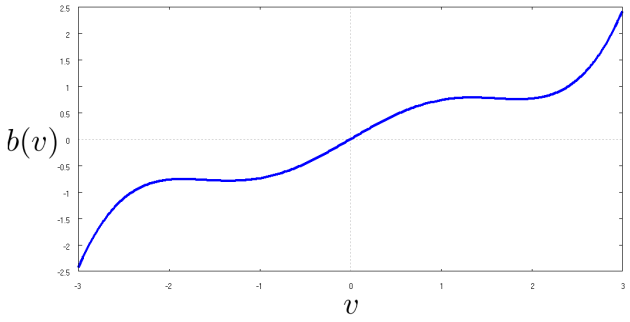

Figure 3.1.1: A First and Third Quadrant Function

74-75]. This is an important result since it highlights that non-linear functions can actually aid in stabilising a system globally.

3.2 Lyapunov's Second Method

It is intuitively obvious that a system that is always dissipating energy into the external environment will eventually settle to some final state, provided that energy is not being added to the system at a rate greater than is being dissipated. The Lyapunov method (Lyapunov's Second Method)[2] for proof of stability is a generalisation of this energy argument [5, p. 110-126]. This section is presented as a brief summary of the excellent work in [5, p. 110-126] and [15, p. 40-91], which the interested reader is urged to read as they are both excellent sources of information on the topic.

Given a general autonomous system which can be described by the differential equation

$$\frac{\mathrm{d}\mathbf{x}}{\mathrm{d}t} = \mathbf{F}(\mathbf{x}),$$

it is possible to show that this system's states $\mathbf{x} \in \mathbb{R}^N$, will *eventually* settle at the origin, $\mathbf{x} = \mathbb{O}$, if a function $V(\mathbf{x})$, called the Lyapunov function, can be found [5, p. 110-126],[15, p. 40-91].

The Lyapunov function $V(\mathbf{x})$ must satisfy:

$$V(\mathbf{x}) > 0$$

for all $\mathbf{x} \neq \mathbb{O}$, which is to say that the function is positive for any value of the states [5, p. 110-126],[15, p. 40-91]. Furthermore, its time derivative must always be negative for any value of the states, mathematically

$$\dot{V}(\mathbf{x}) < 0$$

for all $\mathbf{x} \neq \mathbb{O}$ and

$$\dot{V}(\mathbf{x}) = 0$$

[1] The model can be thought of as a series of coupled, non-linear and time varying mass-spring-dampers

[2] Lyapunov's First Method refers to the technique of linearising the system about a point and checking that all of the poles are strictly in the left half plane [5, p. 110-126]

iff $\mathbf{x} = \mathbb{O}$ which is to say that the function $\dot{V}(\mathbf{x})$ is only zero if every state is zero[5, p. 110-126],[15, p. 40-91].

A question typically arises about how this function, $V(\mathbf{x})$ is at all related to the system under study, since the function can be fabricated without considering the system at all. The answer is simple: consider a Lyapunov candidate function $V(\mathbf{x})$, its time derivative can be computed using the chain rule from multidimensional calculus, as follows

$$\dot{V}(\mathbf{x}) = \frac{\partial V(\mathbf{x})}{\partial \mathbf{x}} \frac{\mathrm{d}\mathbf{x}}{\mathrm{d}t},$$

which when "evaluated along the system trajectories", basically substituting in the model equation,

$$\frac{\mathrm{d}\mathbf{x}}{\mathrm{d}t} = \mathbf{F}(\mathbf{x}),$$

yields

$$\dot{V}(\mathbf{x}) = \frac{\partial V(\mathbf{x})}{\partial \mathbf{x}} \mathbf{F}(\mathbf{x})$$

[5, p. 110-126].

This has to satisfy the properties outlined above in order to prove that the system is globally stable [5, p. 110-126],[15, p. 40-91].

It is important to remember that if a candidate Lyapunov function fails to have the desired properties to prove stability, this does not imply that the system is unstable [5, p. 110-126],[15, p. 40-91]. What remains is to try another candidate Lyapunov function until stability can be proved [5, p. 110-126],[15, p. 40-91].

Subtleties and Uses of the Lyapunov Method

Now the Lyapunov candidate function need not have the properties mentioned throughout the entire state space. If it can be shown that the Lyapunov function has the required properties, *locally,* which is to say within some "ball", B_r within a radius r around a point in the state space, $\mathbf{x_e}$, then it shows stability within that region of the state space [5, p. 110-112]. The region of stability is called a "ball" since in general the state space will be N dimensional and a "ball" is different from an N dimensional sphere since it includes all of the points enclosed by that sphere, mathematically defined as all the points that satisfy $||\mathbf{x}|| < r$ [15, 40-91]. Figure 3.2.1 depicts a Lyapunov function for a system of one state $\mathbf{x}$, which has multiple equilibria, $\mathbf{x_e}$ and the derivative of $V(\mathbf{x})$ is depicted using the arrows visible on the function. It is clear from the figure that the equilibrium point at the origin is *globally* a minimum, whereas the equilibrium point in the negative half of the the state space is a *local* minimum. Now Lyapunov's method for proof of stability will work for both of these points. However, the "ball", B_r for each point will have a different radius. If the "ball" nearest the origin were extended to encompass the entire real line, *global* stability for the origin could not be concluded, since there is a local minimum elsewhere in the space.

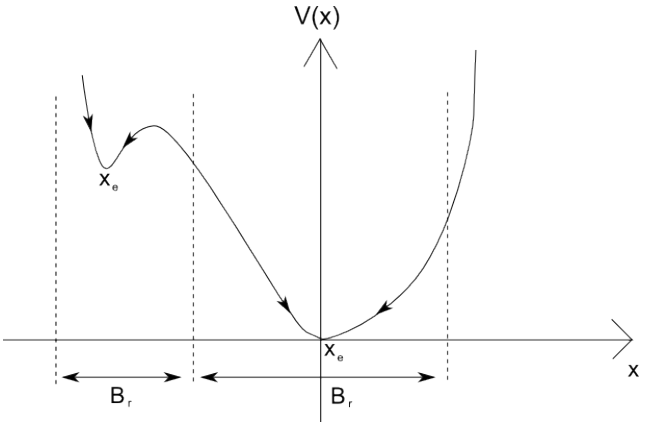

Figure 3.2.1: A one dimensional Lyapunov function

3.3 Contraction Analysis

Contraction analysis is a method used to determine whether all trajectories in some region in the state space, for a given system, converge to a particular trajectory, or point [40, 41]. The basic premise is simple: if the *virtual displacement* [3], $\delta\mathbf{x}$, of any trajectory of the system (with respect to some definition of distance in the state space, also known as a *metric*) inside a *ball*[4] around a point or other some other trajectory (call it $\mathbf{x_d}$) tends to move towards $\mathbf{x_d}$, then the system is said to be *contracting* in that ball [42, 41]. Figure 3.3.1, inspired and adapted from [41], depicts this idea for a two dimensional system where it can be seen that the ball B, surrounds the trajectory x_d and that all the trajectories within the ball move towards x_d. The trajectories outside this ball do not approach x_d.

Given a system described by

$$\dot{\mathbf{x}} \;=\; \mathbf{F}(\mathbf{x},t),$$

where $\mathbf{x}$ may be a vector and $\mathbf{F}$ is a non-linear, possibly time varying function, the *virtual velocity* $\delta\dot{\mathbf{x}}$ is calculated with

$$\delta\dot{\mathbf{x}} \;=\; \frac{\partial\mathbf{F}}{\partial\mathbf{x}}\delta\mathbf{x},$$

note that the virtual displacement, $\delta\mathbf{x}$ can be differentiated with respect to time [41].

Now consider the squared distance of the virtual displacement, defined as $\delta\mathbf{x}^{\mathrm{T}}\delta\mathbf{x}$ differentiated with respect to time to yield

$$\begin{aligned}\frac{\mathrm{d}}{\mathrm{d}t}(\delta\mathbf{x}^{\mathrm{T}}\delta\mathbf{x}) &= 2\delta\mathbf{x}^{\mathrm{T}}\delta\dot{\mathbf{x}}\\ &= 2\delta\mathbf{x}^{\mathrm{T}}\frac{\partial\mathbf{F}}{\partial\mathbf{x}}\delta\mathbf{x}\end{aligned}$$

[3] A *virtual displacement* is the distance between two trajectories in the state space, at a fixed point in time [42, 41]. Essentially, this can be thought of as a *what if* scenario. One considers what would happen if the system started at different initial conditions and were allowed to evolve until the present time. The "distance" between the system's actual trajectory now and this other theoretical trajectory is the virtual displacement.

[4] A ball, described in English, is a filled-in multidimensional sphere which excludes the shell of the sphere. Mathematically a *ball* around the point $\mathbf{x}^*$ is the set of all points in $\mathbf{x}\in\mathbb{R}^N$, satisfying $||\mathbf{x}-\mathbf{x}^*|| < r$ where r is a positive constant [15, pp. 47].

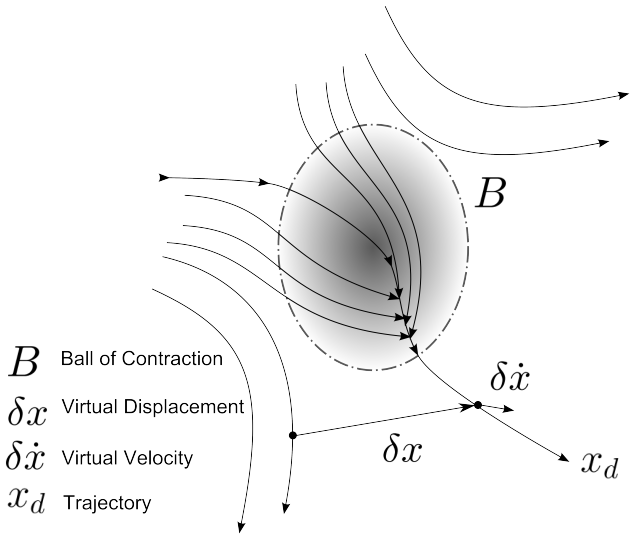

Figure 3.3.1: Contraction for a Two Dimensional System, adapted from Slotine.

which uses the virtual velocity calculated earlier [41].

Now let $\lambda_{max}(\mathbf{x},t)$ denote the largest eigenvalue of the symmetric part[5] of the Jacobian $\frac{\partial \mathbf{F}}{\partial \mathbf{x}}$, where the symmetric part of the Jacobian is $\frac{1}{2}\left(\frac{\partial \mathbf{F}}{\partial \mathbf{x}} + \frac{\partial \mathbf{F}}{\partial \mathbf{x}}^{\mathrm{T}}\right)$ [41].

Substitution of this idea into $\frac{\mathrm{d}}{\mathrm{d}t}(\delta\mathbf{x}^{\mathrm{T}}\delta\mathbf{x})$, yields

$$\begin{aligned}\frac{\mathrm{d}}{\mathrm{d}t}(\delta\mathbf{x}^{\mathrm{T}}\delta\mathbf{x}) &= 2\delta\mathbf{x}^{\mathrm{T}}\frac{\partial \mathbf{F}}{\partial \mathbf{x}}\delta\mathbf{x} \\ &= \delta\mathbf{x}^{\mathrm{T}}\left(\frac{\partial \mathbf{F}}{\partial \mathbf{x}} + \frac{\partial \mathbf{F}}{\partial \mathbf{x}}^{\mathrm{T}}\right)\delta\mathbf{x} \\ &\leq \lambda_{max}(\mathbf{x},t)\delta\mathbf{x}^{\mathrm{T}}\delta\mathbf{x}\end{aligned}$$

which upon integration, bearing in mind that $\delta\mathbf{x}^{\mathrm{T}}\delta\mathbf{x} = (||\delta\mathbf{x}||)^2$ (where $||\,.\,||$ is the 2-norm), yields

$$||\delta\mathbf{x}|| \leq ||\delta\mathbf{x}_0|| e^{\int_0^t \lambda_{max}(\mathbf{x},t)\mathrm{d}t}$$

according to [41].

If $\lambda_{max}(\mathbf{x},t)$ is then *uniformly negative definite*, basically it is less than zero for all $\mathbf{x}$ considered and all time $t > 0$ then any virtual displacement $||\delta\mathbf{x}||$ converges to zero [41]. A finite path would then consist of a number of $||\delta\mathbf{x}||$ and all of these are converging exponentially so therefore an entire finite path would converge exponentially as well [41]. The region where this phenomenon occurs is then called a *contraction region* [41].

In mathematical parlance, a contraction region is defined as a region where

$$\exists\beta > 0, \forall\mathbf{x}, \forall t > 0, \quad \tfrac{1}{2}\left(\frac{\partial \mathbf{F}}{\partial \mathbf{x}} + \frac{\partial \mathbf{F}}{\partial \mathbf{x}}^{\mathrm{T}}\right) < -\beta\mathbb{I} < \mathbb{O},$$

[5] A skew-symmetric matrix, $\mathbf{J}$ has the well-known property $\mathbf{v}^{\mathrm{T}}\mathbf{J}\mathbf{v} = 0$, for any appropriately sized vector $\mathbf{v}$. This is the reason why only the symmetric part of the Jacobian is considered.

a *semi-contraction region* is defined as a region wheres

$$\exists \beta > 0, \forall \mathbf{x}, \forall t > 0, \quad \tfrac{1}{2}\left(\tfrac{\partial \mathbf{F}}{\partial \mathbf{x}} + \tfrac{\partial \mathbf{F}}{\partial \mathbf{x}}^{\mathrm{T}}\right) \quad \leq -\beta \mathbb{I} \leq \mathbb{O},$$

and an *indifferent region* is defined as a region where $\frac{\partial \mathbf{F}}{\partial \mathbf{x}}$ is skew-symmetric [41]. Note that $\mathbb{I}$ is the $N \times N$ identity matrix.

Now the main result of contraction analysis follows:

For a system described by $\dot{\mathbf{x}} = \mathbf{F}(\mathbf{x},t)$, if a ball centred around a trajectory is a contraction region, then all the trajectories that start in that ball remain in that ball and furthermore, they converge exponentially to that trajectory [41, Theorem 1]. If the entire state space is a contraction region, then logically, *all* trajectories converge to the single trajectory considered. There is a further generalisation of this result for cases where the definition of *length* changes with states and time (this is the metric alluded to in the opening paragraph of this section).

Let $\mathbf{M_e}(\mathbf{x},t) = \Theta^{\mathrm{T}}\Theta$ be a *uniformly positive definite* defined metric for the state space $\mathbf{x}$, where Θ is a continuous and smooth transformation $\delta\mathbf{z} = \Theta\delta\mathbf{x}$ [41]. Given a system $\dot{\mathbf{x}} = \mathbf{F}(\mathbf{x},t)$, if there is a region in the state space where

$\frac{\partial \mathbf{F}}{\partial \mathbf{x}}^{\mathrm{T}}\mathbf{M_e} + \dot{\mathbf{M}}_\mathbf{e} + \mathbf{M_e}\frac{\partial \mathbf{F}}{\partial \mathbf{x}} \leq \beta_{\mathrm{M}}\mathbf{M_e}$ with constant $\beta_{\mathrm{M}} > 0$ then that region is a *contraction region* [41].

This result follows from the time derivative of $\delta\mathbf{x}^{\mathrm{T}}\mathbf{M_e}(\mathbf{x},t)\delta\mathbf{x}$ which is

$$\frac{\mathrm{d}}{\mathrm{d}t}\left(\delta\mathbf{x}^{\mathrm{T}}\mathbf{M_e}(\mathbf{x},t)\delta\mathbf{x}\right) \quad = \quad \delta\mathbf{x}^{\mathrm{T}}\left(\frac{\partial \mathbf{F}}{\partial \mathbf{x}}^{\mathrm{T}}\mathbf{M_e} + \dot{\mathbf{M}}_\mathbf{e} + \mathbf{M_e}\frac{\partial \mathbf{F}}{\partial \mathbf{x}}\right)\delta\mathbf{x},$$

and uses the same method and assumptions as before [41]. The interested reader is referred to [40, 42, 41] for more information on the technique.

Subtleties in the use of Contraction Analysis

In [42] the idea of a *virtual system* is introduced, which dramatically simplifies the application of contraction theory. The virtual system is one which contains both the system trajectory and desired trajectory as special cases, which means that if the virtual system is contracting, then the system trajectory exponentially approaches the desired trajectory [42]. Furthermore, for the case of an observer, if the virtual system contains both the estimated state and the true state, then the estimated state will exponentially approach the true state [42]. The difficulty lies in finding this virtual system, which is done by inspection and some clever tricks in [42].

A number of characteristic examples are taken from [42] and presented:

A Simple Autonomous System

Consider a system with states $\mathbf{x} \in \mathbb{R}^N$ and matrix $\mathbf{D}(\mathbf{x}) > 0 \, \forall \mathbf{x}$ described by

$$\dot{\mathbf{x}} \quad = \quad -\mathbf{D}(\mathbf{x})\mathbf{x}.$$

The virtual velocity is

$$\delta\dot{\mathbf{x}} = -\frac{\partial \mathbf{D}}{\partial \mathbf{x}}\mathbf{x}\,\delta\mathbf{x} - \mathbf{D}\,\delta\mathbf{x}$$

which, in general, is difficult to use in a proof of contraction [42].

The trick is to use a *virtual system*, with virtual state χ, described by

$$\dot{\chi} = -\mathbf{D}(\mathbf{x})\chi$$

that has the original system as a solution ($\chi = \mathbf{x}$) as well as the origin ($\chi = \mathbb{O}$) [42]. This is critical, $\mathbf{D}(\mathbf{x})$ is **not** a function of χ and hence it is **not** affected when calculating the virtual velocity, $\delta\dot{\chi}$.

Now the virtual velocity for this *virtual system* is

$$\begin{aligned}\delta\dot{\chi} &= -\left[\mathbf{D}(\mathbf{x})\chi\right]_{\chi}\delta\chi \\ &= -\mathbf{D}(\mathbf{x})\delta\chi\end{aligned}$$

which contracts for all χ since $\mathbf{D}(\mathbf{x}) > 0\ \forall \mathbf{x}, \chi$. This means that the original system, whose trajectory is contained in the virtual system (i.e. $\chi = \mathbf{x}$) contracts as well [42].

Observers and Controllers

This example is an adaptation from an example in [42].

Consider the observer

$$\dot{\hat{x}} = -\sin(\hat{x}) + u + \kappa_p(x - \hat{x}) \tag{3.3.1}$$

which estimates the state, $x \in \mathbb{R}$, for the system

$$\dot{x} = -\sin(x) + u + \kappa_p(x - x) \tag{3.3.2}$$

and $\kappa_p > 0$ is a strictly positive constant [42]. There is a subtlety here introduced by [42]. The subtlety is inclusion of the term $\kappa_p(x-x)$ in the description of the system. This extra term suggests the choice of virtual system

$$\dot{\chi} = -\sin(\chi) + u + \kappa_p(x - \chi), \tag{3.3.3}$$

that has the virtual velocity

$$\delta\dot{\chi} = (-\cos(\chi) - \kappa_p)\delta\chi,$$

which will contract for $\kappa_p > 1$ [42]. Therefore since both the system state $\chi = x$ and the observer estimate $\chi = \hat{x}$ are particular solutions to the virtual system, the observer estimate exponentially approaches the true state [42]. There is a dual result about tracking controllers, which is to say that the system will exponentially approach the reference trajectory provided that the system to be controlled is a particular solution of the contracting controller [42]. Now both the original system $\chi = x$ and the reference signal to be tracked $\chi = x_d$ are

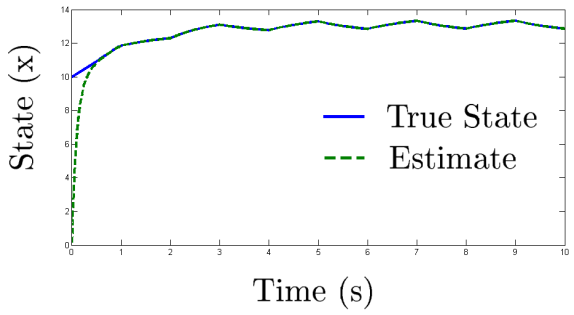

Figure 3.3.2: Observer Response

solutions of the virtual system, therefore a controller of the form (3.3.3) will exponentially track the reference signal. This is highlighted in [42] and considers (3.3.3) as an *implicit* form of the controller that, upon solving for u and letting $\chi = x_d$ yields,

$$u = \dot{x}_d + \sin(x_d) + \kappa_p(x_d - x) \tag{3.3.4}$$

which is a proportional controller with a feed-forward term. Notice that the feed-forward term does *not* cancel the non-linear dynamics of the system. In feed-back linearisation, the control law with feedback linearisation would be of the form $u = \sin(x) + r$ which, upon substitution into the system, would lead to $\dot{x} = r$. It will be shown in Chapter 5.4 that eq (3.3.4) is actually *plant inversion* with a feedback term. This controller is an excellent example of the Controller Complexity Principle in action: the controller has at least the same mathematical structure as the plant in order to get the plant to exponentially track a reference trajectory.

The system (3.3.2), observer (3.3.1) and controller (3.3.4) were simulated using Matlab's Simulink simulation package, a gain of $\kappa_p = 10$ was used in both circumstances, the derivative in the tracking controller was approximated using a filtered derivative with an arbitrary bandwidth of 100 rad/s and the system was given an initial condition of 10. The input to the plant for the observer was a square wave with a period of 2 s and a duty cycle of 50%; the same signal was used as the reference to be tracked for the tracking controller. The observer response is depicted in Figure 3.3.2. The tracking response is depicted in Figure 3.3.3. The exponential stability as predicted by the contraction analysis is clear in both cases.

Contraction Analysis' relationship with Energy and Power: an Example

For a suitably defined metric $\mathbf{M_e}(\chi,t)$ it is possible to relate the system energy to the idea of contraction. Provided that $\delta\chi^{\mathrm{T}}\mathbf{M_e}(\chi,t)\delta\chi$ has units of the system energy, $\frac{\mathrm{d}}{\mathrm{d}t}\left(\delta\chi^{\mathrm{T}}\mathbf{M_e}(\chi,t)\delta\chi\right)$ will have units of power and will therefore represent the energy loss or gain of the system.

Consider the DC motor model

$$\frac{\mathrm{d}}{\mathrm{d}t}\begin{pmatrix}\omega\\ i\end{pmatrix} = \begin{pmatrix}-\frac{B_r}{J_m} & \frac{K_m}{J_m}\\ -\frac{K_m}{L} & -\frac{R_r}{L}\end{pmatrix}\begin{pmatrix}\omega\\ i\end{pmatrix} + \begin{pmatrix}0\\ \frac{1}{L}\end{pmatrix}V,$$

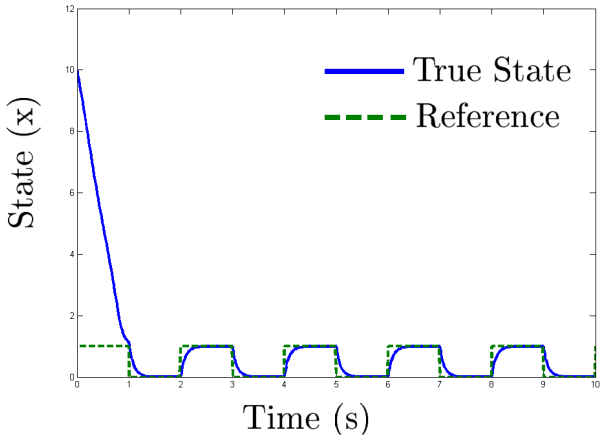

Figure 3.3.3: Tracking Response

with angular speed ω, current i, input voltage V, torque/speed constant K_m, moment of inertia J_m, inductance L, resistance R_r and viscous damping B_r.

Written in this form the system appears as

$$\dot{\mathbf{x}} = \mathbf{F}(\mathbf{x}) + \mathbf{G}u$$

where

$$\mathbf{F}(\mathbf{x}) = \begin{pmatrix} -\frac{B_r}{J_m} & \frac{K_m}{J_m} \\ -\frac{K_m}{L} & -\frac{R_r}{L} \end{pmatrix} \begin{pmatrix} \omega \\ i \end{pmatrix}$$

and

$$\mathbf{G}u = \begin{pmatrix} 0 \\ \frac{1}{L} \end{pmatrix} V.$$

By choosing $\chi = \mathbf{x} = \begin{bmatrix} \omega & i \end{bmatrix}^T$, $\mathbf{M_e}(\mathbf{x},t)$ as

$$\mathbf{M_e} = \begin{pmatrix} \frac{J_m}{2} & 0 \\ 0 & \frac{L}{2} \end{pmatrix},$$

and given that $\delta\mathbf{x} = \begin{bmatrix} \delta\omega & \delta i \end{bmatrix}^{\mathrm{T}}$ leads to

$$\delta\mathbf{x}^{\mathrm{T}}\mathbf{M_e}(\mathbf{x},t)\delta\mathbf{x} = \frac{J_m}{2}\delta\omega^2 + \frac{L}{2}\delta i^2.$$

This is exactly the incremental kinetic energy of the load and the incremental magnetic energy stored in the inductor. Now calculating the power,

$$\frac{\mathrm{d}}{\mathrm{d}t}\left(\delta\mathbf{x}^{\mathrm{T}}\mathbf{M_e}(\mathbf{x},t)\delta\mathbf{x}\right) = \delta\mathbf{x}^{\mathrm{T}}\left(\frac{\partial\mathbf{F}}{\partial\mathbf{x}}^{\mathrm{T}}\mathbf{M_e} + \dot{\mathbf{M}}_\mathbf{e} + \mathbf{M_e}\frac{\partial\mathbf{F}}{\partial\mathbf{x}}\right)\delta\mathbf{x},$$

leads to $-B_r\delta\omega^2 - R_r\delta i^2$ which is expected from energy reasoning alone, considering that this term is the loss due to the rotational friction and resistance in the armature.

3.4 Phase Portraits

Henri Poincare was one of the mathematicians who developed the idea of phase plane analysis in the late 1800's [15, pp. 17]. The idea is to plot a dynamic system's trajectories in a plane defined by the state (eg. x) on one axis and the rate (eg. $\dot{x}$) on an axis perpendicular to that, making time an implicit variable [15, pp. 17]. This plot is called a phase portrait for the system [15, pp. 17-18]. A point in the phase space, $(x, \dot{x})$, is the instantaneous position and velocity of the system [43, Ch. 3]. If the system which the phase space describes were to change its position or velocity or both, it is clear that it would rely on the present states and the equations of motion. Hence the system would (uniquely) evolve with time by following a sequence of points in the phase space [43, Ch. 3]. All of these successive points form a trajectory in the phase plane [15, pp. 17-18]. It should be noted that due to determinism, each trajectory in the phase portrait may not cross any other trajectory, for that would imply that a particular initial condition would lead to two different outcomes [43, Ch. 3].

The beauty of this graphical representation of a dynamic system is that qualitative features, response to various initial conditions and equilibrium points of the system can all be pictorially represented [15, pp. 19]. This plot also obviates the need to solve the equations of motion analytically [15, pp. 17]. The most useful property of phase portraits is that the system models can be non-linear and hence the non-linear behaviour of a system may be analysed [5, pp. 28-29]. Phase portraits are useful for up to second order non-linear ordinary differential equations (ODE's) since one can obtain global information about the system under study simply by looking at a picture of the various trajectories [15, Ch. 2], [43, Ch. 3].

Method of Construction

All of the phase portraits in this dissertation were constructed using *wxMaxima*, a free computer algebra system, and *Matlab*.

First Order Systems

For any first order non-linear ODE, the phase portrait may be drawn explicitly [15, Ch. 2, pp 21-22]. Consider the equation,

$$\dot{x} \quad = \quad f(x),$$

the phase portrait can be drawn under the premise that $\dot{x}$ becomes the dependent variable in the plot and x becomes the independent variable in the plot, in the usual spirit of $y = f(x)$ [15, Ch. 2, pp 21-22].

Once the system has been drawn, the trajectory that the system takes given some initial x_0, may be found by inspection [15, Ch. 2, pp 21-22]. Wherever $\dot{x}$ is positive, the state trajectory will move in the direction of increasing x and wherever $\dot{x}$ is negative, the trajectory will move in the direction of decreasing x [15, Ch. 2, pp 21-22]. The values where $\dot{x} = 0$ are the equilibrium points of the system and the stability of the equilibrium point is assessed by considering whether the two state trajectories are moving away from the point or towards it [15, Ch. 2, pp 21-22].

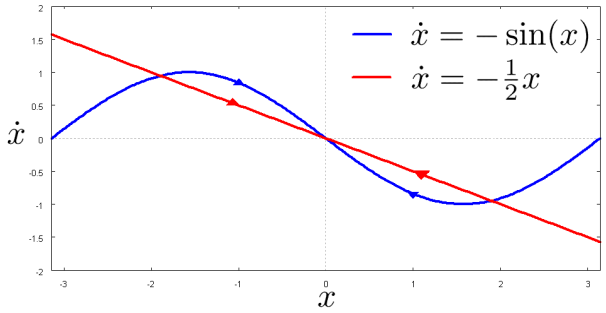

Figure 3.4.1: Phase Portrait of $\dot{x} = -\sin(x)$ and $\dot{x} = -\frac{1}{2}x$

It is worth noting that a linear first order ODE with a time constant τ, written as

$$\frac{dx}{dt} = -\frac{x}{\tau},$$

is a straight line in the phase portrait [10]. This means that one may estimate a given non-linear first order ODE's rate of convergence to a stable point (divergence from an unstable point respectively) by drawing a straight line through the origin and comparing where the non-linear ODE is above the line. Wherever the non-linear ODE is above the line, its rate of convergence (divergence respectively) will be at least as fast as an exponential with time constant τ, where $\frac{1}{\tau}$ is the slope of the straight line in phase space. Figure 3.4.1 depicts the function,

$$\dot{x} = -\sin(x),$$

with $\dot{x} = -\frac{1}{2}x$ overlaid on the plot.

It should be noted that when x is in the region $[-1.89, 1.89]$, then the system has a (converging) time constant that is greater than 2 seconds, and outside of this region the time constant is less than 2 seconds.

This procedure makes it visually obvious that non-linear systems can have different time constants for different regions of the state space.

Furthermore, it is clear that the origin, $(x, \dot{x}) = (0, 0)$, is a point of stability for this system since all the system trajectories within $x \in (-\pi, \pi)$ move towards it.

Second Order Systems

There are a number of ways to draw a phase portrait for second order non-linear ODE's [15, Ch 2.]. Since time is an implicit variable in the phase portrait, by solving the set of ODE's and eliminating time, the equations that govern the phase portrait are readily arrived at [15, Ch. 2, pp. 18-19]. Another method is to integrate the second order ODE with respect to $d\dot{x}$ and dx respectively, using the identity from calculus

$$\ddot{x} = \dot{x}\frac{d\dot{x}}{dx}$$

as described in [15, Ch. 2, pp. 24-25]. This integration will yield the same phase portrait as the first method which solves for time [15, Ch. 2, pp 24-25].

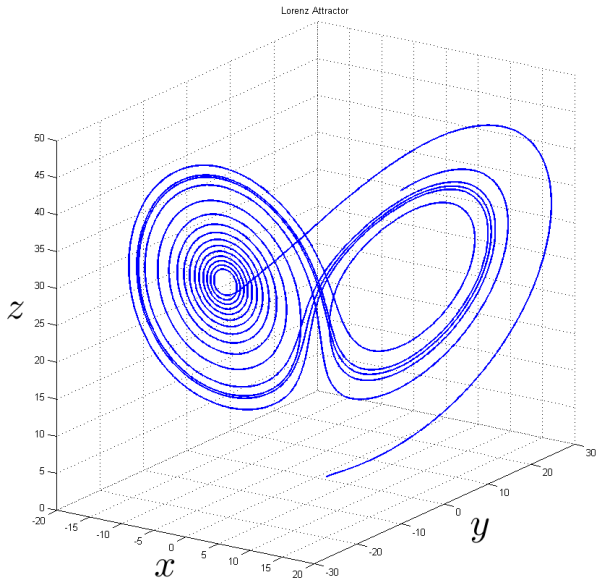

Figure 3.4.2: Lorenz Attractor $\rho = 28$, $\sigma = 10$, $\beta = \frac{8}{3}$

Third Order Systems

The Lorentz attractor is an excellent example of a well known phase portrait for a third order system [43, Ch. 18]. The Lorenz attractor is depicted in Figure 3.4.2 and shows what a trajectory for the system starting from $(x,y,z) = (1,1,0)$ looks like.

The phase portrait of a third order system is useful for the visualisation of Proportional Integral Derivative (PID) control of a second-order system, as will be shown. It is possible to construct phase portraits of third order ODE's using modern software packages designed for visualisation of volumetric fluid flow, indeed Figure (3.4.2) was constructed using *Matlab*'s functions intended for visualising volumetric flows. The type of systems that can easily be visualised in this way are systems of equations of the form,

$$\begin{aligned} \dot{x} &= f_x(x,y,z) \\ \dot{y} &= f_y(x,y,z) \\ \dot{z} &= f_z(x,y,z). \end{aligned}$$

Fortunately the general PID controller for a second-order ODE can be put into this form.

Given a second-order ODE of the form,

$$\ddot{x} = f(x,\dot{x}) + gu,$$

a PID controller with set-point weighting for the system has the form [5, pp. 309],

$$\begin{aligned} u &= \kappa_{p1}x^* - \kappa_{p2}x + \kappa_{d1}v^* - \kappa_{d2}v + \zeta \\ \dot{\zeta} &= \kappa_i(x^* - x), \end{aligned}$$

where x^* is the desired state, x is the measured state, κ_p is a proportional gain, κ_d is a derivative gain and κ_i is the integral gain.

This yields the closed loop dynamics,

$$\begin{aligned}\dot{x} &= v \\ \dot{v} &= f(x,\dot{x}) + g\left[\kappa_{p1}x^* - \kappa_{p2}x + \kappa_{d1}v^* - \kappa_{d2}v + \zeta\right] \\ \dot{\zeta} &= \kappa_i(x^* - x),\end{aligned}$$

which is of the required form for three dimensional visualisation.

This is visualised in Chapter 6.2.

Relationship of Phase Portrait to Energy

The phase portrait for a physical system has a particularly useful interpretation in terms of energy. The view presented here was inspired by Riemann who saw complex mappings as projections from an object on the surface of a three dimensional sphere onto the complex plane, the so called "Riemann Sphere" [44, pp. 142-145].

Consider a subset of the prototypical model eq (3.1.1) for a one dimensional system,

$$m\ddot{x} = -k(x) - b(x,\dot{x})\dot{x} + F,$$

with m the inertia, $k(x)$ the force dependent on position, $x \in \mathbb{R}$, $b(x,\dot{x})\dot{x}$ the force dependent on velocity, $\dot{x}$ and F the external applied force. This equation can readily be seen to be Newton II in disguise i.e. $ma = \sum F$.

Now using the identity,

$$\ddot{x} = \dot{x}\frac{\mathrm{d}\dot{x}}{\mathrm{d}x},$$

the following can be integrated,

$$m\dot{x}\mathrm{d}\dot{x} = -k(x)\,\mathrm{d}x - b(x,\dot{x})\dot{x}\,\mathrm{d}x + F\,\mathrm{d}x. \tag{3.4.1}$$

It is pertinent at this point to examine the units of the equation,

$$\begin{aligned}[m\dot{x}\,\mathrm{d}\dot{x}] &= kg\frac{m}{s}\frac{m}{s} \\ [k(x)\,\mathrm{d}x] &= Nm \\ [b(x,\dot{x})\dot{x}\,\mathrm{d}x] &= Nm \\ [F\,\mathrm{d}x] &= Nm,\end{aligned}$$

which are all units of energy. This means that equation (3.4.1) which governs the phase portrait will be the energy of the system!

Recall,

$$m\ddot{x} = -k(x) - b(x,\dot{x})\dot{x} + F,$$

which leads to the differential,

$$m\dot{x}\,\mathrm{d}\dot{x} = -k(x)\,\mathrm{d}x - b(x,\dot{x})\dot{x}\,\mathrm{d}x + F\,\mathrm{d}x$$

after using the identity $\ddot{x} = \dot{x}\frac{\mathrm{d}\dot{x}}{\mathrm{d}x}$.

Integrating both sides leads to,

$$\frac{1}{2}m\dot{x}^2 + \int k(x)\mathrm{d}x \quad = \quad E_0 - \int b(x,\dot{x})\dot{x}^2\mathrm{d}t + \int F\,\mathrm{d}x,$$

where the chain rule has been applied to the integral of $b(x,\dot{x})\dot{x}$ and the constants of integration are lumped into E_0. This is exactly of the form of the energy balance for the system, in words, the energy stored by the system, kinetic $\frac{1}{2}m\dot{x}^2$ plus potential $\int k(x)\,\mathrm{d}x$, is equal to the initial energy, E_0 minus the energy lost by friction forces, $\int b(x,\dot{x})\dot{x}^2\mathrm{d}t$ plus the work done on the system, $\int F\,\mathrm{d}x$.

For the application of this idea to constructing and interpreting phase portraits, consider the simple frictionless mass spring system,

$$m\ddot{x} \quad = \quad -kx.$$

Applying the identity $\ddot{x} = \dot{x}\frac{\mathrm{d}\dot{x}}{\mathrm{d}x}$ leads to the equation,

$$m\dot{x}\mathrm{d}\dot{x} \quad = \quad -kx\,\mathrm{d}x,$$

which, when integrated, yields,

$$\frac{1}{2}m\dot{x}^2 \quad = \quad -\frac{1}{2}kx^2 + c.$$

As expected, this is the energy for the frictionless mass-spring system, which implies that the constant of integration, c is the initial energy, E_0 i.e.

$$\frac{1}{2}m\dot{x}^2 + \frac{1}{2}kx^2 \quad = \quad E_0. \tag{3.4.2}$$

Now, in the spirit of the Riemann sphere, consider the energy as a two dimensional function, $E(x,\dot{x}) = \frac{1}{2}m\dot{x}^2 + \frac{1}{2}kx^2$ perpendicular to the plane of the phase portrait. The energy of a mass spring system is simply a paraboloid with its stationary point at the origin, $(x,\dot{x}) = (0,0)$. Figure 3.4.3 depicts this paraboloid, as well as contour lines projected into the phase plane.

A solution to the equation (3.4.2) is seen to actually be a contour line of constant energy, E_0, on the function $E(x,\dot{x})$ and is depicted as a projection down from the energy surface, $E(x,\dot{x})$ onto the phase plane in Figure 3.4.3. Juxtapose this perspective now with the phase portrait of the system drawn directly from equation (3.4.2) and depicted in Figure 3.4.4. The two views of equation (3.4.2), that of a projection down from a higher dimensional energy function and the solutions to a planar equation (3.4.2), are congruent.

The only remaining issues are those of dissipation and applied forces, $-\int b(x,\dot{x})\dot{x}^2\mathrm{d}t + \int F\,\mathrm{d}x$. The problem with these forces is that they are, in general, dependent on time[6] and the phase portrait has time as an implicit variable. These can be dealt with by considering only the system energy

$$E_s \quad = \quad \frac{1}{2}m\dot{x}^2 + \int k(x)\,\mathrm{d}x \tag{3.4.3}$$

[6] If F is dependent only on the state x or a constant then it may be integrated and added to the system energy, $\frac{1}{2}m\dot{x}^2 + \int k(x)\,\mathrm{d}x$.

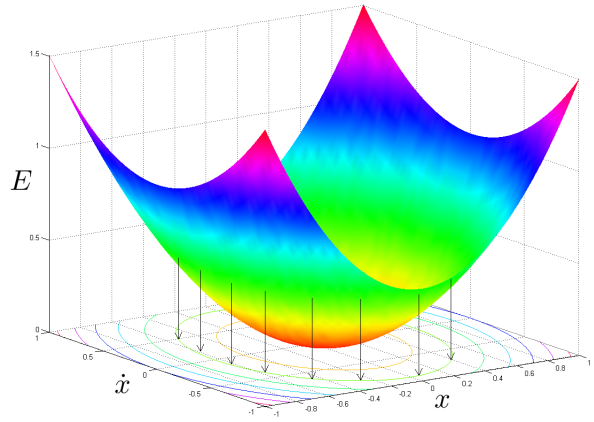

Figure 3.4.3: Energy of the mass spring system, $m = 1$ kg, $k = 2$ N/m

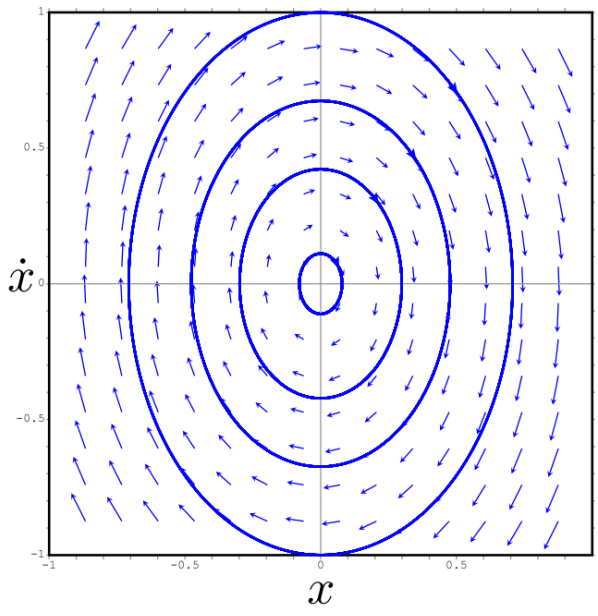

Figure 3.4.4: Phase portrait of mass spring system, $m = 1$ kg, $k = 2$ N/m

which implies that the dissipated energy and added work are

$$E_s = E_0 - \int b(x,\dot{x})\dot{x}^2 \mathrm{d}t + \int F \,\mathrm{d}x. \tag{3.4.4}$$

Consider that the contours of the energy function $E(x,\dot{x})$ are found by the intersection of a plane $E(x,\dot{x}) = const$ and $E(x,\dot{x})$ which is the first graph in Figure 3.4.5. It should be duly noted in this figure that the trajectory is a closed orbit, just as in the case of the lossless mass spring system. Now, since the system energy, E_s is varying with time, the plane of intersection $E(x,\dot{x}) = const$ must be moving up and down, depending on whether energy is being dissipated, or added into, the system. The second graph in Figure 3.4.5 shows dissipation of energy and it should be noted that the trajectory now takes on a spiral as the surface, $E(x,\dot{x})$ tightens in towards the origin. Now the phase portrait of the system with dissipation is depicted in Figure 3.4.6. It should be clear that the spiral on the surface of the paraboloid in Figure 3.4.5 will appear as Figure 3.4.6 when projected down into the $(x,\dot{x})$ plane.

Hence the trajectories in any two dimensional phase plane can be understood in terms of projections down from a higher dimensional energy function.

Note that a closed circle will look like a cosine wave when x is plotted against t . Furthermore, a spiral will look like a damped cosine in time [5, pp. 28-29]. Phase portraits are not simply a useful tool for analysing second-order, non-linear system ODE's, but are also a valuable aid for energy-shaping control. This will be further demonstrated in this dissertation.

3.5 Applications of Phase Portraits to Energy Shaping Control

In practice, one does not need to bother with solving equation (3.4.1) each time to construct the phase portrait, if the energy function is known. It can be plotted directly and furthermore, the effect of a controller (if its effect in the energy domain is known) can immediately be observed, without having to run numerous simulation experiments. Phase portrait analysis is an extremely powerful analysis tool which, when coupled with energy shaping, allows the control engineer to visually design non-linear controllers and understand their effect, globally. The only restriction is that analysis is restricted to second order, scalar, ordinary differential equations [15, Ch. 2]. Phase portraits represent the link between the energy and the time domain. By shaping the energy, the possible trajectories that can be taken by the closed loop system are altered. Those trajectories can then be compared to a known time domain performance trajectory, similar to what was done in Figure 3.4.1. Consider that for an arbitrary second order system, a spiral of known time domain performance can be started with the same initial condition and the trajectory that the closed loop system takes can be compared.

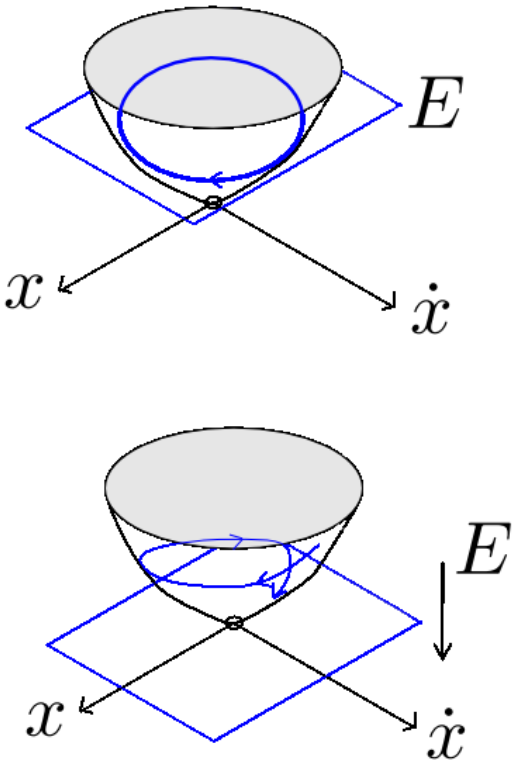

Figure 3.4.5: The effect of time-varying forces on the system energy

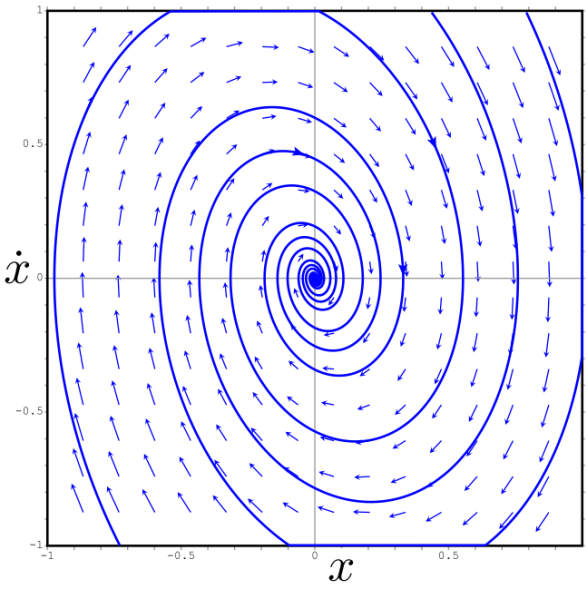

Figure 3.4.6: Mass Spring System with Viscous Damping ($b(x,\dot{x})\dot{x} = b\dot{x}$), $m = 1$ kg, $k = 2$ N/m, $b = 0.5$ Ns/m, $F = 0$ N

4 Modelling of Systems using Energy

"*For those who want some proof that physicists are human, the proof is in the idiocy of all the different units which they use for measuring energy.*"

- Richard P. Feynman, The Character of Physical Law

Energy Viewed as an Integral Transform

Inspired by *The Energy Method* taught extensively in undergraduate physics courses, the following general derivation is presented [23, Ch. 7]. What is new in this derivation is the inclusion of input force and dissipation, which, to the best of the author's knowledge, has not been done explicitly before. Note: all integral limits are from $t_0 \to t$, unless otherwise stated and all initial conditions are lumped into the value E_0, where E_0 is the initial energy of the system. This framework offers an alternative to the well known Hamiltonian and Lagrangian methods of modelling complicated systems and can be considered a generalisation of *The Energy Method.*

Given a set of N equations of motion in the prototypical form,

$$\mathbf{M}(\mathbf{x},t)\ddot{\mathbf{x}} + \mathbf{D}(\mathbf{x},\mathbf{v})\mathbf{v} + \mathbf{K}(\mathbf{x}) \quad = \quad \mathbf{G}(\mathbf{x})\mathbf{u},$$

with state $\mathbf{x} \in \mathbb{R}^N$ and $\mathbf{v} = \dot{\mathbf{x}}$, let

$$\mathbf{y} \quad := \quad \mathbf{M}(\mathbf{x},t)\ddot{\mathbf{x}} + \mathbf{D}(\mathbf{x},\mathbf{v})\mathbf{v} + \mathbf{K}(\mathbf{x}) - \mathbf{G}(\mathbf{x})\mathbf{u}.$$

Hence the prototypical model equation is reduced to $\mathbf{y} = \mathbb{O}$ with this definition.

Note that $\int (\mathbf{G}(\mathbf{x})\mathbf{u})^{\mathrm{T}}\, \mathrm{d}\mathbf{x}$ has units of work. Without loss of generality, let $\mathbf{G}(\mathbf{x})\mathbf{u} = \mathbf{F}$. The $N \times 1$ force vector, $\mathbf{F}$, may be zero for some row entries, which would correspond to co-ordinates that are not directly acted upon via the input forces.

Now the total energy of the system, including all loss and gain appears as an integral transform[1] via

$$\mathscr{E}\{\mathbf{y}\} \quad = \quad \int \mathbf{v}^T \mathbf{y}\, \mathrm{d}t.$$

[1] Juxtapose this with the well known Fourier Transform $\mathscr{F}\{y\} = \int e^{-j\omega t} y\, \mathrm{d}t$, where the integral is taken over all time from $-\infty \to \infty$

Note that the units of each row of $\mathbf{y}$ are identical to each row of the generalised force vector, $\mathbf{F}$ as per definition. As per the definition, $\int \mathbf{F}^{\mathrm{T}}\,\mathrm{d}\mathbf{x}$ has units of work. This integral may be transformed via the chain rule in calculus,

$$\begin{aligned}\int \mathbf{F}^{\mathrm{T}}\mathrm{d}\mathbf{x} &= \int \mathbf{F}^{\mathrm{T}}\frac{\mathrm{d}\mathbf{x}}{\mathrm{d}t}\mathrm{d}t \\ &= \int \mathbf{v}^{\mathrm{T}}\mathbf{F}\,\mathrm{d}t.\end{aligned}$$

Note that the term, $\mathbf{F}^{\mathrm{T}}\mathbf{v}$, is a scalar and hence $\mathbf{F}^{\mathrm{T}}\mathbf{v} = \mathbf{v}^{\mathrm{T}}\mathbf{F}$.

Including each term in $\mathbf{y}$ into the work integral leads to

$$\int \mathbf{v}^{\mathrm{T}}\mathbf{y}\,\mathrm{d}t = \int \mathbf{v}^{\mathrm{T}}\mathbf{M}(\mathbf{x},t)\ddot{\mathbf{x}}\,\mathrm{d}t + \int \mathbf{v}^{\mathrm{T}}\mathbf{D}(\mathbf{x},\mathbf{v})\mathbf{v}\,\mathrm{d}t + \int \mathbf{v}^{\mathrm{T}}\mathbf{K}(\mathbf{x})\,\mathrm{d}t - \int \mathbf{v}^{\mathrm{T}}\mathbf{F}\,\mathrm{d}t + E_0$$

Each term will be looked at individually:

Firstly, the "spring-like" term can be re-written as

$$\int \mathbf{v}^{\mathrm{T}}\mathbf{K}(\mathbf{x})\,\mathrm{d}t = \int \mathbf{K}(\mathbf{x})^{\mathrm{T}}\,\mathrm{d}\mathbf{x},$$

where the chain rule was again used to transform the integral. It is clear that this is the total work done by moving N position dependent springs[2] with force equal to $\mathbf{K}(\mathbf{x})$ through a displacement $\mathrm{d}\mathbf{x}$. This work is given the name of potential energy which is stored in the system by virtue of its displacement and is recovered when the system is allowed to return to rest [23, Ch. 8].

The second term is given by

$$\int \mathbf{v}^{\mathrm{T}}\mathbf{D}(\mathbf{x},\mathbf{v})\mathbf{v}\,\mathrm{d}t,$$

which is, in part, the time integral of the power lost due to internal heating of the system [23, Ch. 7.7 , 8.4]. The other part of this term will also contain the Coriolis and Centripetal forces present [15, pp. 393-403]. It must be stressed that this term is *not* only a representation of loss of energy of the system. It will be shown that it contains terms that represent energy exchange within the system itself.

Lastly, the "mass-like" term, $\mathbf{M}(\mathbf{x},t)$ must be symmetric and positive definite [10]. This is because it is used in the kinetic energy, and if it didn't have these properties then a negative kinetic energy could be possible [10]. A negative kinetic energy is disallowed [10]. The integral transform for the "mass-like" term is

$$\begin{aligned}\int \mathbf{v}^{\mathrm{T}}\mathbf{M}(\mathbf{x},t)\ddot{\mathbf{x}}\,\mathrm{d}t &= \mathbf{v}^{\mathrm{T}}\mathbf{M}(\mathbf{x},t)\mathbf{v} - \int \mathbf{v}^{\mathrm{T}}\dot{\mathbf{M}}(\mathbf{x},t)\mathbf{v}\,\mathrm{d}t - \int \ddot{\mathbf{x}}^{\mathrm{T}}\mathbf{M}(\mathbf{x},t)\mathbf{v}\mathrm{d}t \\ 2\int \mathbf{v}^{\mathrm{T}}\mathbf{M}(\mathbf{x},t)\ddot{\mathbf{x}}\,\mathrm{d}t &= \mathbf{v}^{\mathrm{T}}\mathbf{M}(\mathbf{x},t)\mathbf{v} - \int \mathbf{v}^{\mathrm{T}}\dot{\mathbf{M}}(\mathbf{x},t)\mathbf{v}\,\mathrm{d}t \\ \int \mathbf{v}^{\mathrm{T}}\mathbf{M}(\mathbf{x},t)\ddot{\mathbf{x}}\,\mathrm{d}t &= \frac{1}{2}\mathbf{v}^{\mathrm{T}}\mathbf{M}(\mathbf{x},t)\mathbf{v} - \frac{1}{2}\int \mathbf{v}^{\mathrm{T}}\dot{\mathbf{M}}(\mathbf{x},t)\mathbf{v}\,\mathrm{d}t\end{aligned}$$

[2] In fact any potential derived force that is displaced from equilibrium can be modelled using this equation. The term "potential derived" force was avoided so that a more concrete example (springs) could be offered.

where integration by parts has been used[3] and the repeated integral, $\int \ddot{\mathbf{x}}^{\mathrm{T}}\mathbf{M}(\mathbf{x},t)\mathbf{v}\,\mathrm{d}t = \int \mathbf{v}^{\mathrm{T}}\mathbf{M}(\mathbf{x},t)\ddot{\mathbf{x}}\,\mathrm{d}t$, is factored out. This is the energy stored in the system by virtue of its motion, called the kinetic energy of the system and is a direct consequence of the well known work-kinetic energy theorem [23, Ch. 7.5]. The other term dependent on the time rate of change of the mass is not normally associated with the kinetic energy of the system. This term will be dealt with in the sequel.

Hence, each term in the integral is a recognisable energy term and the total energy of a system is the sum of all the individual energies in the system, which means,

$$\mathscr{E}\{\mathbf{y}\} \quad = \quad \int \mathbf{v}^{\mathrm{T}}\mathbf{y}\,\mathrm{d}t. \tag{4.0.1}$$

Given that the criteria for dimensional consistency are satisfied, one can transform any set of such equations from the time domain into the energy domain.

To reverse this and transform from the energy domain back to the time domain, it is necessary to solve

$$\frac{\mathrm{d}}{\mathrm{d}t}\mathscr{E}\{\mathbf{y}\} \quad = \quad \mathbb{O}.$$

This is simply a statement of the conservation of energy, that is that the total stored energy (kinetic plus potential) plus internal energy minus the work done on the system does not change with time.

Proof

From the definition,

$$\frac{\mathrm{d}}{\mathrm{d}t}\mathscr{E}\{\mathbf{y}\} \quad = \quad \frac{\mathrm{d}}{\mathrm{d}t}\int \mathbf{v}^{\mathrm{T}}\mathbf{y}\,\mathrm{d}t.$$

Using the fundamental theorem of calculus,

$$\frac{\mathrm{d}}{\mathrm{d}t}\int \mathbf{v}^{\mathrm{T}}\mathbf{y}\,\mathrm{d}t \quad = \quad \mathbf{v}^{\mathrm{T}}\mathbf{y}.$$

Now setting this equal to zero results in

$$\mathbf{v}^{\mathrm{T}}\mathbf{y} \quad = \quad \mathbb{O}$$

which implies that either: every generalised velocity, $\mathbf{v} = 0$ for all time; or each co-efficient, $\mathbf{y} = \mathbb{O}$. By definition $\mathbf{y} = \mathbb{O}$ are the equations of motion for the system. ■

There are two matters outstanding; the $\frac{1}{2}\int \mathbf{v}^{\mathrm{T}}\dot{\mathbf{M}}(\mathbf{x},t)\mathbf{v}\,\mathrm{d}t$ term and the exact description of $\mathbf{D}(\mathbf{x},\mathbf{v})$. At this point it is worth mentioning that what we choose to call the various energies is artificial and a matter of convenience. An example illustrating this fact is the energy associated with an object's temperature. This energy is not available to do any work

[3] $\int fgh' = fgh - \int fg'h - \int f'gh$

by itself and is sometimes called "heat". However, if there is another object nearby with a different temperature, then one can construct a heat engine which can do useful work. In this case the energy in the first object can be thought of as a form of potential energy, relative to the second object. The energy content in the first object has not changed, it is only the label that the user applies to it that has changed. This simple example illustrates the point that the partitioning of the system energy is a matter of convenience. This has a direct consequence on the $\frac{1}{2}\int \mathbf{v}^{\mathrm{T}}\dot{\mathbf{M}}(\mathbf{x},t)\mathbf{v}\,\mathrm{d}t$ term as well as the interpretation of the energy associated with the $\mathbf{D}(\mathbf{x},\mathbf{v})$ term. The energy $\frac{1}{2}\int \mathbf{v}^{\mathrm{T}}\dot{\mathbf{M}}(\mathbf{x},t)\mathbf{v}\,\mathrm{d}t$, is complicated since it can arise due to the reconfiguration of the mass elements in the system (since $\mathbf{M}$ is a function of $\mathbf{x}$) or due to genuine mass loss (for instance in a thrust powered aircraft). In the first case the energy does not leave the system and in the second case, it does and is hence not recoverable. Thus one can call it both an internal energy reshuffling or a dissipation term, depending on the context. The decomposition of $\mathbf{D}(\mathbf{x},\mathbf{v})$ is addressed next. It is organised into a convenient form and it should be noted again, that the reader may choose to represent it differently.

Decomposition of the $\mathbf{D}(\mathbf{x},\mathbf{v})$ term

The system energy E_s is defined here as the kinetic plus the potential energy of the system i.e.

$$E_s \;:=\; \frac{1}{2}\mathbf{v}^{\mathrm{T}}\mathbf{M}(\mathbf{x},t)\mathbf{v} + \int \mathbf{K}(\mathbf{x})^{\mathrm{T}}\,\mathrm{d}\mathbf{x}. \tag{4.0.2}$$

This is the energy that is, in principle, recoverable and is an artificial partitioning of the energy of the system. The only way the system can gain energy is via the input and the only way the system can lose energy is via dissipation into the environment, mathematically this means that

$$\frac{\mathrm{d}}{\mathrm{d}t}E_s \;=\; -\mathbf{v}^{\mathrm{T}}\mathbf{R}(\mathbf{x},\mathbf{v})\mathbf{v} + \mathbf{v}^{\mathrm{T}}\mathbf{G}(\mathbf{x})\mathbf{u} + -\mathbf{v}^{\mathbf{T}}\mathbf{J}(\mathbf{x},\mathbf{v})\mathbf{v}. \tag{4.0.3}$$

Note that the term $\mathbf{R}(\mathbf{x},\mathbf{v})$ is symmetric and positive definite and is used to capture the power loss. The extra term representing loss-less internal power transformations, $\mathbf{J}(\mathbf{x},\mathbf{v})$, is skew symmetric i.e. $\mathbf{v}^{\mathrm{T}}\mathbf{J}(\mathbf{x},\mathbf{v})\mathbf{v} = 0$, which means that nothing has been added to the physical power equation.

This is a purely physical argument and is not derived from other considerations.

Furthermore, this term is different from the $\mathbf{D}(\mathbf{x},\mathbf{v})$ present in the prototypical model. This was done to allow for Coriolis and Centripetal forces in the spirit of Robotics [15, pp. 393-403][14], include dissipation as is done in IDAPBC [19, 18] and include the $\frac{1}{2}\int \mathbf{v}^{\mathrm{T}}\dot{\mathbf{M}}(\mathbf{x},t)\mathbf{v}\,\mathrm{d}t$ as is done in [14].

Looking at the power of the physical system, $\frac{\mathrm{d}}{\mathrm{d}t}E_s$, which is the time derivative of eq. (4.0.2) gives

$$\frac{\mathrm{d}}{\mathrm{d}t}E_s \;=\; \mathbf{v}^{\mathrm{T}}\mathbf{M}(\mathbf{x},t)\dot{\mathbf{v}} + \mathbf{v}^{T}\frac{\dot{\mathbf{M}}(\mathbf{x},t)}{2}\mathbf{v} + \mathbf{v}^{T}\mathbf{K}(\mathbf{x}),$$

where the chain rule has been used on the potential function integral, $\int \mathbf{K}(\mathbf{x})^{\mathrm{T}}\,\mathrm{d}\mathbf{x}$, and the transpose has been taken of the resulting 1×1 entity, namely $\mathbf{K}(\mathbf{x})^{\mathrm{T}}\mathbf{v} = \mathbf{v}^{\mathrm{T}}\mathbf{K}(\mathbf{x})$.

Now using the prototypical model equation, eq (3.1.1) and substituting in for $\mathbf{M}(\mathbf{x},t)\ddot{\mathbf{x}}$

$$\begin{aligned}\frac{\mathrm{d}}{\mathrm{d}t}E_s &= \underbrace{\mathbf{v}^{\mathrm{T}}\mathbf{G}(\mathbf{x})\mathbf{u}-\mathbf{v}^{\mathrm{T}}\mathbf{K}(\mathbf{x})-\mathbf{v}^{\mathrm{T}}\mathbf{D}(\mathbf{x},\mathbf{v})\mathbf{v}}_{\mathbf{v}^{\mathrm{T}}\mathbf{M}(\mathbf{x},t)\ddot{\mathbf{x}}} \\ &\quad +\mathbf{v}^{\mathrm{T}}\frac{\dot{\mathbf{M}}(\mathbf{x},t)}{2}\mathbf{v}+\mathbf{v}^{\mathrm{T}}\mathbf{K}(\mathbf{x}) \\ &= \mathbf{v}^{\mathrm{T}}\mathbf{G}(\mathbf{x})\mathbf{u}-\mathbf{v}^{\mathrm{T}}\mathbf{D}(\mathbf{x},\mathbf{v})\mathbf{v}+\mathbf{v}^{\mathrm{T}}\frac{\dot{\mathbf{M}}(\mathbf{x},t)}{2}\mathbf{v}. \qquad (4.0.4)\end{aligned}$$

Therefore by making eq. (4.0.3) equal to eq. (4.0.4),

$$\begin{aligned}\mathbf{v}^{\mathrm{T}}\mathbf{G}(\mathbf{x})\mathbf{u}-\mathbf{v}^{\mathrm{T}}\mathbf{D}(\mathbf{x},\mathbf{v})\mathbf{v}+\mathbf{v}^{\mathrm{T}}\frac{\dot{\mathbf{M}}(\mathbf{x},t)}{2}\mathbf{v} &= -\mathbf{v}^{\mathrm{T}}\mathbf{R}(\mathbf{x},\mathbf{v})\mathbf{v}+\mathbf{v}^{\mathrm{T}}\mathbf{G}(\mathbf{x})\mathbf{u}-\mathbf{v}^{\mathrm{T}}\mathbf{J}(\mathbf{x},\mathbf{v})\mathbf{v} \\ \mathbf{v}^{\mathrm{T}}\mathbf{D}(\mathbf{x},\mathbf{v})\mathbf{v} &= \mathbf{v}^{\mathrm{T}}\mathbf{R}(\mathbf{x},\mathbf{v})\mathbf{v}+\mathbf{v}^{\mathrm{T}}\frac{\dot{\mathbf{M}}(\mathbf{x},t)}{2}\mathbf{v}+\mathbf{v}^{\mathrm{T}}\mathbf{J}(\mathbf{x},\mathbf{v})\mathbf{v}\end{aligned}$$

which is to say that

$$\mathbf{D}(\mathbf{x},\mathbf{v}) = \mathbf{J}(\mathbf{x},\mathbf{v})+\mathbf{R}(\mathbf{x},\mathbf{v})+\frac{1}{2}\dot{\mathbf{M}}(\mathbf{x},t). \qquad (4.0.5)$$

This decomposition of $\mathbf{D}(\mathbf{x},\mathbf{v})$ is hence an amalgamation of [18, 14].

This result is a mathematical description of what is intuitive from physics, which is to say that the power flow in the system is the sum of the power gained via the input and the power lost due to dissipation.

Stationary points

An important feature of the system energy is that the stationary points of the energy function, $\nabla E = 0$, are the equilibrium points of the system [6]. Hence, if the energy function is shaped, so too are the stationary points. In order to determine the stability of the stationary points, a variety of techniques may be used: stability of the linearised system about that point as in Lyapunov's First method [45, 30]; or La Salle's invariance principle as described in [15, Chapter 3.4.3]; or the well known result about the sign of $\nabla^2 E$ around the stationary point i.e. if $\nabla^2 E > 0$ around the stationary point, it is a local minimum and hence stable. The value of energy-based reasoning is that it is not an abstract mathematical concept, but something that is used daily by engineers to reason about the physical world. Thus, by placing the design of controllers in this domain, all of the insight and experience with the system to be controlled is automatically included in the design considerations.

4.1 Modelling using the Conservation of Energy

The purpose of the previous derivation is to present an alternative to the well known Hamiltonian and Lagrangian methods of modelling. This alternative is a generalisation of the *The Energy Method* which exploits the conservation of energy in order to derive the equations of motion [23, Ch. 7].

The basic idea is as follows:

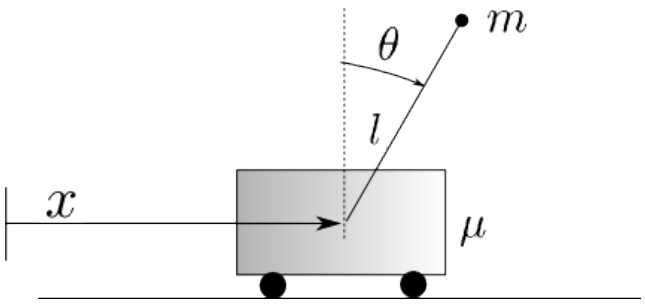

Figure 4.1.1: Inverted Pendulum on a Cart System

1. Describe the kinetic and potential energy in terms of co-ordinates appropriate to the problem; call the sum E_s.
2. Compute $\frac{\mathrm{d}}{\mathrm{d}t}E_s$.
3. Describe power loss, $-\mathbf{v}^{\mathrm{T}}\mathbf{R}(\mathbf{x},\mathbf{v})\mathbf{v}$, and power gain, $\mathbf{v}^{\mathrm{T}}\mathbf{G}(\mathbf{x})\mathbf{u}$, into the system and let it equal $\frac{\mathrm{d}}{\mathrm{d}t}E_s$.
4. Include known work-less forces in the power loss equation via $-\mathbf{v}^{\mathrm{T}}\mathbf{J}(\mathbf{x},\mathbf{v})\mathbf{v}$.
5. Solve the resulting equation power equation: $\frac{\mathrm{d}}{\mathrm{d}t}E_s = -\mathbf{v}^{\mathrm{T}}\mathbf{R}(\mathbf{x},\mathbf{v})\mathbf{v} - \mathbf{v}^{\mathrm{T}}\mathbf{J}(\mathbf{x},\mathbf{v})\mathbf{v} + \mathbf{v}^{\mathrm{T}}\mathbf{G}(\mathbf{x})\mathbf{u}$.

Two possible solutions are: either the equations of motion (eq (3.1.1)) or all velocities equal zero for all time ($\mathbf{v} = \mathbb{O}, \forall t > 0$), as proved above. Two characteristic examples follow which illustrate the method.

Energy Domain to Time Domain Example: Pendulum on a Cart

Consider the classical pendulum on a cart system with cart position x, cart velocity v, pendulum angle θ, pendulum angular velocity ω, pendulum length l, pendulum mass m and cart mass μ depicted in Figure 4.1.1.

1.) To begin, the position of the mass of the pendulum in the lab frame is given by

$$r(t) \quad = \quad [x + l\sin(\theta), l\cos(\theta)],$$

with generalised velocity,

$$\dot{r}(t) \quad = \quad [v + l\cos(\theta)\omega, -l\sin(\theta)\omega].$$

The Kinetic energy of the pendulum T_p is given by

$$\begin{aligned} T_p &= \frac{1}{2}m\dot{r}\cdot\dot{r} \\ &= \frac{1}{2}mv^2 + \frac{1}{2}ml^2\omega^2 + ml\cos(\theta)\omega v. \end{aligned}$$

The Kinetic energy of the cart T_c is given by

$$T_c \quad = \quad \frac{1}{2}\mu v^2.$$

Let $ml^2 = I$ which is immediately seen to be the moment of inertia of the rod about the end tip and let $\gamma = ml\cos(\theta)$ which is the coupling between the two degrees of freedom of the cart and pendulum system.

Now the total Kinetic energy, $T_p + T_c$, for the cart pendulum system is,

$$T = \frac{1}{2}mv^2 + \frac{1}{2}I\omega^2 + \gamma\omega v + \frac{1}{2}\mu v^2.$$

It is imperative at this point to describe the kinetic energy using matrix notation [4]. To begin, choose the generalised co-ordinate as $\mathbf{x} = \begin{bmatrix} x & \theta \end{bmatrix}^{\mathbf{T}}$ and hence the generalised velocity is $\mathbf{v} = \begin{bmatrix} v & \omega \end{bmatrix}^{\mathbf{T}} = \dot{\mathbf{x}}$. The mass matrix is therefore,

$$\mathbf{M}(\mathbf{x},t) = \begin{pmatrix} m+\mu & \gamma \\ \gamma & I \end{pmatrix},$$

such that

$$T = \frac{1}{2}\mathbf{v}^{\mathbf{T}}\mathbf{M}(\mathbf{x},t)\mathbf{v}.$$

The potential energy of the system with respect to the down position of the pendulum is given by,

$$\begin{aligned} U &= mgl(1+\cos(\theta)) \\ &= mgl + g\gamma. \end{aligned}$$

In integral form the potential energy is,

$$U = \int \mathbf{K}(\mathbf{x})^{\mathbf{T}} \mathrm{d}\mathbf{x},$$

which produces the well known result,

$$\begin{aligned} \mathbf{K}(\mathbf{x}) &= \frac{\partial U}{\partial \mathbf{x}} \\ &= \begin{pmatrix} 0 \\ g\frac{\partial \gamma}{\partial \theta} \end{pmatrix}. \end{aligned}$$

This is the potential derived force.

Now the system energy, E_s is

$$\begin{aligned} E_s &= T + U \\ &= \frac{1}{2}\mathbf{v}^{\mathbf{T}}\mathbf{M}(\mathbf{x},t)\mathbf{v} + \int \mathbf{K}(\mathbf{x})^{\mathbf{T}} \mathrm{d}\mathbf{x}. \end{aligned}$$

2.) Computing $\frac{\mathrm{d}}{\mathrm{d}t}E_s$ is now a simple matter and results in,

[4] It is possible to follow the procedure without matrices, however substantially more algebra is needed.

$$\frac{\mathrm{d}}{\mathrm{d}t}E_s \quad = \quad \mathbf{v}^{\mathbf{T}}\mathbf{M}(\mathbf{x},t)\dot{\mathbf{v}} + \frac{1}{2}\mathbf{v}^{\mathbf{T}}\dot{\mathbf{M}}(\mathbf{x},t)\mathbf{v} + \mathbf{v}^{\mathbf{T}}\mathbf{K}(\mathbf{x})$$

3.) The power loss due to frictional forces is modelled using viscous damping,

$$\mathbf{v}^{\mathbf{T}}\mathbf{R}(\mathbf{x},\mathbf{v})\mathbf{v} \quad = \quad \mathbf{v}^{\mathbf{T}}\begin{pmatrix} B & 0 \\ 0 & B_r \end{pmatrix}\mathbf{v},$$

where B is the friction co-efficient for the x co-ordinate and B_r is the friction co-efficient for the θ co-ordinate. Notice that there is room to include cross-coupling between the friction co-ordinates in the off-diagonal terms. The only proviso is that the resulting matrix must be positive definite. The input forces enter only in the x co-ordinate and hence the power gained by the system is given by,

$$\mathbf{v}^{\mathbf{T}}\mathbf{G}(\mathbf{x})\mathbf{u} \quad = \quad \mathbf{v}^{\mathbf{T}}\begin{pmatrix} 1 & 0 \\ 0 & 1 \end{pmatrix}\begin{pmatrix} u \\ 0 \end{pmatrix},$$

where u is the applied force on the cart.

4.) There is no other shuffling of energy within the system and hence $\mathbf{J}(\mathbf{x},\mathbf{v}) = \mathbf{0}$.

5.) Using the result from step 2 and 3, the resulting power equation to be solved is,

$$\mathbf{v}^{\mathbf{T}}\mathbf{M}(\mathbf{x},t)\dot{\mathbf{v}} + \frac{1}{2}\mathbf{v}^{\mathbf{T}}\dot{\mathbf{M}}(\mathbf{x},t)\mathbf{v} + \mathbf{v}^{\mathbf{T}}\mathbf{K}(\mathbf{x}) \quad = \quad -\mathbf{v}^{\mathbf{T}}\mathbf{R}(\mathbf{x},\mathbf{v})\mathbf{v} + \mathbf{v}^{\mathbf{T}}\mathbf{G}(\mathbf{x})\mathbf{u},$$

which has the solutions

$$\mathbf{M}(\mathbf{x},t)\ddot{\mathbf{x}} + \mathbf{D}(\mathbf{x},\mathbf{v})\mathbf{v} + \mathbf{K}(\mathbf{x}) \quad = \quad \mathbf{G}(\mathbf{x})\mathbf{u},$$

or $\mathbf{v} = \mathbb{O}$, $\forall t$, recalling that $\dot{\mathbf{v}} = \ddot{\mathbf{x}}$.

Each term is given explicitly by

$$\mathbf{M}(\mathbf{x},t)\ddot{\mathbf{x}} \quad = \quad \begin{pmatrix} m+\mu & \gamma \\ \gamma & I \end{pmatrix}\begin{pmatrix} \ddot{x} \\ \ddot{\theta} \end{pmatrix}$$

$$\mathbf{D}(\mathbf{x},\mathbf{v})\mathbf{v} \quad = \quad \begin{pmatrix} B & \frac{1}{2}\frac{\partial\gamma}{\partial\theta}\omega \\ \frac{1}{2}\frac{\partial\gamma}{\partial\theta}\omega & B_r \end{pmatrix}\begin{pmatrix} v \\ \omega \end{pmatrix}$$

$$\mathbf{K}(\mathbf{x}) \quad = \quad \begin{pmatrix} 0 \\ g\frac{\partial\gamma}{\partial\theta} \end{pmatrix}$$

and

$$\mathbf{G}(\mathbf{x})u \quad = \quad \begin{pmatrix} 1 \\ 0 \end{pmatrix}u$$

with $u = F$ and $\gamma = ml\cos(\theta)$. These are exactly the equations of motion derived by other means [7, 38].

4.2 Time Domain to Energy Domain

The beauty of eq. (4.0.1) is that it is possible to reverse the modelling procedure, which is to say that one can take the model equations and analyse the energy structure present. This can be done uniquely as follows:

Represent the system in prototypical model form i.e. eq. (3.1.1).

Decompose the $\mathbf{D}(\mathbf{x},\mathbf{v})$ in terms of $\mathbf{R}(\mathbf{x},\mathbf{v})$and $\mathbf{J}(\mathbf{x},\mathbf{v})$.

Compute $\int \mathbf{v}^T\mathbf{y}\,\mathrm{d}t$.

The various partitions of energy should be evident from the previous sections. Recall that the $\mathbf{J}(\mathbf{x},\mathbf{v})$ matrix does not add anything to the power equation and hence would be lost if the integral in step 3 was performed without first finding $\mathbf{J}(\mathbf{x},\mathbf{v})$ in the time domain. This is the term that uniquely specifies the energy structure of the system since it is lost in general.

Time Domain to Energy Domain Example: DC Motor

This example serves to show that step 2 is of paramount importance when computing eq. (4.0.1), as claimed. The well known DC motor model, with: moment of inertia, J_m; angle of shaft, θ; angular speed of shaft, ω; inductance of stator, L; charge in stator circuit, q; current in stator, i; viscous rotational friction, B_r; resistance in stator circuit, R_r; input voltage, V and motor constant K_m. Describing the system with $\mathbf{x} = \begin{bmatrix} \theta & q \end{bmatrix}^T$ and $\mathbf{v} = \begin{bmatrix} \omega & i \end{bmatrix}^T$,

the model equations are

$$\frac{\mathrm{d}}{\mathrm{d}t}\begin{pmatrix} J_m\omega \\ Li \end{pmatrix} = \begin{pmatrix} -B_r & K_m \\ -K_m & -R_r \end{pmatrix}\begin{pmatrix} \omega \\ i \end{pmatrix} + \begin{pmatrix} 0 \\ 1 \end{pmatrix} V,$$

and can be put into prototypical form

$$\mathbf{M}\dot{\mathbf{x}} + \mathbf{D}\mathbf{v} + \mathbf{K}(\mathbf{x}) = \mathbf{G}u.$$

1.) The matrices of the prototypical form are,

$$\mathbf{M}\dot{\mathbf{x}} = \begin{pmatrix} J_m & 0 \\ 0 & L \end{pmatrix}\frac{\mathrm{d}}{\mathrm{d}t}\begin{pmatrix} \omega \\ i \end{pmatrix},$$

$$\mathbf{D}\mathbf{v} = \begin{pmatrix} B_r & -K_m \\ K_m & R_r \end{pmatrix}\begin{pmatrix} \omega \\ i \end{pmatrix},$$

$$\mathbf{K}(\mathbf{x}) = \begin{pmatrix} 0 \\ 0 \end{pmatrix},$$

and

$$\mathbf{G}u = \begin{pmatrix} 0 \\ 1 \end{pmatrix} V.$$

2.) The decomposition to be followed is $\mathbf{D} = \mathbf{J} + \mathbf{R} + \frac{1}{2}\dot{\mathbf{M}}$. Due to the constant $\mathbf{M}$ the term $\frac{1}{2}\dot{\mathbf{M}}$ is a non-issue. The $\mathbf{J}$ matrix will not appear in the energy of the system. Hence when trying to go from the energy domain back to the time domain, $\mathbf{J}$ will be missing in the dynamics.

Observe that by computing the integral transform, $\int \mathbf{v}^{\mathrm{T}}\,\mathrm{d}t$, without completing step 2, the result is,

$$\begin{aligned} E_s &= \frac{1}{2}\mathbf{v}^{\mathrm{T}}\mathbf{M}\mathbf{v} + 0 \\ &= E_0 - \int \mathbf{v}^{\mathrm{T}}\mathbf{D}\mathbf{v}\,\mathrm{d}t + \int \mathbf{v}^{\mathrm{T}}\mathbf{G}u\,\mathrm{d}t \end{aligned}$$

therefore

$$\begin{aligned} \frac{\mathrm{d}}{\mathrm{d}t}E_s &= \mathbf{v}^{\mathrm{T}}\mathbf{M}\dot{\mathbf{v}} \\ &= -B_r\omega^2 - R_r i^2 + \mathbf{v}^{\mathrm{T}}\mathbf{G}u \end{aligned}$$

which upon solving this power equation leads to

$$\mathbf{M}\dot{\mathbf{v}} = \begin{pmatrix} -B_r & 0 \\ 0 & -R \end{pmatrix}\mathbf{v} + \begin{pmatrix} 0 \\ 1 \end{pmatrix}V$$

and it is clear that the loss-less power transformation between current and angular velocity through K_m is lost. This is because $\mathbf{J}$ does not store or leak energy and hence does not participate in the energy accounting. Decomposing $\mathbf{D}$ leads to

$$\begin{aligned} \mathbf{R} &= \frac{1}{2}\left((\mathbf{D} - \frac{1}{2}\dot{\mathbf{M}}) + (\mathbf{D} - \frac{1}{2}\dot{\mathbf{M}})^{\mathrm{T}}\right) \\ &= \begin{pmatrix} B_r & 0 \\ 0 & R_r \end{pmatrix} \end{aligned}$$

as expected and

$$\begin{aligned} \mathbf{J} &= \frac{1}{2}\left((\mathbf{D} - \frac{1}{2}\dot{\mathbf{M}}) - (\mathbf{D} - \frac{1}{2}\dot{\mathbf{M}})^{\mathrm{T}}\right) \\ &= \begin{pmatrix} 0 & -K_m \\ K_m & 0 \end{pmatrix} \end{aligned}$$

which was lost when taking the product $\mathbf{v}^{\mathrm{T}}\mathbf{D}\mathbf{v}$. The reader is reminded again that $\mathbf{v}^{\mathrm{T}}\mathbf{J}\mathbf{v} = 0$, for any $\mathbf{v}$, due to $\mathbf{J}$ being skew-symmetric.

3.) Keeping this in mind leads to the energy equation

$$\begin{aligned} E_s &= \frac{1}{2}\mathbf{v}^{\mathrm{T}}\mathbf{M}\mathbf{v} + 0 \\ &= E_0 - \int \mathbf{v}^{\mathrm{T}}\mathbf{R}\mathbf{v}\,\mathrm{d}t - \int \mathbf{v}^{\mathrm{T}}\mathbf{J}\mathbf{v}\,\mathrm{d}t + \int \mathbf{v}^{\mathrm{T}}\mathbf{G}\mathbf{u}\,\mathrm{d}t \end{aligned}$$

which will yield the correct equations of motion by differentiating with respect to time and solving the power equation.

5 Energy-Shaping Methods for Control

"*A method is a trick I use twice.*"
- George Polya

Energy-Shaping will fundamentally consist of either changing the closed-loop energy or the closed-loop power or both. Energy-Balancing is a general methodology that *matches* an open-loop energy structure to a closed-loop energy structure, as will be shown. Power-shaping on the other hand, asymptotically approaches a desired closed-loop energy structure. The problem remains with *how* to choose a desired closed-loop energy. This is addressed in the three constructive techniques used to assign a desired closed-loop energy structure. These techniques are: controller interpolation via a common Lyapunov function; energy-shaping Robot control and Interconnection and Damping Assignment Passivity Based Control (IDAPBC). All of these techniques require a controller that has full state access and is at least as computationally complex as the plant, in line with the Controller Complexity principle.

At the end of this section, a simple physical system with rich dynamics, namely the simple pendulum, under the influence of gravity with a torque acting on a frictionless hinge is modelled and described. The control algorithms will be *tested* on this system, however they will be *developed* for the prototypical model and hence have wide applicability.

Energy Balancing

The basic idea of energy balancing is to have the system energy appear as some desired energy in closed loop [6]. The presentation of this idea is modified from the conventional energy balancing controllers, which are presented in the Controlled Lagrangian and IDAPBC framework [6, 26]. The presentation here is original and has an intuitive interpretation. Furthermore, it follows on naturally to the power shaping ideas of [10].

The equivalence of the system energy, E_s, with a desired energy, E_d, is mathematically

$$E_s = E_d,$$

which is to say that

$$\begin{aligned} \tilde{E} &= E_s - E_d \\ &= 0. \end{aligned}$$

The detailed presentation and design using Energy Balancing is presented in 5.1.

Power Shaping

The idea of power shaping presented here is originally presented as an "energy swing up" controller by [11], and further presented in [10]. See [12] for the idea of power shaping as applied to the process control problem of an unstable Continuously Stirred Tank Reactor.

The basic idea is to add energy into the system until the system reaches the energy level which corresponds to a particular desired trajectory in the state space [10, 11]. It was shown in Chapter 3.4 how energy relates to time domain performance using phase portraits as a tool.

Explicitly (for the lossless case): given the system energy, E_s, and desired *constant* energy associated with a certain system behaviour, E_d, the rate of change of the difference $E_s - E_d = \tilde{E}$ is

$$\frac{\mathrm{d}}{\mathrm{d}t}\tilde{E} = \dot{E}_s,$$

because E_d is a constant. Now

$$\dot{E}_s = Fv$$

which is simply the input power, as expected in the lossless case. There is a valuable trick which [11] employed. The trick is to let

$$F = -\kappa_p \tilde{E} v$$

where $\kappa_p > 0$ is a constant and implies that

$$\begin{aligned} \dot{E}_s &= \frac{\mathrm{d}}{\mathrm{d}t}\tilde{E} \\ &= -\kappa_p \tilde{E} v^2. \end{aligned}$$

Using contraction analysis,

$$\delta\dot{\tilde{E}} = -\kappa_p v^2 \, \delta\tilde{E},$$

is contracting therefore the control law $F = -\kappa_p \tilde{E} v$ will exponentially cause $\tilde{E} \to 0$ i.e. the system energy $E_s \to E_d$.

An integrator in the power shaping control law has been included to allow for robust performance in the presence of model uncertainty, as well as removing the problem of dissipation. This idea was inspired by the understanding of energy in terms of phase portraits, as well as the well known problem of disturbance rejection in linear control. Furthermore, the idea has been extended into many degree of freedom systems by vectorising this result for the prototypical system.

The detailed method and design using Power shaping is in Chapter 5.2.

The three constructive techniques are briefly described next.

Constructive Techniques for Energy-Shaping

Controller Interpolation via a Common Lyapunov function

The main idea was presented in [13, 32] as a Heuristic Fuzzy Logic controller. The basic idea is first to define regions in the state space, $\mathbf{x} \in \mathbb{R}^N$ using fuzzy membership functions $\mu_i(\mathbf{x}) : \left\{\mathbb{R}^N \to [0,1]\right\}$ [13, 32]. Then using a Lyapunov function, $V(\mathbf{x})$, choose a control input $\mathbf{u}_i(\mathbf{x})$ which makes the derivative of the Lyapunov function, $\dot{V}(\mathbf{x})$ negative definite *in that region* [13, 32]. Using the *same* Lyapunov function, look at each of the defined regions in turn and choose a control input function which makes each region's $\dot{V}(\mathbf{x})$ negative definite [13, 32]. Finally, each of the functions are interpolated using the weighted sum defuzzification method

$$\mathbf{u}(\mathbf{x}) \quad = \quad \frac{\sum_i \mu_i(\mathbf{x})\mathbf{u}_i(\mathbf{x})}{\sum_i \mu_i(\mathbf{x})},$$

where $\mathbf{u}(\mathbf{x})$ is the total input to the system [13, 32]. Since each controller stabilises each region of the state space, their interpolation via the weighted sum defuzzification method, stabilises the system over the entire state space [13, 32].

As an example; a rule leading to a consequent might be:

IF $Positive(x_1)$ AND $Positive(x_2)$ THEN $\mathbf{u}_1(\mathbf{x}) = x_1 - x_2$,

where the membership function

$\mu_1(\mathbf{x}) = Positive(x_1)$ AND $Positive(x_2)$ which can be defined as $min\left(Positive(x_1), Positive(x_2)\right)$.

The rule can then composed as,

$$\mu_1(\mathbf{x})\mathbf{u}_1(\mathbf{x}) \quad = \quad min\left(Positive(x_1), Positive(x_2)\right)(x_1 - x_2),$$

if the definition for AND has been chosen as the $min()$ function [46, Ch. 2.2.4].

The name used in [13, 32] was *Heuristic Fuzzy Controller,* but this detracts from the key point of using a Lyapunov function.

Another view provided in this dissertation is the reinterpretation of the results which the fuzzy control system terminology obfuscates; this technique is really just an interpolation amongst controllers bearing a Lyapunov function in mind. Chapter 5.3 presents the method and design technique.

Energy-Shaping Robot Control

The techniques from Robot Control apply directly to the class of problems considered in this dissertation and are based on energy shaping arguments for stability proofs and understanding of the algorithm [15, Ch. 9]. The idea of considering the actuator in a multiple degree of freedom robot system as a device which regulates the energy flow in a system was first done in [2].

The model considered for this class of problem is near identical in structure to the prototypical model, eq (3.1.1), but does not include dissipation, and the inputs enter directly:

$$\mathbf{H}(\mathbf{q})\ddot{\mathbf{q}} + \mathbf{C}(\mathbf{q},\dot{\mathbf{q}})\dot{\mathbf{q}} + \mathbf{g}(\mathbf{q}) \quad = \quad \tau,$$

where $\mathbf{q} \in \mathbb{R}^N$ is the vector of the N generalised co-ordinates, $\mathbf{H}(\mathbf{q})$ is the inertia matrix, $\mathbf{C}(\mathbf{q}, \dot{\mathbf{q}})$ is the Coriolis and Centripetal matrix, $\mathbf{g}(\mathbf{q})$ is the gravitational force matrix and τ are the applied torques [15, Ch. 9]. The main results of this method are translatable to the prototypical model, eq (3.1.1), but will require a few subtle adjustments.

The controllers available in this framework, adapted for the prototypical model, are presented in Chapter 5.4.

Interconnection and Damping Assignment

This dissertation would not be complete if the method of IDAPBC were not presented. The basic idea is again one on matching, but in this case the matching condition is that the well known input affine nonlinear model

$$\dot{\mathbf{x}} = \mathbf{F}(\mathbf{x}) + \mathbf{G}(\mathbf{x})\mathbf{u}$$

be made to look like

$$\dot{\mathbf{x}} = (\mathbf{J_d}(\mathbf{x}) - \mathbf{R_d}(\mathbf{x})) \frac{\partial}{\partial \mathbf{x}} H_d(\mathbf{x}) \tag{5.0.1}$$

where each of the terms $\mathbf{J_d}$, $\mathbf{R_d}$ and H_d have physical interpretations as interconnection, damping and energy respectively [19, 18]. The minima of $H_d(\mathbf{x})$ are the stable equilibrium points for a suitably chosen $\mathbf{J_d}$ and $\mathbf{R_d}$ [19, 18]. If the system is already in the form

$$\dot{\mathbf{x}} = (\mathbf{J}(\mathbf{x}) - \mathbf{R}(\mathbf{x})) \frac{\partial}{\partial \mathbf{x}} H(\mathbf{x})$$

called a Port-Controlled Hamiltonian model, then the matching problem is to make this system match the eq (5.0.1), which is the desired closed loop system [19, 18]. The solution for the control law involves finding the solution to a set of partial differential equations, which prevents the ease of application of IDAPBC [19, 18].

The method and detailed design of the technique is presented in Chapter 5.5.

The Simple Pendulum

An example used to demonstrate each control technique is the simple pendulum, under the influence of gravity with a torque acting on a frictionless hinge. The pendulum is suspended by a mass-less rigid rod. There are a number of reasons for choosing this example: the system is a scalar second order differential equation and can therefore be represented on a phase portrait; it has a trigonometric non-linearity due to gravity, which leads to interesting behaviour (notably multiple equilibria); the system is well understood and the system has different behaviour at different energy levels. By choosing such a simple, yet rich, system, the various influences from each of the control techniques can be readily appreciated [1].

This simple pendulum, under the influence of gravity on a frictionless hinge is depicted in Figure 5.0.1. It has a mass m, at the end of a rigid rod of length l, angle θ, angular speed $\omega = \dot{\theta}$, applied torque τ, gravitational constant g and moment of inertia measured about the hinge, I.

[1] However, the control techniques are developed for the multi-dimensional, multiple-input prototypical model and hence are valid for a much broader class of problems.

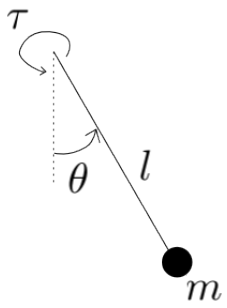

Figure 5.0.1: A Simple Pendulum

The system has an energy,

$$E_s = \frac{1}{2}I\omega^2 + U_0 - mgl\cos(\theta), \tag{5.0.2}$$

with $U_0 := mgl$ in order to have zero potential energy when $\theta = 0$. The power input to the system is

$$\dot{E}_s = \tau\omega. \tag{5.0.3}$$

Now the equations of motion are derived using the technique from Chapter 4, by taking the time derivative of eq. (5.0.2) and setting it equal to eq. (5.0.3),

$$\begin{aligned} \dot{E}_s &= \dot{E}_s \\ \omega\left(I\ddot{\theta} + mgl\sin(\theta)\right) &= \omega\tau, \end{aligned}$$

and therefore either $\omega = 0$ for all $t > 0$ or

$$I\ddot{\theta} + mgl\sin(\theta) = \tau. \tag{5.0.4}$$

Put into prototypical form, the system is,

$$m_{sp}(\theta)\ddot{\theta} + d_{sp}(\theta,\omega)\omega + k_{sp}(\theta) = g_{sp}(\theta)\tau, \tag{5.0.5}$$

with

$$\begin{aligned} m_{sp}(\theta) &= I, \\ d_{sp}(\theta,\omega) &= 0, \\ k_{sp}(\theta) &= mgl\sin(\theta), \\ g_{sp}(\theta) &= 1, \\ \dot{\theta} &= \omega. \end{aligned}$$

The values of $m = 0.5$ kg, $l = 1$ m, g =9.81 m/s^2, $I = ml^2$ kg m^2 will be used throughout.

The natural energy function and phase portrait are depicted in Figure 5.0.2 and Figure 5.0.3 respectively. Firstly, there are multiple equilibria, as evidenced by the orbiting trajectories around multiples of 2π [10]. This should be juxtaposed with the mass-spring system which had a single equilibrium point in Chapter 3.4.

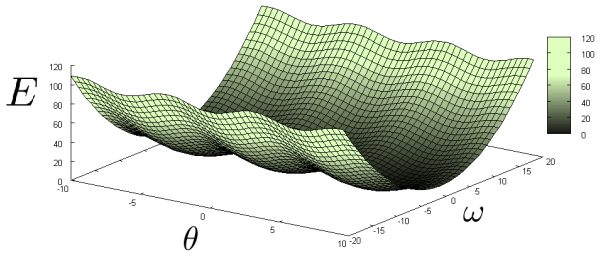

Figure 5.0.2: The Simple Pendulum Energy Function

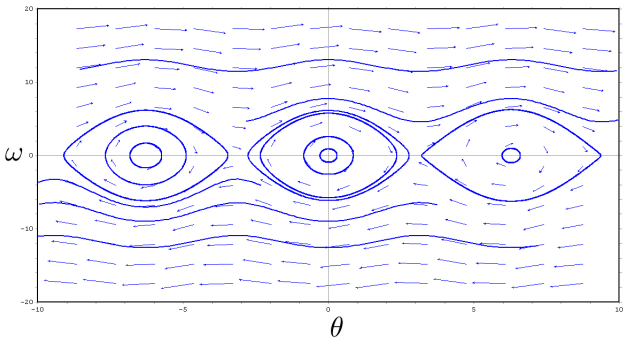

Figure 5.0.3: The Simple Pendulum Phase Portrait for Various Initial Conditions

Secondly, it should be apparent that for low energy levels, the pendulum behaves as a mass-spring system (simple harmonic oscillator) [10]. This is clearly shown by the circular trajectories near each multiple of 2π. As higher and higher energy levels are attained, the period of the pendulum must change, since the circular trajectories distort and become ellipses. In fact, the exact analytic solution to this period is given by "*the complete elliptic integral of the first kind*" [47]. Note that the mass-spring system must have exactly the same period, regardless of energy level, due to its linearity. Even though the arc-length of the circle becomes larger in the mass-spring system, for higher energy levels, the maximum speed attained is larger and hence the same time per round trip must be taken. Whereas for the pendulum, this is not the case.

Now, if the energy function is viewed locally around $(\theta,\omega) = (0,0)$ (see Figure 5.0.4), then it is apparent that the approximation to a mass-spring system is valid. This region corresponds to the circular orbits around the origin of Figure 5.0.3. If the energy function is viewed locally around $(\theta,\omega) = (\pi,0)$ (see Figure 5.0.5), then it is clear that this is a saddle point in the energy function. Calculating $\nabla^2 E$ confirms this:

$$\nabla^2 E(\theta,\omega) \quad = \quad \begin{pmatrix} mgl\cos(\theta) \\ I \end{pmatrix},$$

which evaluated at $(\theta,\omega) = (\pi,0)$ leads to

$$\nabla^2 E(\pi,0) \quad = \quad \begin{pmatrix} -mgl \\ I \end{pmatrix}.$$

This demonstrates a local maximum, ($\nabla^2 E < 0$), in the θ direction and a local minimum,

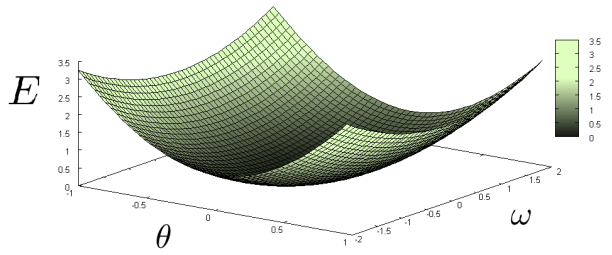

Figure 5.0.4: Energy of Simple Pendulum viewed locally around $\theta = 0$

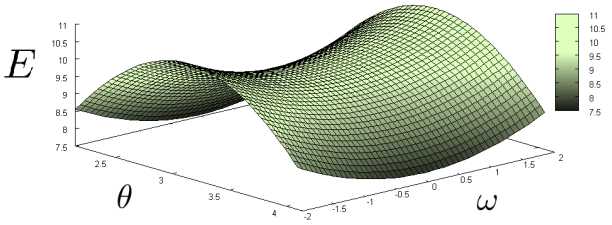

Figure 5.0.5: Energy of Simple Pendulum viewed locally around $\theta = \pi$

($\nabla^2 E > 0$), in the ω direction [2]. Hence this is classified as a saddle point. Due to the trigonometric term in θ, this local minimum and saddle point pattern repeats every $k2\pi$, $k \in \mathbb{Z}$.

[2] Note that the point $(\theta, \omega) = (\pi, 0)$ is an equilibrium point since, $\nabla E(\pi, 0) = (0, 0)$ and therefore the assertion of minima and maxima is valid.

5.1 Energy Balancing

The idea of an Energy Balancing controller is presented in the literature in a number of different contexts, most notably in the Controlled Lagrangian method [7, 8] and the IDAPBC framework [6].

The presentation here is of the same basic idea, but modified for the prototypical system presented in eq (3.1.1). It includes the ability to shape the dissipation, interconnection and Coriolis/Centripetal terms as done in IDAPBC [6], but avoids having to solve partial derivative equations, since the potential and kinetic energies are kept separate and discernable.

Given the prototypical model eq (3.1.1), the energy of the system E_s is given by

$$\begin{aligned} E_s &= \frac{1}{2}\mathbf{v}^{\mathrm{T}}\mathbf{M}(\mathbf{x},t)\mathbf{v} + \int \mathbf{K}(\mathbf{x})^{\mathrm{T}}\,\mathrm{d}\mathbf{x} \\ &= E_0 - \int \mathbf{v}^{\mathrm{T}}\mathbf{D}(\mathbf{x},\mathbf{v})\mathbf{v}\,\mathrm{d}t + \int \mathbf{v}^{\mathrm{T}}\mathbf{G}(\mathbf{x})\mathbf{u}\,\mathrm{d}t \end{aligned} \tag{5.1.1}$$

as is derived in Chapter 4. An energy balancing controller essentially makes the controller supply the difference between the stored and the desired energy E_d.

It requires that

$$E_s = E_d$$

and furthermore that

$$\begin{aligned} \frac{\mathrm{d}}{\mathrm{d}t}\left(E_s - E_d\right) &= \frac{\mathrm{d}}{\mathrm{d}t}\tilde{E} \\ &= 0, \end{aligned}$$

which is to say that the difference in energy *is* zero for all time. This should be juxtaposed with the power shaping method where the difference in energy exponentially approaches zero as $t \to \infty$ which is described in Chapter 5.2.

Now given a basic desired energy

$$\begin{aligned} E_d &= \frac{1}{2}\mathbf{v}^{\mathrm{T}}\mathbf{M}_{\mathbf{d}}(\mathbf{x},t)\mathbf{v} + \int \mathbf{K}_{\mathbf{d}}(\mathbf{x})^{\mathrm{T}}\,\mathrm{d}\mathbf{x} \\ &= E_0 - \int \mathbf{v}^{\mathrm{T}}\mathbf{D}_{\mathbf{d}}(\mathbf{x},\mathbf{v})\mathbf{v}\,\mathrm{d}t \end{aligned}$$

and using the difference in power equation results in

$$\begin{aligned} \int \mathbf{v}^{\mathbf{T}}\mathbf{y}\mathrm{d}t &= E_d \\ \mathbf{v}^{\mathrm{T}}\left(\mathbf{M}(\mathbf{x},t)\ddot{\mathbf{x}} + \mathbf{D}(\mathbf{x},\mathbf{v})\mathbf{v} + \mathbf{K}(\mathbf{x}) - \mathbf{G}(\mathbf{x})\mathbf{u}\right) &= \mathbf{v}^{\mathrm{T}}\left(\mathbf{M}_{\mathbf{d}}(\mathbf{x},t)\ddot{\mathbf{x}} + \mathbf{D}_{\mathbf{d}}(\mathbf{x},\mathbf{v})\mathbf{v} + \mathbf{K}_{\mathbf{d}}(\mathbf{x})\right), \end{aligned}$$

which permits the solution

$$\mathbf{u} = \mathbf{G}(\mathbf{x})^{-1}\left(\mathbf{M}(\mathbf{x},t)\ddot{\mathbf{x}} + \mathbf{D}(\mathbf{x},\mathbf{v})\mathbf{v} + \mathbf{K}(\mathbf{x}) - \mathbf{u}^{*}\right), \tag{5.1.2}$$

where

$$\mathbf{u}^* \quad = \quad \mathbf{M_d}(\mathbf{x},t)\ddot{\mathbf{x}} + \mathbf{D_d}(\mathbf{x},\mathbf{v})\mathbf{v} + \mathbf{K_d}(\mathbf{x}).$$

This result has the basic form of feedback linearisation [15, Ch. 6]. The key difference here is that, the target dynamics $\mathbf{u}^*$ are derived using physical considerations of the desired closed loop system's energy, and not arbitrarily, as in Feedback Linearisation[3]. The second major difference between this technique and feedback linearisation is that, eq (5.1.2) is actually an *inversion of the plant,* in that the plant dynamics are completely cancelled and replaced by other dynamics i.e. the substitution of eq (5.1.2) into eq (3.1.1) leads to

$$\mathbf{M_d}(\mathbf{x},t)\ddot{\mathbf{x}} + \mathbf{D_d}(\mathbf{x},\mathbf{v})\mathbf{v} + \mathbf{K_d}(\mathbf{x}) \quad = \quad 0.$$

Strictly speaking, feedback linearisation comes from the requirement that,

$$\begin{aligned} \mathbf{M_d} &= \mathbb{I} \\ \mathbf{D_d} &= \mathbb{O} \\ \mathbf{K_d} &= \mathbb{O}, \end{aligned}$$

which implies that,

$$E_d \quad = \quad \frac{1}{2}\mathbf{v}^{\mathrm{T}}\mathbf{v},$$

and

$$\dot{E}_d \quad = \quad \mathbf{v}^{\mathrm{T}}\mathbf{r}$$

where $\mathbf{r}$ is a new external input i.e. the control of a double integrator. This has the control law

$$\mathbf{u} \quad = \quad \mathbf{G}(\mathbf{x})^{-1}\left([\mathbf{M}(\mathbf{x},t) - 1]\,\ddot{\mathbf{x}} + \mathbf{D}(\mathbf{x},\mathbf{v})\mathbf{v} + \mathbf{K}(\mathbf{x}) + \mathbf{r}\right)$$

which can be simplified using the model eq (3.1.1), substituting for $\ddot{\mathbf{x}}$ and a great deal of algebra into

$$\mathbf{u} \quad = \quad \mathbf{G}(\mathbf{x})^{-1}\left(\mathbf{D}(\mathbf{x},\mathbf{v})\mathbf{v} + \mathbf{K}(\mathbf{x}) + \mathbf{M}(\mathbf{x},t)\mathbf{r}\right).$$

Substituting the control law into eq (3.1.1) leads to

$$\ddot{\mathbf{x}} \quad = \quad \mathbf{r}$$

as required. Of course the general method rests on choosing an appropriate desired energy E_d, a few situations are presented next. It should be remembered here that the general theory has been presented and creativity and insight has been used in the example for this section. Other techniques which constructively modify the closed-loop energy and power functions are presented later in this Chapter.

[3]The one key point to mention is that acceleration terms are needed in the target dynamics u^* if the mass matrix is to be modified

Choosing E_d: Modification of Existing Plant

If the desired energy functions are modifications of the existing plant, which is to say:

$$F_d = F_p + \Delta F$$

where F_d is the desired function[4], F_p is the plant function and ΔF is the modification then the control law eq (5.1.2) becomes

$$\mathbf{u} = -\mathbf{G}(\mathbf{x})^{-1}\left(\Delta\mathbf{M}(\mathbf{x},t)\ddot{\mathbf{x}} + \Delta\mathbf{D}(\mathbf{x},\mathbf{v})\mathbf{v} + \Delta\mathbf{K}(\mathbf{x})\right)$$

which appears exactly like a general state feedback control law except with the additional acceleration term $\Delta\mathbf{M}(\mathbf{x},t)\ddot{\mathbf{x}}$. The acceleration terms may be kept if they are being measured (say via accelerometers) or may be eliminated using the model eq. (3.1.1) and a great deal of algebra into

$$\mathbf{u} = -\left[\mathbf{M_d}(\mathbf{x},t)\mathbf{G}(\mathbf{x})\right]^{-1}\left\{\mathbf{M}(\mathbf{x},t)\left(\Delta\mathbf{K}(\mathbf{x}) + \Delta\mathbf{D}(\mathbf{x},\mathbf{v})\mathbf{v}\right) - \Delta\mathbf{M}(\mathbf{x},t)\left(\mathbf{K}(\mathbf{x}) - \mathbf{D}(\mathbf{x},\mathbf{v})\mathbf{v}\right)\right\}$$

Choosing E_d: New Plant

If the desire is to have the closed loop system behave completely differently from the existing plant, then eq (5.1.2) is exactly what will be derived.

Design of Energy-Balancing Controllers

The general design steps are:

1. Get the system model into prototypical model form.
2. Identify $\mathbf{M}(\mathbf{x},t)$, $\mathbf{D}(\mathbf{x},\mathbf{v})$, $\mathbf{K}(\mathbf{x})$ and $\mathbf{G}(\mathbf{x})\mathbf{u}$ in the open loop system.
3. Choose desired kinetic and potential functions[5].
4. Choose a desired dissipation, interconnection and Coriolis/Centripetal matrix $\mathbf{D_d}(\mathbf{x},\mathbf{v})$.
5. Solve the energy and power matching equation for $\mathbf{u}$.

Energy-Balancing Control of a Simple Pendulum

Given the system energy of the pendulum as,

$$E_s = \frac{1}{2}I\omega^2 + U_0 - mgl\cos(\theta),$$

with input power,

$$\dot{E}_s = \tau\omega,$$

[4] An example is $\mathbf{M_d}(\mathbf{x},t) = \mathbf{M}(\mathbf{x},t) + \Delta\mathbf{M}(\mathbf{x},t)$

[5] Steps 3 and 4 represent the design freedom of the control engineer. Constructive methods to assign the desired energy structure will be introduced later in this chapter.

the energy-balancing methodology can begin. Note that θ^* is a desired angle.

It is important to actually have the uncontrolled energy of the system to be controlled or otherwise there can be no energy-balancing. Provided that $\mathbf{M}(\mathbf{x},t)$, $\mathbf{D}(\mathbf{x},\mathbf{v})$ and $\mathbf{K}(\mathbf{x})$ can be identified, the system energy can easily be calculated using the energy transform in Chapter 4.

The equations of motion are, given by eq. (5.0.4) and repeated here for reference,

$$I\ddot{\theta} + mgl\sin(\theta) \quad = \quad \tau.$$

1.) The prototypical form of this equation is given by eq. (5.0.5) and is repeated here,

$$m_{sp}(\theta)\ddot{\theta} + d_{sp}(\theta,\omega)\omega + k_{sp}(\theta) \quad = \quad g_{sp}(\theta)\tau.$$

2.) The parameters of the model are given by

$$\begin{aligned} m_{sp}(\theta) &= I, \\ d_{sp}(\theta,\omega) &= 0, \\ k_{sp}(\theta) &= mgl\sin(\theta), \\ g_{sp}(\theta) &= 1. \end{aligned}$$

As stipulated, the design freedom of the control engineer is in steps 3.) and 4.). A selection of energy balancing designs are worked through next.

Viscous Damping

3.) The kinetic energy and potential energy are left untouched and hence,

$$\begin{aligned} \frac{1}{2}m_{spd}(\theta)\omega^2 &= m_{sp}(\theta)\omega^2, \\ \int k_{spd}(\theta)\mathrm{d}\theta &= \int k_{sp}(\theta)\mathrm{d}\theta. \end{aligned}$$

4.) The inclusion of viscous damping is given by the desired power,

$$\begin{aligned} \dot{E}_d &= -d_{spd}(\theta,\omega)\omega^2 \\ &= -\kappa_d\omega^2. \end{aligned}$$

5.) Each of the adjustments to the energy structure of the system can be classed under the "modification of an existing plant" which implies that,

$$\begin{aligned} m_{spd} &= m_{sp} + \Delta m, \\ d_{spd} &= d_{sp} + \Delta d, \\ k_{spd} &= k_{sp} + \Delta k, \end{aligned}$$

with $\Delta m = 0$, $\Delta d = \kappa_d$, $\Delta k = 0$ and hence the control law is given by,

$$\begin{aligned} \tau &= -g_{sp}(\theta)^{-1}\left[\Delta m\ddot{\theta} + \Delta d\omega + \Delta k\right] \\ &= -\frac{1}{1}\left[0\,\ddot{\theta} + \kappa_d\omega + 0\right] \\ &= -\kappa_d\omega. \end{aligned}$$

It may be more transparent to the reader to approach the problem from first principles. This is the presentation that will be followed throughout the rest of the energy balancing section. If the reader so desires, it is possible to follow the "modification of an existing plant" paradigm and write the control laws directly for the following examples.

3.) The inclusion of viscous damping leads to,

$$E_d = \frac{1}{2}I\omega^2 + U_0 - mgl\cos(\theta).$$

4.) The desired power loss is,

$$\dot{E}_d = -\kappa_d\,\omega^2.$$

5.) The matching equation is therefore, the derivative of the system energy minus the derivative of the desired energy equal to the system power minus the desired power,

$$\begin{aligned} \dot{E}_s - \dot{E}_d &= \dot{E}_s - \dot{E}_d \\ \omega\left(I\ddot{\theta} + mgl\sin(\theta) - I\ddot{\theta} - mgl\sin(\theta)\right) &= \tau\omega + \kappa_d\,\omega^2 \\ 0 &= \tau\omega + \kappa_d\,\omega^2 \end{aligned}$$

and therefore,

$$\begin{aligned} \tau\omega &= -\kappa_d\,\omega^2 \\ \tau &= -\kappa_d\,\omega. \end{aligned}$$

Spring-like Desired Potential Function

3.) The desire to have the potential function appear as a spring-like potential function, with a single equilibrium point, θ^*, leads to

$$E_d = \frac{1}{2}I\omega^2 + \frac{1}{2}\kappa_p\,(\theta - \theta^*)^2.$$

4.) The dissipation of the system is left alone.

5.) The matching equation is then,

$$\begin{aligned} \dot{E}_s - \dot{E}_d &= \dot{E}_s - \dot{E}_d \\ \omega\left(I\ddot{\theta} + mgl\sin(\theta) - I\ddot{\theta} - \kappa_p(\theta - \theta^*)\right) &= \tau\omega, \end{aligned}$$

which has solution

$$\tau = mgl\sin(\theta) - \kappa_p(\theta - \theta^*).$$

This is a proportional controller with feedback linearisation.

Translation of Stationary Points in the Potential Function

3.) Now if the potential function were chosen to have a new minimum, at θ^* say, then

$$E_d = \frac{1}{2}I\omega^2 + U_0 - mgl\cos(\theta - \theta^*).$$

4.) The dissipation of the system is left alone.

5.) The matching equation is,

$$\begin{aligned} \dot{E}_s - \dot{E}_d &= \dot{E}_s - \dot{E}_d \\ \omega\left(I\ddot{\theta} + mgl\sin(\theta) - I\ddot{\theta} - mgl\sin(\theta - \theta^*)\right) &= \tau\omega, \end{aligned}$$

which leads to

$$\tau = mgl\sin(\theta) - mgl\sin(\theta - \theta^*).$$

Again, feedback linearisation with a new potential function. Notice that this feedback controller honours the symmetry of the system in that the new potential function has an infinite number of stationary points. Observe,

$$\nabla E_d = \begin{pmatrix} mgl\sin(\theta - \theta^*) \\ I\omega \end{pmatrix} = \begin{pmatrix} 0 \\ 0 \end{pmatrix}$$

has solutions $(\theta, \omega) = (\theta^* + k\pi, 0)$ with $k \in \mathbb{Z}$. Take note of the $k\pi$, this means that *all* of the equilibrium points have translated, including the saddle points. This problem is alleviated in the following control method.

Target Torque Position Controller

A strange potential function, which reappears in Chapter 5.4 under the "target torque" controller[6], is

$$\int k_{spd}(\theta)\mathrm{d}\theta = U_0 - mgl\cos(\theta) - mgl\sin(\theta^*)\theta.$$

3.) The desired kinetic and potential energy is,

$$E_d = \frac{1}{2}I\omega^2 + U_0 - mgl\cos(\theta) - mgl\sin(\theta^*)\theta.$$

4.) The dissipation of the system is left alone.

5.) The matching equation is,

[6] In fact this potential function was calculated using the energy transform from Chapter 4.

$$\begin{aligned} \dot{E}_s - \dot{E}_d &= \dot{E}_s - \dot{E}_d \\ \omega\left(I\ddot{\theta} + mgl\sin(\theta) - I\ddot{\theta} - mgl\sin(\theta) + mgl\sin(\theta^*)\right) &= \tau\omega, \end{aligned}$$

and therefore the controller is,

$$\tau = mgl\sin(\theta^*).$$

Although the effect of the new potential function is not obvious, the gradient of the energy function is

$$\nabla E_d = \begin{pmatrix} mgl\sin(\theta) - mgl\sin(\theta^*) \\ I\omega \end{pmatrix}.$$

This can be made to solve for the stationary points of the system via,

$$\begin{pmatrix} 0 \\ 0 \end{pmatrix} = \begin{pmatrix} mgl\sin(\theta) - mgl\sin(\theta^*) \\ I\omega \end{pmatrix},$$

which has the solutions $(\theta, \omega) = (\theta^* + 2k\pi, 0)$ with $k \in \mathbb{Z}$, as required. Note the $2k\pi$ which ensures that no saddle points are included in solutions to the system's steady state. This controller is also less computationally involved than the translation of stationary points method previously, since the control law is essentially a calculated constant. This stationary point is not at a minimum of the energy function though since $\nabla^2 E_d$ remains unchanged.

Gravity Inversion

Consider the case of gravity inversion, where the potential function changes sign,

3.) The desired kinetic and potential energy are,

$$E_d = \frac{1}{2}I\omega^2 + U_0 + mgl\cos(\theta).$$

4.) The dissipation is left as is.

5.) The matching equation is,

$$\begin{aligned} \dot{E}_s - \dot{E}_d &= \dot{E}_s - \dot{E}_d \\ \omega\left(I\ddot{\theta} + mgl\sin(\theta) - I\ddot{\theta} + mgl\sin(\theta)\right) &= \tau\omega, \end{aligned}$$

that leads to the controller,

$$\tau = 2mgl\sin(\theta).$$

Again, the saddle points have not been removed from the possible equilibria of the system.

Of course, it is possible to combine these different controllers.

Combined Dissipation and Potential Shaping

It is possible to combine the effects of potential and dissipation shaping.

Spring-like potential and Viscous dissipation

3.) The desired energy is,

$$E_d = \frac{1}{2}I\omega^2 + \frac{1}{2}\kappa_p(\theta - \theta^*)^2.$$

4.) The desired power dissipation is,

$$\dot{E}_d = -\kappa_d\,\omega^2.$$

5.) The resulting controller (after solving the matching equation) is then,

$$\tau = mgl\,\sin(\theta) - \kappa_p(\theta - \theta^*) - \kappa_d\,\omega,$$

which is feedback linearisation with a PD controller. Notice that the derivative is not taken of the error, $\theta - \theta^*$ but rather the output, θ only [7] as with a set-point weighted PD controller.

Target torque, Spring-like potential and Viscous dissipation

3.) If the combination is the target torque, spring-like potential function with dissipation then:

$$E_d = \frac{1}{2}I\omega^2 + \frac{1}{2}\kappa_p(\theta - \theta^*)^2 + U_0 - mgl\,\cos(\theta) - mgl\,\sin(\theta^*)\theta.$$

4.) The desired power dissipation is,

$$E_d = -\kappa_d\,\omega^2.$$

5.) The resulting control law is,

$$\tau = mgl\,\sin(\theta^*) - \kappa_p(\theta - \theta^*) - \kappa_d\,\omega.$$

Both of these combinations are well known in the Robotics literature, and are discussed in Chapter 5.4.

[7] $\frac{\mathrm{d}}{\mathrm{d}t}\theta = \omega$.

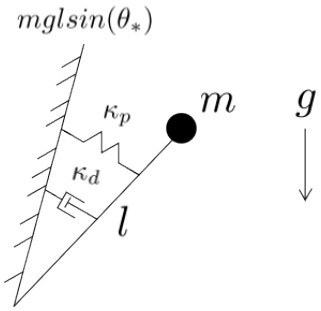

Figure 5.1.1: Physical Representation of Pendulum Controller, adapted from Ortega et al.

Stability

Given that the matching equation has been solved, it means that the closed loop energy *is* the desired energy. In the combination of the spring-like function with dissipation, asymptotic stability of $(\theta,\omega) = (\theta^*,0)$ can easily be shown using E_d as a Lyapunov function and employing La Salle's Invariance principle [15, Chapter 3.4.3]. Remember this is at the cost of online computation of $mgl\sin(\theta)$.

The stability of the target torque, spring-like function and dissipation combination requires more subtlety. Solving for the stationary points of the energy function, E_d,

$$\nabla E_d \quad = \quad \begin{pmatrix} mgl\sin(\theta) - mgl\sin(\theta^*) + \kappa_p(\theta-\theta^*) \\ I\omega \end{pmatrix} = \begin{pmatrix} 0 \\ 0 \end{pmatrix},$$

yields the unique solution $(\theta,\omega) = (\theta^*,0)$ if $\kappa_p > 0$. Next, $\nabla^2 E_d$ must be greater than zero at the desired equilibrium point θ^* in order for it to be a global minimum. Calculating this,

$$\nabla^2 E_d \quad = \quad \begin{pmatrix} mgl\cos(\theta) + \kappa_p \\ I \end{pmatrix},$$

and ensuring that $\nabla^2 E_d > 0$ for any θ^* implies, that $\kappa_p > mgl$. If this condition on κ_p is validated, then the point $(\theta,\omega) = (\theta^*,0)$ will be a global minimum of the energy function, E_d. Hence if $\kappa_d > 0$, this point will be asymptotically approached as per Figure 3.4.5 in Chapter 3.4. Appreciate that only physical reasoning about the energy was used to conclude global stability. No linearisation was needed, no complicated partial differential equations (PDE's) had to be solved, no invariance principles had to be invoked, only physical insight and reasoning about the closed loop system's energy was needed. It is valuable to have a visual representation of the forces that have been added to the pendulum system. This is depicted in Figure 5.1.1 and adapted from [25, pp. 47]. Essentially, the target torque acts as a plane that a spring, κ_p term, and a damper, κ_d term, are coupled to with the pendulum [25, pp. 47]. The action of each of the terms should be clear now.

The phase portraits of these two control laws are depicted in Figures 5.1.2 and 5.1.3. For the parameters chosen, $mgl = 4.905$ and hence $\kappa_p = 5$. Choosing, $\kappa_d = 0.5$ and θ^* (arbitrarily) as 1 rad completes the design. It is clear from the phase portraits that both control laws are globally asymptotically stable, and further that $(\theta,\omega) \to (\theta^*,0)$ as the theory predicts.

It is trivial to generalise these controllers, to the multi-variable, prototypical case: formally replace all $mgl\sin()$ with $\mathbf{K}()$, ω with $\mathbf{v}$, θ with $\mathbf{x}$ and θ^* with $\mathbf{x}^*$. Define κ_p and κ_d as $N \times N$ matrices, $\boldsymbol{\kappa_p}$, $\boldsymbol{\kappa_d}$ and finally replace τ with $\mathbf{G}(\mathbf{x})\mathbf{u}$. If $\mathbf{G}(\mathbf{x})$ has an inverse, an assumption

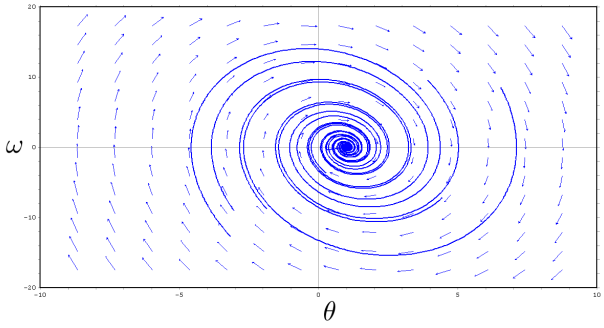

Figure 5.1.2: Phase Portrait with Desired Spring-like Potential and Dissipation ($\kappa_p = 5$, $\kappa_d = 0.5$ and $\theta^* = 1$)

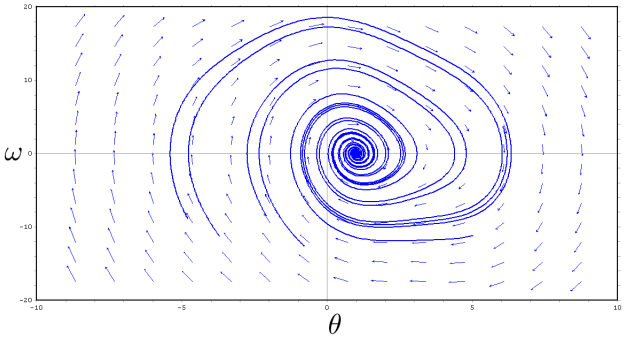

Figure 5.1.3: Phase Portrait with Target Torque, Spring-like Potential and Dissipation ($\kappa_p = 5$, $\kappa_d = 0.5$ and $\theta^* = 1$)

used throughout this dissertation and explained in Chapter 3.1, then the input, $\mathbf{u}$, can be solved for explicitly.

The analogues to these control laws are shown in [14] and [15, Ch. 9] to be well suited for position regulation. If trajectory following is the control problem, then the techniques from Chapter 5.2 and Chapter 5.4 are better suited to this task.

5.2 Power Shaping

The ideal objective for any control problem would be for the system to do already what the designer would like it to do. Now the phase portrait shows all the possible trajectories which the system can take and if any one of them is a desirable behaviour, then the goal of the controller is merely to make sure that the system has exactly the energy needed to follow that trajectory [10, 11]. This means that the controller is exploiting what the system would do naturally anyway as opposed to forcing it to do what the designer wants and wasting energy fighting the dynamics. By combining phase portrait analysis, bearing Figure 3.4.5 in mind, and energy-shaping control, the designer can elegantly solve non-linear control objectives by considering how much energy the system has at a given point in time and therefore what trajectory the system will be on.

The development presented here mirrors the scalar system described in [10]. However, extensions to the paradigm and adaptation to the prototypical model are included in this development and are presented next.

The basic idea is as follows: given a system energy E_s and a desired energy E_d, let the difference in energy be $\tilde{E} = E_s - E_d$.

The desired energy E_d is given by

$$E_d = \frac{1}{2}\mathbf{v}^{\mathrm{T}}\mathbf{M_d}(\mathbf{x},t)\mathbf{v} + \int \mathbf{K_d}(\mathbf{x})^{\mathrm{T}}\,\mathrm{d}\mathbf{x}$$

with the desired power

$$\dot{E}_d = \mathbf{v}^{\mathrm{T}}\Phi(\mathbf{x},\mathbf{v})$$

where $\Phi(\mathbf{x},\mathbf{v})$ is the desired $\mathbf{D}(\mathbf{x},\mathbf{v})\mathbf{v}$ and desired inputs lumped together. Note that E_d and $\dot{E}_d$ together represent the desired closed loop dynamics.

Looking now at the difference in actual and desired energy $\tilde{E}$,

$$\tilde{E} = \frac{1}{2}\mathbf{v}^{\mathrm{T}}\Delta\mathbf{M}\mathbf{v} + \int \Delta\mathbf{K}^{T}\,\mathrm{d}\mathbf{x},$$

where $\Delta\mathbf{M} = \mathbf{M}(\mathbf{x},t) - \mathbf{M_d}(\mathbf{x},t)$ and $\Delta\mathbf{K} = \mathbf{K}(\mathbf{x}) - \mathbf{K_d}(\mathbf{x})$.

The difference in power is

$$\frac{\mathrm{d}}{\mathrm{d}t}\tilde{E} = -\mathbf{v}^{\mathrm{T}}\mathbf{R}(\mathbf{x},\mathbf{v})\mathbf{v} + \mathbf{v}^{\mathrm{T}}\mathbf{G}(\mathbf{x})\mathbf{u} - \mathbf{v}^{\mathrm{T}}\Phi(\mathbf{x},\mathbf{v})$$

and the goal is for

$$\frac{\mathrm{d}}{\mathrm{d}t}\tilde{E} = -\kappa_p\mathbf{v}^{\mathrm{T}}\tilde{E}\mathbf{v}$$

where $\kappa_p > 0$ is a scalar constant. This is similar to the scalar system in [10].

This condition leads to

$$-\kappa_p\mathbf{v}^{\mathrm{T}}\tilde{E}\mathbf{v} = -\mathbf{v}^{\mathrm{T}}\mathbf{R}(\mathbf{x},\mathbf{v})\mathbf{v} + \mathbf{v}^{\mathrm{T}}\mathbf{G}(\mathbf{x})\mathbf{u} - \mathbf{v}^{\mathrm{T}}\Phi(\mathbf{x},\mathbf{v})$$

which results in the control law,

$$\mathbf{u} = \mathbf{G}(\mathbf{x})^{-1}\left(\underbrace{\Phi(\mathbf{x},\mathbf{v})+\mathbf{R}(\mathbf{x},\mathbf{v})\mathbf{v}}_{\text{cancels}} - \kappa_p\tilde{E}\mathbf{v}\right)$$

which requires exact cancellation of the dissipation structure $\Phi(\mathbf{x},\mathbf{v})+\mathbf{R}(\mathbf{x},\mathbf{v})\mathbf{v}$ i.e. partial feedback linearisation of the dissipation of the system. Now if there are any model inaccuracies in $\mathbf{R}(\mathbf{x},\mathbf{v})$ then $\tilde{E}$ will not go to zero[8]. The inspiration for solving this problem was from the investigations into phase portraits in terms of energy in Chapter 3.4 as well as a PID controller's effect in the phase plane in Chapter 3.5.

Consider using just the control law

$$\mathbf{u} = -\kappa_p\mathbf{G}(\mathbf{x})^{-1}\tilde{E}\mathbf{v}$$

and for simplicity's sake, E_d is constant, then

$$\frac{\mathrm{d}}{\mathrm{d}t}\tilde{E} = -\kappa_p\mathbf{v}^{\mathrm{T}}\tilde{E}\mathbf{v} - \mathbf{v}^{\mathrm{T}}\mathbf{R}(\mathbf{x},\mathbf{v})\mathbf{v}$$

which looks like $\dot{x} = -kx - d$ i.e. the dissipation acts like a disturbance in the power equation! Hence, the well known method of disturbance rejection using an integrator was used to remove the dissipation, *without* cancelling it in the control law.

This idea leads to the control law,

$$\begin{aligned}\mathbf{u} &= \mathbf{G}(\mathbf{x})^{-1}\left(\zeta\mathbf{v} - \kappa_p\tilde{E}\mathbf{v}\right)\\ \dot{\zeta} &= -\kappa_i\tilde{E}\end{aligned}$$

and the power equation becomes

$$\begin{aligned}\frac{\mathrm{d}}{\mathrm{d}t}\tilde{E} &= -\mathbf{v}^{\mathrm{T}}\mathbf{R}(\mathbf{x},\mathbf{v})\mathbf{v} - \kappa_p\mathbf{v}^{\mathrm{T}}\tilde{E}\mathbf{v} + \mathbf{v}^{\mathrm{T}}\zeta\mathbf{v}\\ \frac{\mathrm{d}}{\mathrm{d}t}\zeta &= -\kappa_i\tilde{E}\end{aligned}$$

if E_d is a constant, where $\kappa_i > 0$ is a constant and ζ is a scalar integrator. This is an extension of the method in [10], and can be considered as a non-linear energy PI controller.

The equilibrium points for this system are found by setting the derivatives equal to zero (and assuming $\mathbf{v} \neq \mathbb{O}$) and hence

$$\begin{aligned}\tilde{E} &= 0\\ \mathbf{v}^{\mathrm{T}}\zeta\mathbf{v} &= \mathbf{v}^{\mathrm{T}}\mathbf{R}(\mathbf{x},\mathbf{v})\mathbf{v}\end{aligned}$$

which has clearly negated the effect of the dissipation.

In the general case when E_d is not a constant,

$$\frac{\mathrm{d}}{\mathrm{d}t}\tilde{E} = -\mathbf{v}^{\mathrm{T}}\mathbf{R}(\mathbf{x},\mathbf{v})\mathbf{v} + \mathbf{v}^{\mathrm{T}}\mathbf{G}(\mathbf{x})\mathbf{u} - \mathbf{v}^{\mathrm{T}}\Phi(\mathbf{x},\mathbf{v})$$

[8] $\Phi(\mathbf{x},\mathbf{v})$ is user defined and therefore there are no model inaccuracies to worry about

with the control law

$$\begin{aligned} \mathbf{u} &= \mathbf{G}(\mathbf{x})^{-1}\left(\zeta\mathbf{v} - \kappa_p\tilde{E}\mathbf{v} + \Phi(\mathbf{x},\mathbf{v})\right) \\ \dot{\zeta} &= -\kappa_i\tilde{E} \end{aligned} \tag{5.2.1}$$

results in the equilibrium points

$$\begin{aligned} \tilde{E} &= 0 \\ \mathbf{v}^{\mathrm{T}}\zeta\mathbf{v} &= \mathbf{v}^{\mathrm{T}}\mathbf{R}(\mathbf{x},\mathbf{v})\mathbf{v} \end{aligned}$$

as expected. To assess the stability, contraction analysis is used. Define the virtual system,

$$\begin{aligned} \frac{\mathrm{d}}{\mathrm{d}t}\mathscr{E} &= -\mathbf{v}^{\mathrm{T}}\mathbf{R}(\mathbf{x},\mathbf{v})\mathbf{v} - \kappa_p\mathbf{v}^{\mathrm{T}}\mathscr{E}\mathbf{v} + \mathbf{v}^{\mathrm{T}}\mathscr{Z}\mathbf{v} \\ \frac{\mathrm{d}}{\mathrm{d}t}\mathscr{Z} &= -\kappa_i\mathscr{E}, \end{aligned}$$

which contains the actual system for $\mathscr{E} = \tilde{E}$ and $\mathscr{Z} = \zeta$. The virtual velocity is now,

$$\begin{pmatrix} \delta\dot{\mathscr{E}} \\ \delta\dot{\mathscr{Z}} \end{pmatrix} = \begin{pmatrix} -\kappa_p\mathbf{v}^{\mathrm{T}}\mathbf{v} & \mathbf{v}^{\mathrm{T}}\mathbf{v} \\ -\kappa_i & 0 \end{pmatrix}\begin{pmatrix} \delta\mathscr{E} \\ \delta\mathscr{Z} \end{pmatrix}.$$

The eigenvalues, $s_{1,2}$ of the system are

$$s_1 = \frac{-\left(\mathbf{v}^{\mathrm{T}}\mathbf{v}\right)\kappa_p + \sqrt{\kappa_p^2\left(\mathbf{v}^{\mathrm{T}}\mathbf{v}\right)^2 - 4\kappa_i\mathbf{v}^{\mathrm{T}}\mathbf{v}}}{2}$$

and

$$s_2 = \frac{-\left(\mathbf{v}^{\mathrm{T}}\mathbf{v}\right)\kappa_p - \sqrt{\kappa_p^2\left(\mathbf{v}^{\mathrm{T}}\mathbf{v}\right)^2 - 4\kappa_i\mathbf{v}^{\mathrm{T}}\mathbf{v}}}{2}.$$

The system is stable as long as the real part of s_1 is negative i.e.

$$\begin{aligned} \sqrt{\kappa_p^2\left(\mathbf{v}^{\mathrm{T}}\mathbf{v}\right)^2 - 4\kappa_i\mathbf{v}^{\mathrm{T}}\mathbf{v}} &< \mathbf{v}^{\mathrm{T}}\mathbf{v}\kappa_p \\ \implies \kappa_p^2\left(\mathbf{v}^{\mathrm{T}}\mathbf{v}\right)^2 - 4\kappa_i\mathbf{v}^{\mathrm{T}}\mathbf{v} &< \kappa_p^2\left(\mathbf{v}^{\mathrm{T}}\mathbf{v}\right)^2 \end{aligned}$$

and therefore

$$\kappa_i\mathbf{v}^{\mathrm{T}}\mathbf{v} > 0,$$

which is validated as long as $\mathbf{v} \neq \mathbb{O}$.

Consider the case that $\mathbf{v} = \mathbb{O}$ and $\tilde{E} \neq 0$. This leads to $\dot{\zeta} \neq 0$, with $\mathbf{u} = 0$ from the definition of eq (5.2.1), the power shaping control law. Therefore the integrator will continue to wind-up whilst no input is applied to the system. By applying a small impulse, enough to

overcome stiction and make $\mathbf{v} \neq \mathbb{O}$, when $\mathbf{v} = \mathbb{O}$ this issue can be resolved. Hence the full and final power shaping control law is

$$\begin{aligned} \mathbf{u} &= \mathbf{G}(\mathbf{x})^{-1}\left\{\zeta \mathbf{v} - \kappa_p \tilde{E}\mathbf{v} + \Phi(\mathbf{x},\mathbf{v}) + A\,\delta(\mathbf{v})\right\} \\ \dot{\zeta} &= -\kappa_i \tilde{E} \end{aligned}$$

where $A > |\mathbf{v}^{\mathrm{T}}\mathbf{D}(\mathbf{x},\mathbf{v})\mathbf{v}|$ for small $\mathbf{v}$, if stiction is a problem and $A > 0$ if it isn't. Furthermore, $\delta(x)$ is the well known, one dimensional Kronecker delta function. This is defined as,

$$\delta(x) = \begin{cases} 1 & x = 0 \\ 0 & \text{otherwise.} \end{cases}$$

Design of Power-Shaping Controllers

The general design steps are:

1. Get the system model into prototypical model form.
2. Identify which of the level curves of the energy function are a desired trajectory. Call this energy level, E_d.
3. If none exist, use an energy shaping controller to generate them. Go back to 2.
4. Use eq. 5.2.1 as the control law.
5. Design appropriate values for κ_p and κ_i, depending on performance requirements.

Swing-up Control of a Pendulum

Step 1.) has been completed previously in eq. (5.0.5).

This example is adapted from the lecture series of [10]. For reference purposes, the equation of motion for the pendulum is repeated here,

$$I\ddot{\theta} = -mgl\sin(\theta) + \tau.$$

Remember that $\theta = 0$ is the straight down position of the pendulum.

Now the energy for the system is,

$$\frac{1}{2}I\omega^2 + U_0 - mgl\cos(\theta) = E_0 + \int \tau\omega\,\mathrm{d}t$$

which is to say that,

$$E_s = \frac{1}{2}I\omega^2 + U_0 - mgl\cos(\theta),$$

with U_0 the reference potential energy.

2.) The phase portrait for this system is depicted in Figure 5.2.1. A trajectory that has exactly enough energy to swing up to vertical position, stop briefly and then fall back over is highlighted i.e. $(\theta,\omega) = (-\pi, 0.1)$.

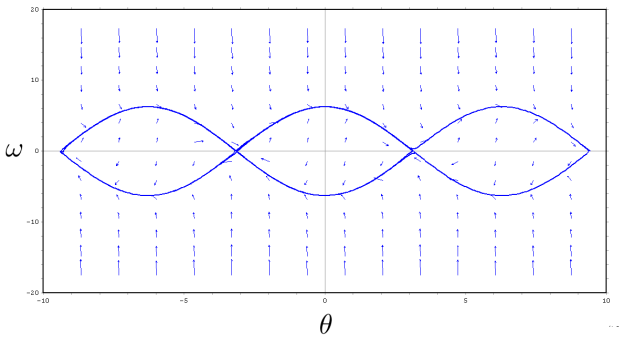

Figure 5.2.1: Pendulum Phase Portrait with critical swing up trajectory

Now if the control algorithm could asymptotically approach this energy, $E_d = 2mgl$ and maintain the system energy there, the pendulum would follow this trajectory and achieve the goal of swinging the pendulum up. If the energy function is suitably shaped such that a desirable trajectory already exists in the system, then this technique can be used to exponentially track this trajectory. Mathematically the goal is to have $E_s \to E_d$ i.e. $E_s - E_d = \tilde{E} \to 0$.

So the goal is to lift the system energy or lower the system energy plane, in the spirit of Figure 3.4.5, until it attains the correct level. This can be done by looking at the time derivative of $\tilde{E}$ i.e. the power, which, after some algebra, turns out to be,

$$\begin{aligned} \frac{\mathrm{d}}{\mathrm{d}t}\tilde{E} &= \dot{E}_s \\ &= \tau\omega. \end{aligned}$$

This is completely expected since E_d and E_0 are constants and more importantly, since there is no dissipation, the only power loss or gain is through the input torque, τ.

4.) The trick now is to make $\tau = -\kappa_p \omega \tilde{E}$ which yields,

$$\frac{\mathrm{d}}{\mathrm{d}t}\tilde{E} = -\kappa_p \omega^2 \tilde{E}. \tag{5.2.2}$$

Juxtapose equation (5.2.2) with a simple linear ODE $\dot{x} = -kx$ and it should be clear that as long as $\kappa_p > 0$, then $\tilde{E}$ will exponentially approach 0 as required. Figure 5.2.2 shows the system under this control law, $\kappa_p = 1$, for various initial conditions; it is clear that these initial conditions all reach the required swing up trajectory. The drawback being if the initial condition is $(\theta, \omega) = (k2\pi, 0)$, $k = \mathbb{Z}$, then the system will not swing-up due to the system being at a local minimum in the energy and $\tau = -\kappa_p(0)\tilde{E}$. The inclusion of the small impulse defined earlier will alleviate this problem.

Lastly, the swing-up problem with dissipation is solved using the integrator previously defined. Consider the dissipation function,

$$d(\omega)\omega = 5\,sgn(\omega) + 2\omega$$

which (loosely) models stiction at low speeds and viscous friction otherwise. This function is depicted in Figure 5.2.3.

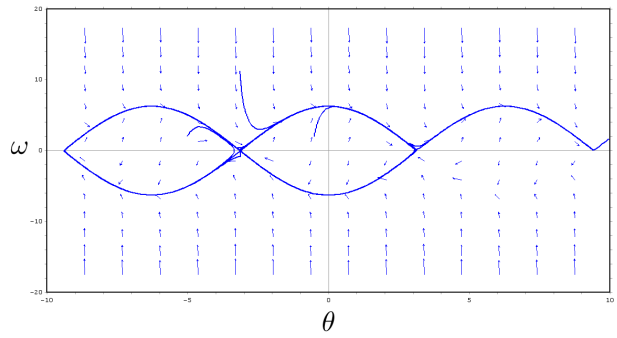

Figure 5.2.2: Phase Portrait of Pendulum System under Swing-up Control ($\kappa_p = 1$) for three different initial conditions, $[\theta, \omega] = \{[-0.5, 2], [-\pi, 11.25], [-5, 2]\}$

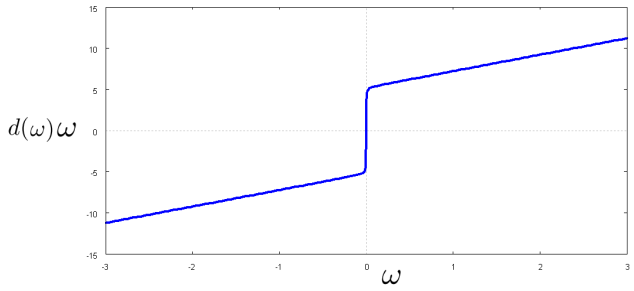

Figure 5.2.3: Dissipation function modelling Stiction and Viscous Damping

The system with dissipation is now,

$$I\ddot{\theta} + d(\omega)\omega + mgl\sin(\theta) \quad = \quad \tau.$$

With the existing control law, it is clear that the swing-up trajectory is never reached, as depicted in Figure 5.2.4.

4.) The control law is now

$$\begin{aligned} \tau &= -\kappa_p \omega \tilde{E} + \omega\zeta + A\,\delta(\omega) \\ \dot{\zeta} &= -\kappa_i \tilde{E}, \end{aligned}$$

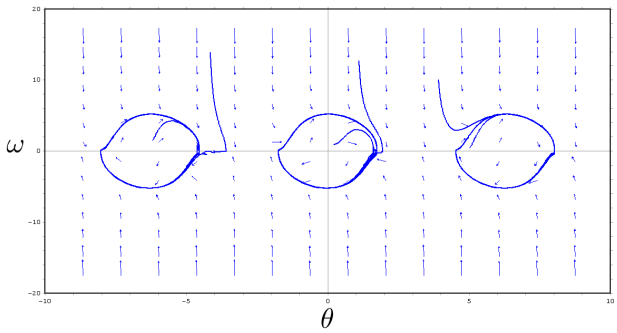

Figure 5.2.4: Phase plot for Pendulum under Swing-up Control with Dissipation

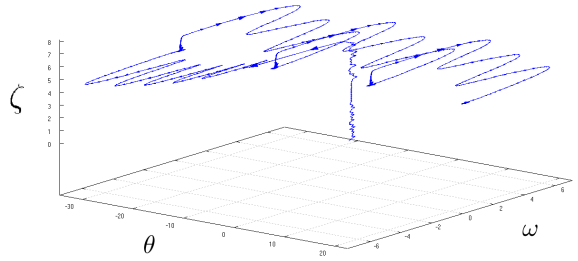

Figure 5.2.5: Three-dimensional Phase Portrait of Pendulum under Swing-Up Control with Integrator ($\kappa_p = 1$, $\kappa_i = 0.2$)

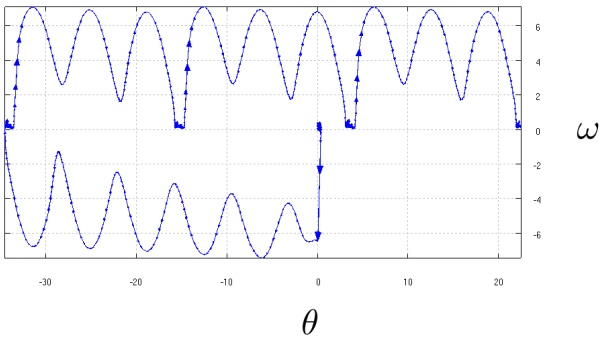

Figure 5.2.6: Two-dimensional Phase Portrait of Pendulum under Swing-Up Control with Integrator ($\kappa_p = 1$, $\kappa_i = 0.2$)

with constants $\kappa_p > 0$ and κ_i, A to be determined.

5.) Firstly $A > |d(\omega)\omega^2|$ for small ω which leads to $A > 5$, hence $A = 6$ is chosen. For a chosen κ_p, as long as $\kappa_i < \frac{\kappa_p^2}{4}$ then the eigenvalues for the virtual system will remain real. For comparison sake, $\kappa_p = 1$ as before and hence $\kappa_i < \frac{1}{4}$. Therefore a $\kappa_i = 0.2$ is chosen.

The three-dimensional phase portrait for initial condition $(\theta, \omega, \zeta) = (0,0,0)$, using this control law is depicted in Figure 5.2.5. It should be clear that the integrator ζ oscillates between 5 and 7 due to the dissipation changing with angular speed ω. Figure 5.2.6 depicts the system, viewed along the ζ axis i.e. the two-dimensional phase portrait. In both cases there appears to be an oscillation during the swinging phase but the system is swinging-up. The phase portrait does not appear as Figure 5.2.2, however it should be remembered that the system cannot swing-up without this integrator (See Figure 5.2.4). So at the very least the control problem is solved, although not ideally.

By modifying κ_i to allow for non-real eigenvalues the performance is improved, at the cost of overshoot (as with linear PI control). To ensure this condition, κ_i is chosen to be 4. The three-dimensional phase portrait is depicted in Figure 5.2.7. The overshoot is well evidenced in this figure since the value of ζ oscillates dramatically. However, at low speeds, the integrator almost tracks the dissipation function, as evidenced by the step-like rises along the ζ axis. It should be clear though, that the ideal swing-up trajectory of Figure 5.2.1 is more closely followed. The two-dimensional phase portrait (the system viewed along the ζ axis) is portrayed in Figure 5.2.8. The system is clearly seen to be oscillating between π

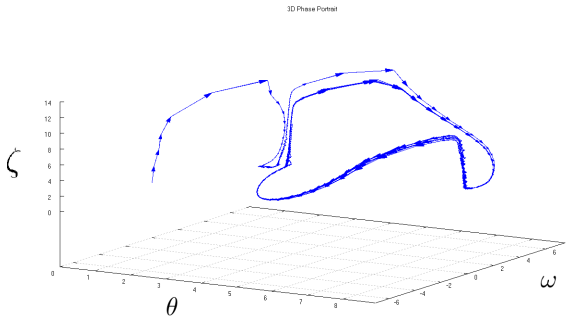

Figure 5.2.7: Three-dimensional Phase Portrait of Pendulum under Swing-Up Control with Integrator ($\kappa_p = 1$, $\kappa_i = 4$)

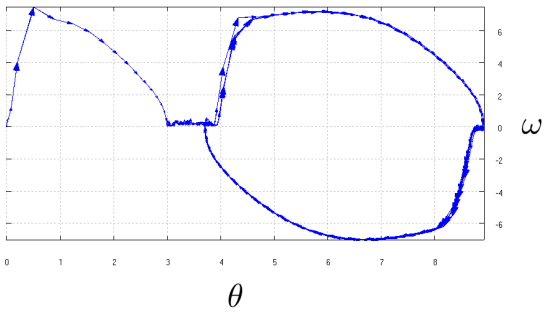

Figure 5.2.8: Two-dimensional Phase Portrait of Pendulum under Swing-Up Control with Integrator ($\kappa_p = 1$, $\kappa_i = 4$)

and 3π, as desired.

The inclusion of a non-linear integrator and impulse only at zero speed has clearly extended the technique of power shaping. It is now possible to actively compensate for a non-linear dissipation function, without feedback linearisation, in the power-shaping methodology. Furthermore, the method has been extended to include multi-dimensional systems as well as non-constant desired energy levels, E_d. So it should be possible now to have a given multi-variable, non-linear system , characterised by E_s, exponentially approach a desired system, characterised by E_d, using this technique, regardless of dissipation. The beauty of the Power-Shaping control law is that it causes the system to exponentially reach a natural trajectory i.e. a trajectory that the system is already capable of via the energy function.

Constructive methods for shaping the closed loop energy are presented next.

Constructive Methods for Energy-Shaping

5.3 Common Lyapunov Controller Interpolation

The so called "Heuristic Fuzzy Logic" controller of [13, 32] is a constructive method of choosing "fuzzy rules" that make a common Lyapunov function negative definite over the entire state space.

The basic idea in [13, 32] is to consider a number of "membership functions" $\mu_i(\mathbf{x}) : \left\{\mathbb{R}^N \to [0,1]\right\}$ (which are used for measuring the extent that the system is "in" the various regions of the state space), and associated outputs, $\mathbf{u}_i(\mathbf{x})$ (which are really just controllers) with k rules that are "defuzzified" via the algorithm

$$\mathbf{u}(\mathbf{x}) \quad = \quad \frac{\sum_i \mu_i(\mathbf{x})\mathbf{u}_i(\mathbf{x})}{\sum_i \mu_i(\mathbf{x})}.$$

The method is perhaps best grasped by way of a simple example.

Consider a scalar subset of the prototypical model,

$$m\ddot{x} + d(v)v + k(x) \quad = \quad u$$

with (for interest's sake) $k(x) = sin(x)$, $d(v) = |v|$ and m a constant. It is good to identify what this system appears as, and for all intents and purposes it appears as a pendulum in a viscous medium.

Choose the Lyapunov function as the energy

$$E(x,v) \quad = \quad \frac{1}{2}mv^2 + U_0 - cos(x)$$

where $U_0 = 1$ is the zero potential energy reference. This system has the derivative

$$\frac{\mathrm{d}}{\mathrm{d}t}E \quad = \quad -d(v)v^2 + u$$

which is expected from the methodology expounded upon in Chapter 4. Letting $u = 0$ and finding the equilibrium points of the system by looking at $\nabla E = 0$ yields the set

$$(x^*, v^*) \quad \in \quad [k\pi, 0]$$

for $k \in \mathbb{Z}$. Due to symmetry and because $k\pi$ (k odd) is a saddle point, it is best to limit the stability argument to $-\pi < x < \pi$. Now the power is zero iff $-d(v)v^2 = 0$ and hence the points (x^*, v^*), with $(k-2)\pi < x^* < k\pi$ and k odd, are locally asymptotically stable[9] as per the reasoning around La Salle's invariance principle in [15, Chapter 3.4.3]. Consider defining, as is usually done, three membership functions that determine whether a variable is positive, negative or zero [13]. Now to construct the two dimensional membership functions in the (x,v) state space the following is defined,

$$\mu_{XY}(x,v) \quad := \quad X(x)\,\mathrm{AND}\,Y(v)$$

[9] Getting a system like this to stabilise around $(x,v) = (0,0)$ is simple. All that is needed is a proportional controller with a gain large enough to overcome the energy in the minima of the potential function i.e. $u = -\kappa_p x$ with $\kappa_p > 1$.

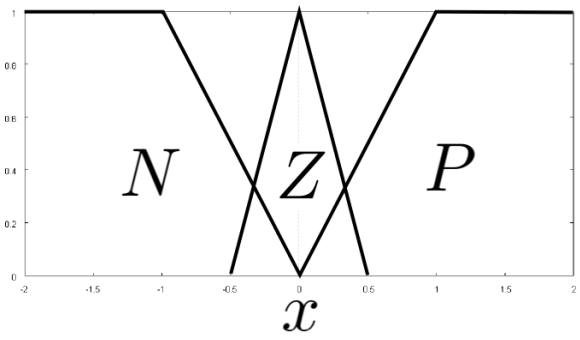

Figure 5.3.1: Positive, Negative and Zero membership functions

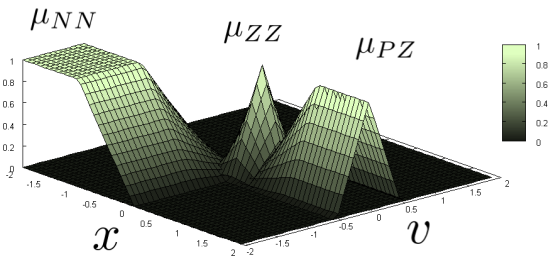

Figure 5.3.2: Membership Functions for 2D Phase Space

where μ_{XY} is the two dimensional membership function composed of one dimensional membership functions $X()$ AND $Y()$.

The fuzzy definition for AND is

$$X(x) \text{ AND } Y(v) \quad := \quad X(x)Y(v)$$

which can alternatively be defined as $min(X(x), Y(v))$ [46, Ch. 2.2.4].

As an example, three membership functions μ_{ZZ}, μ_{NN} and μ_{PZ} of the two dimensional state space (x, v) are depicted in Figure 5.3.2. These should be read as, for example, $\mu_{ZZ} := Z(x)$ AND $Z(v)$ in other words x is zero and v is zero. For comparison, the same sets are plotted using the alternate definition for AND, it is clear that the difference is in the gradients of the membership functions which takes on a stepped appearance in Figure 5.3.3.

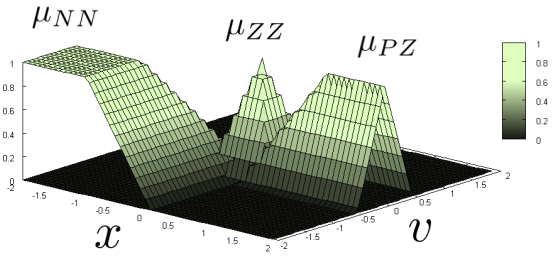

Figure 5.3.3: Membership functions for 2D Phase space using alternate definition of AND

Table 5.1: Fuzzy Rule Base (Control Law Interpolation Table)

Rule	Membership Function	Control Input	Lyapunov Function Derivative $\dot{V}$
1	μ_{PP}	$-u_{max}$	$\dot{V} = xv + v\frac{1}{m}\left(-\lvert v\rvert v - sin(x) - u_{max}\right)$
2	μ_{PZ}	$-\kappa_2 x$	$\dot{V} = xv + v\frac{1}{m}\left(-\lvert v\rvert v - sin(x) - \kappa_2 x\right)$
3	μ_{PN}	$-\kappa_3 x$	$\dot{V} = xv + v\frac{1}{m}\left(-\lvert v\rvert v - sin(x) - \kappa_3 x\right)$
4	μ_{ZP}	$-\kappa_4 x$	$\dot{V} = xv + v\frac{1}{m}\left(-\lvert v\rvert v - sin(x) - \kappa_4 x\right)$
5	μ_{ZZ}	$-\kappa_5 x - \delta_5 v$	$\dot{V} = xv + v\frac{1}{m}\left(-\lvert v\rvert v - sin(x) - \kappa_5 x - \delta_5 v\right)$
6	μ_{ZN}	$-\kappa_6 x$	$\dot{V} = xv + v\frac{1}{m}\left(-\lvert v\rvert v - sin(x) - \kappa_6 x\right)$
7	μ_{NP}	$-\kappa_7 x$	$\dot{V} = xv + v\frac{1}{m}\left(-\lvert v\rvert v - sin(x) - \kappa_7 x\right)$
8	μ_{NZ}	$-\kappa_8 x$	$\dot{V} = xv + v\frac{1}{m}\left(-\lvert v\rvert v - sin(x) - \kappa_8 x\right)$
9	μ_{NN}	u_{max}	$\dot{V} = xv + v\frac{1}{m}\left(-\lvert v\rvert v - sin(x) + u_{max}\right)$

Now each of the membership functions defined like this are given corresponding control inputs, which is the "fuzzy rule base" in [13, 32]. The rule base will typically take on the form of Table 5.1, where u_{max} is the desired saturation limit of the control law [13, 32]. The derivative of the Lyapunov function is included to show the negative definiteness under the various control inputs. The great part about the technique is that assumptions can be made about the sign of the various co-ordinates (x, v) due to the membership functions defining this region of the state space. Note that a different Lyapunov function,

$$V = \frac{1}{2}(x^2 + v^2)$$

is used here to illustrate the method, with

$$\dot{V} = xv + v\frac{1}{m}\left(u - \lvert v\rvert v - sin(x)\right).$$

If the energy of the system is used as the Lyapunov function, then the resulting control laws are trivially shown to stabilise the system. A few select rules are analysed to show the logic behind these rules, which are similar to [13, 32]. Look at Rule 1, bearing in mind that since μ_{PP} defines the region that this control law is valid, it implies that both x and v are positive. Now the derivative of the Lyapunov function V needs to be negative definite in this region to prove stability, hence $\lvert u_{max}\rvert > \lvert mx + sin(x)\rvert$ since $-\frac{1}{m}\lvert v\rvert v^2$ is negative already. In this discussion $-\frac{1}{m}\lvert v\rvert v^2$ is *always* negative hence it is not referred to explicitly from now on.

Rule 2, x is positive and $\lvert v\rvert < 0.5$ therefore $\kappa_2 x > mx + sin(x)$ and so $\kappa_2 = 2.1m$ suffices.

Rule 3, now x is positive and v is negative which makes the term xv negative hence all that is required is that $\kappa_3 x > sin(x)$ which means that $\kappa_3 = 1.1$ suffices.

Rule 4, $\lvert x\rvert < 0.5$ and v is positive, therefore $\kappa_4 x > m0.5 + sin(x)$ and so $\kappa_4 = 1.1m$.

Rule 5 has a PD controller with $|x| < 0.5$ and $|v| < 0.5$ and therefore $\kappa_5 x + \delta_5 v > mxv + sin(x)$ which has $\kappa_5 = 1.1$ and $\delta_5 = 1.1m$ as a solution.

Rule 6, 7 and 8 all have the same relations as κ_4, κ_3 and κ_2 respectively due to symmetry.

Rule 9 has some subtlety to it, since x is negative and v is negative. Therefore the trick is to factorise into $v\left(-x - \frac{1}{m}sin(x) + \frac{1}{m}u_{max}\right)$, remembering that x is negative and again ignore $-\frac{1}{m}|v|v^2$. Now if $\left(-x - \frac{1}{m}sin(x) + \frac{1}{m}u_{max}\right)$ is positive then the product $v\left(-x - \frac{1}{m}sin(x) + \frac{1}{m}u_{max}\right)$ will be negative as required. Therefore $|u_{max}| > |mx + sin(x)|$ which is the same as Rule 1. The engineering reason for making u_{max} positive and adopting this strategy is easier to see; if the position is negative and moving away from the origin, then push as hard as possible in the direction of the origin i.e. the positive direction.

Employing now the weighted sum "defuzzification", the controller interpolation is readily apparent i.e.

$$u(x) = \frac{\mu_{PP}(-u_{max}) + \mu_{PZ}(-\kappa_2 x) + \ldots \mu_{NN}(u_{max})}{\mu_{PP} + \mu_{PZ} + \ldots \mu_{NN}}$$

with all the μ expanded it is,

$$u(x) = \frac{P(x)P(v)(-u_{max}) + P(x)Z(v)(-\kappa_2 x) + \ldots N(x)N(v)(u_{max})}{P(x)P(v) + P(x)Z(v) + \ldots N(x)N(v)}.$$

In the resulting control algorithm, it is mostly proportional feedback and the footnote in the introduction of this problem shows why this is all that was really needed. The system initially used to demonstrate this technique in [13] had exactly the same global stability properties as this example and could have used proportional feedback exclusively as well.

Some special cases of the technique which are worth mentioning follow on from this.

Consider a uniform control strategy, $-\mathbf{Kx}$ say, adopted for all regions in a general state space, $\mathbf{x}$.

Then

$$\begin{aligned}\mathbf{u}(\mathbf{x}) &= \frac{\mu_1(-\mathbf{Kx}) + \mu_2(-\mathbf{Kx}) + \ldots \mu_N(-\mathbf{Kx})}{\mu_1 + \mu_2 + \ldots \mu_N} \\ &= \frac{(\mu_1 + \mu_2 + \ldots \mu_N)(-\mathbf{Kx})}{(\mu_1 + \mu_2 + \ldots \mu_N)} \\ &= -\mathbf{Kx}\end{aligned}$$

i.e. the control law is pure state feedback with a gain $\mathbf{K}$ that satisfies stability in all of the regions considered due to the common Lyapunov considerations.

Consider that the states $\mathbf{x}$ are such that they belong exclusively[10] to a membership function, μ_k, then

$$\begin{aligned}\mathbf{u}(\mathbf{x}) &= \frac{\mu_k(\mathbf{u}_k(\mathbf{x}))}{\mu_k} \\ &= \mathbf{u}_k(\mathbf{x})\end{aligned}$$

[10]Which is to say that all other membership functions return zero

which is just the control law for that region of the state space. Hence the denominator of the "defuzzification" algorithm has normalised the influence of the membership function, μ_k, on the control law, $\mathbf{u}_k(\mathbf{x})$.

Consider now that the states, $\mathbf{x}$, are in a region which belongs to two membership functions, $\mu_1 = 0.25$ and $\mu_2 = 0.75$, and no others then

$$\begin{aligned}\mathbf{u}(\mathbf{x}) &= \frac{\mu_1(\mathbf{u}_1(\mathbf{x})) + \mu_2(\mathbf{u}_2(\mathbf{x}))}{\mu_1 + \mu_2} \\ &= 0.25(\mathbf{u}_1(\mathbf{x})) + 0.75(\mathbf{u}_2(\mathbf{x}))\end{aligned}$$

which demonstrates an interpolation between the two different control strategies. The system is 0.75 in the μ_2 region of the state space and hence the control law consists of 0.75 the control law appropriate to that region of the state space.

It should be clear now that this technique is really one of controller interpolation using a common Lyapunov function for stability assessment.

Design of Common Lyapunov Interpolated Controllers

The general design technique adapted from [13, 32] is now presented.

1. Choose a Lyapunov function appropriate for the problem.
2. Choose regions of the state space to consider and define them using overlapping membership functions. The membership functions must be functions defined such that they map $\mathbb{R}^N \to [0,1]$ only, where $\mathbb{R}^N$ is the dimension of the state space.
3. Go through each membership function and find a controller that makes the Lyapunov function negative definite. Honour the bounds on the states set by the membership functions.
4. Lastly, interpolate amongst the controllers using the weighted defuzzification algorithm.

It is possible to use more extravagant membership functions which solve the problem more elegantly and require fewer rules. One such example is in [32], where a sliding mode controller was combined with a state feedback controller such that, when the system was away from the switching surface, the sliding mode controller was employed and when on the switching surface, the state feedback controller was employed. Not mentioned in that paper was that, the state feedback controller included feedback linearisation. Nevertheless, the combination proved successful when applied in simulation to the inverted pendulum on a cart control problem. Moreover, the control problem only required two controllers to be interpolated for a four dimensional system, instead of the nine for the simple second order problem presented previously.

An idea, inspired by the work in [32], as a general non-linear control paradigm is to form a linear controller, in the usual way, around an equilibrium point, and define a membership function for this region of linearity and then to find a non-linear controller which will drive the system to this region. This sort of strategy is often employed in control of the inverted pendulum and its ilk, where a "swing-up" controller is switched out for an LQR controller when the pendulum reaches the linear region [11, 48]. The drawback of the strategy is that there is a "hard" switch between the different controllers which introduces transients [11, 48]. This switching transient problem is alleviated by interpolating between the controllers using the weighted sum defuzzification method, just as the alleviation of chattering in the sliding mode control was achieved in [32].

Control Interpolation for the Simple Inverted Pendulum

Consider the well known simple pendulum with energy

$$E = \frac{1}{2}I\omega^2 + U_0 - mgl\cos(\theta)$$

and power

$$\dot{E} = \tau\omega$$

which has the model (using the conservation of energy from Chapter 4)

$$I\ddot{\theta} + mgl\sin(\theta) = \tau.$$

Note $g = 9.81$ m/s^2 is the gravitational constant, $l = 1$ m is the length of the pendulum, $m = 0.5$ kg is the mass at the tip of the pendulum, $I = ml^2$ is the moment of inertia about the hinge and τ is the input torque. Notice that this is a frictionless model.

The goal is to get θ to stabilise about the upright position $k\pi$ with k odd.

1.) The energy is chosen as a Lyapunov function.

First Attempt: Constant Torque with State Feedback

Membership Functions

2.) The upright position is really an infinite number of equilibrium points since it is $\theta = k\pi$ with k odd. So to try to have membership functions which are positive, negative and zero about the equilibrium points it is necessary to have an infinite number of such membership functions. Fortunately, this problem was addressed in [49], in which a trigonometric potential function in the IDAPBC methodology solved a similar problem. Now, by borrowing this idea and adapting it for the purposes here, the desired infinite number of membership functions is elegantly solved. In other words, a trigonometric membership function will honor the required equivalence of $\theta = k\pi$, k odd. Hence the membership functions for the θ co-ordinate are chosen as,

$$\begin{aligned} \mu_Z &= \cos(\frac{1}{2}(x-\pi))^2 \\ \mu_{\bar{Z}} &= 1-\mu_z, \end{aligned}$$

with μ_z read as zero and $\mu_{\bar{Z}}$ read as not zero, these are depicted in Figure 5.3.4. 3.) Consider the control strategy: if the angle is not near zero apply a constant torque, if the angle is near zero then use a PD controller (State Feedback) that honours $\theta = k\pi$, k odd. It is intuitive that this strategy should be feasible. The control law is presented in Table 5.2. It should be noticed that the first controller is not actually negative definite unless $\omega < 0$. However, due to the symmetry of the problem, this presents no challenge as the pendulum can only rotate and hence, an equilibrium point is always available as long as the pendulum spins far enough around. It is also interesting to note that in the Lyapunov framework, if the Lyapunov function's derivative is not negative (semi) definite then no conclusion can be drawn about stability. However, since the energy of the system has been chosen as the

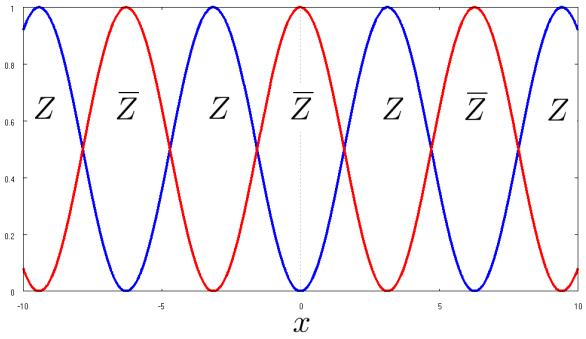

Figure 5.3.4: Zero and Non-Zero Membership Functions for $\theta = k\pi$

Table 5.2: Pendulum Control Law Interpolation Table

Membership Function	Controller	Lyapunov Function Derivative
$\mu_{\bar{Z}}(\theta)$	u_{max}	$\dot{E} = u_{max}\omega$
$\mu_Z(\theta)$	$-\kappa_p \sin(\theta-\pi) - \kappa_d\,\omega$	$\dot{E} = -\kappa_p \sin(\theta-\pi)\omega - \kappa_d\,\omega^2$

Lyapunov function, physical grounds can be used to reason that this is, in fact, a stabilising controller.

The controller for the region $\mu_Z(\theta)$ requires some explanation: the $-\sin(\theta-\pi)$ has the required "first and third quadrant" behaviour around any odd multiple for $2n\pi < |\theta| < 2(n+1)\pi$ for $n \in \mathbb{N}$ and therefore asymptotically stabilises the system, as per Chapter 3.1. The Lyapunov function's derivative (power) is only negative definite when $\kappa_d > \kappa_p$. It will be shown next that this restriction can be relaxed using an energy argument.

Now at its heart, this control law is $-\kappa_p \sin(\theta-\pi) - \kappa_d\,\omega$, which can be interpreted via the energy-balancing methodology from Chapter 5.1. Essentially, what has happened is an adjustment of the potential function i.e. a desired energy of,

$$\begin{aligned} E_d &= \frac{1}{2}I\omega^2 + \int \kappa_p \sin(\theta-\pi)\,\mathrm{d}\theta + mgl\int \sin(\theta)\,\sin\mathrm{d}\theta + U_0 \\ &= \frac{1}{2}I\omega^2 + U_0 + \kappa_p\cos(\theta) - mgl\cos(\theta), \end{aligned}$$

which is tantamount to an inversion of the potential function for $\kappa_p = 2mgl$, and the inclusion of viscous friction,

$$\dot{E}_d = -\kappa_d\,\omega^2.$$

So, what once needed some dancing around and a bit of luck in arriving at, namely, $u = -\kappa_p \sin(\theta-\pi)$, is arrived at in a straight forward manner in the energy balancing framework. As with the first example in this section, all that is really needed is a relatively simple control law $u = -\kappa_p \sin(\theta-\pi) - \kappa_d\,\omega$, which will globally stabilise the pendulum at $\theta = k\pi$ for k odd, provided that $\kappa_p = 2mgl$ exactly and $\kappa_d > 0$, which will eventually dampen out the oscillations about $\theta = k\pi$ for k odd.

4.) The phase portrait in Figure 5.3.5 for this control scheme shows the global stability of the points $(\theta,\omega) = (k\pi, 0)$ for k odd. For comparison's sake, the potential inversion controller

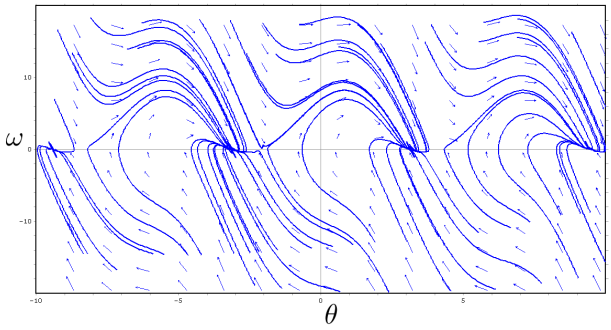

Figure 5.3.5: Phase Portrait of Constant Torque/PD Controller ($\kappa_p = 10$, $\kappa_d = 4.5$, $u_{max} = 10$)

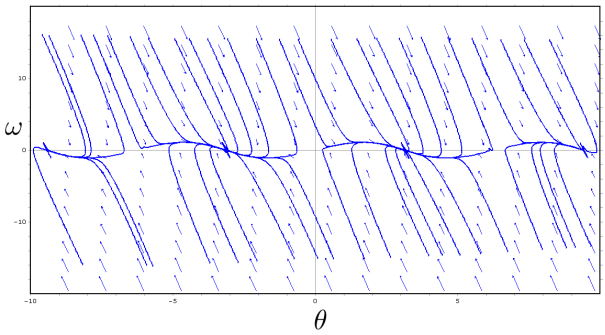

Figure 5.3.6: Phase Portrait of Gravity Inversion/Damping ($\kappa_d = 4.5$)

alluded to has the phase portrait depicted in Figure 5.3.6. It, too, globally stabilises the system.

Second Attempt: Swing-up Controller with State Feedback

2.) The membership functions that are employed in this technique are two-dimensional, since ω is part of the swing up control strategy. An additional membership function for low angular speeds is

$$\mu_L = e^{-x^2},$$

which is the Gaussian function. Now the two regions for the state space (θ, ω) are given as

$$\begin{aligned} \mu_{ZL} &= \mu_Z(\theta)\mu_L(\omega) \\ \mu_{\bar{Z}L} &= 1 - \mu_{ZL}, \end{aligned}$$

which should be read as "near equilibrium" AND "near low speeds" for μ_{ZL}. Finally, $\mu_{\bar{Z}L}$ should be read as, "not near zero equilibrium" AND "not near low speeds". These membership functions are depicted in Figure 5.3.7 and Figure 5.3.8 respectively.

3.) The control scheme is to use the swing up controller if the system is not near the equilibrium point and not at low speeds i.e. $u_{\bar{Z}L}$ is the swing-up power shaping controller from Chapter 5.2, $-(E_s - mgl)\omega$. The same controller as the first attempt is used for the region μ_{ZL} which is, $-\kappa_p \sin(\theta - \pi) - \kappa_d \omega$. 4.) The resulting phase portrait (Figure 5.3.9) shows the global stability of the control strategy around $(\theta, \omega) = (k\pi, 0)$ for k odd.

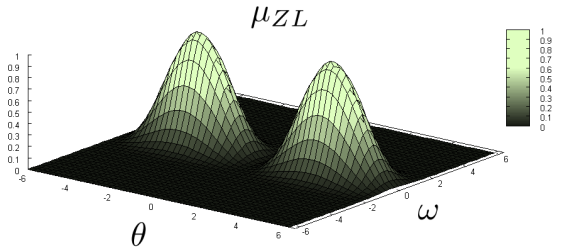

Figure 5.3.7: Zero Angle and Low Speed Membership Functions

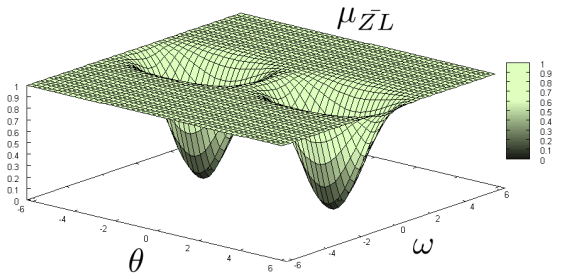

Figure 5.3.8: Not Zero Angle and Not Low speed Membership Functions

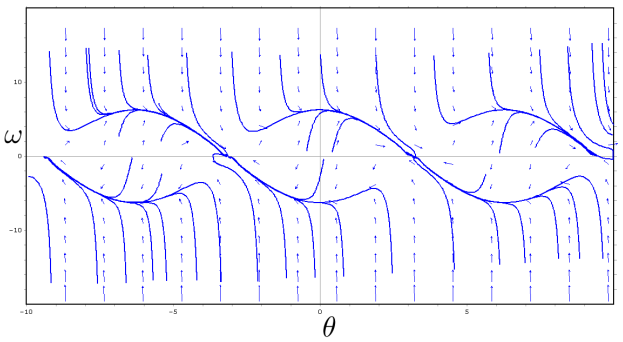

Figure 5.3.9: Phase Portrait of Swing-up/PD ($\kappa_p = 10$, $\kappa_d = 4.5$)

The usefulness of being able to smoothly interpolate between different controllers has clearly been demonstrated with this technique. Moreover, the framework guarantees stability in a constructive manner, using a common Lyapunov function. It is hoped that light has been shed on an idea that was obscured in fuzzy control system terminology.

5.4 Energy Shaping Robot Control

Robotics has a rich history and is an excellent example of how physical insight and energy considerations lead to a successful and intuitive non-linear control methodology [2, 14], [15, Ch. 9]. In [15, Ch. 9] the idea was put forward of using robotics as a template for non-linear control of multiple input multiple output (MIMO) systems. The model equations for a general N degree of freedom robot appear similar to the prototypical model eq (3.1.1), indeed robotics was one of the inspirations for settling on this structure.

The N degree of freedom robot equations are given by [15, Ch. 9.1] and [14] as

$$\mathbf{H}(\mathbf{q})\ddot{\mathbf{q}} + \mathbf{C}(\mathbf{q},\dot{\mathbf{q}})\dot{\mathbf{q}} + \mathbf{g}(\mathbf{q}) \quad = \quad \tau$$

where $\mathbf{q} \in \mathbb{R}^N$ is the vector of the N generalised co-ordinates, $\mathbf{H}(\mathbf{q})$ is the inertia matrix, $\mathbf{C}(\mathbf{q},\dot{\mathbf{q}})$ is the Coriolis and Centripetal matrix, $\mathbf{g}(\mathbf{q})$ is the gravitational force matrix and $\tau \in \mathbb{R}^N$ are the applied torques[11]. There is a slight difference in that [14] includes the time derivative of the inertia matrix with $\mathbf{C}(\mathbf{q},\dot{\mathbf{q}})$ as

$$\mathbf{H}(\mathbf{q})\ddot{\mathbf{q}} + \left(\mathbf{C}(\mathbf{q},\dot{\mathbf{q}}) + \frac{\mathbf{1}}{\mathbf{2}}\dot{\mathbf{H}}(\mathbf{q})\right)\dot{\mathbf{q}} + \mathbf{g}(\mathbf{q}) \quad = \quad \tau, \tag{5.4.1}$$

however the energy balance is the same (as it must be) in both cases. It should be clear that τ is an $N \times 1$ vector of input torques and hence the robotic system must be fully actuated. This fact is crucial for the development of the control laws that follow.

What is not considered in neither [14] nor [15, Ch. 9], is the inclusion of dissipation in the term linear in $\dot{\mathbf{q}}$. This term is present in the prototypical model. It is interesting to note that [14] has also solved robotics problems where constraints are considered and which is also presented in this section.

The robot equation eq (5.4.1) is clearly a subset of the prototypical model eq (3.1.1) which is repeated for reference purposes

$$\mathbf{M}(\mathbf{x},t)\ddot{\mathbf{x}} + \mathbf{D}(\mathbf{x},\mathbf{v})\mathbf{v} + \mathbf{K}(\mathbf{x}) \quad = \quad \mathbf{G}(\mathbf{x})\mathbf{u}$$

with $\mathbf{D}(\mathbf{x},\mathbf{v}) = \mathbf{R}(\mathbf{x},\mathbf{v}) + \mathbf{J}(\mathbf{x},\mathbf{v}) + \frac{1}{2}\dot{\mathbf{M}}(\mathbf{x},t)$, $\mathbf{x} \in \mathbb{R}^N$ and $\mathbf{v} = \dot{\mathbf{x}}$. There are a number of energy shaping controllers for robotics and are presented separately as solutions appropriate to position regulation and trajectory tracking.

Position Regulation

For position regulation, [15, Ch. 9.1.1] uses energy considerations to show that the control law

$$\tau \quad = \quad -\mathbf{K_p}\tilde{\mathbf{q}} - \mathbf{K_d}\dot{\mathbf{q}}, \tag{5.4.2}$$

with $\tilde{\mathbf{q}} = \mathbf{q} - \mathbf{q}^*$ and $\mathbf{q}^*$ the desired position vector, causes the system states $\mathbf{q}$ in eq (5.4.1) to reach the desired states $\mathbf{q}^*$, iff $\mathbf{g}(\mathbf{q}) = \mathbb{O}$ and $\mathbf{K_p} > 0$ and $\mathbf{K_d} > 0$ [15, Ch. 9.1.1]. Note

[11] Note that the condition on the torques implicitly defines the system as fully actuated.

that there is a subtlety here in that the error $\tilde{\mathbf{q}}$ is composed in the position but not the velocity as in conventional PD control. This is further enhanced in [14] via the celebrated PD plus gravity compensation via

$$\tau = -\mathbf{K_p}\tilde{\mathbf{q}} - \mathbf{K_d}\dot{\mathbf{q}} + \mathbf{g}(\mathbf{q}) \tag{5.4.3}$$

which cancels out the gravity term in eq (5.4.1). However eq (5.4.3) requires online computation of the gravity term and adds to the computational burden of the control law, eq (5.4.2), in line with the Controller Complexity principle. Notice that this is the exact same control law derived via Energy-Balancing in Chapter 5.1.

To reduce this computational burden, eq (5.4.3) is modified into,

$$\tau = -\mathbf{K_p}\tilde{\mathbf{q}} - \mathbf{K_d}\dot{\mathbf{q}} + \mathbf{g}(\mathbf{q_d}), \tag{5.4.4}$$

and is referred to as a PD plus target torque regulation controller [14]. This control law is analysed in terms of its energy effects in Chapter 5.1.

Proof of Position Regulation

All three position regulation techniques have Lyapunov stability proofs to show their asymptotic stability properties. These are presented here and are adapted from [14] and [15, Ch. 9] .

All three proofs use a Lyapunov function,

$$\frac{\mathrm{d}}{\mathrm{d}t}\left(\frac{1}{2}\dot{\mathbf{q}}^{\mathbf{T}}\mathbf{H}(\mathbf{q})\dot{\mathbf{q}} + \bar{\mathbf{P}}(\tilde{\mathbf{q}})\right) = -\dot{\mathbf{q}}^{\mathbf{T}}\left(\mathbf{C}(\mathbf{q},\dot{\mathbf{q}}) + \mathbf{K_d}\right)\dot{\mathbf{q}},$$

where $\bar{\mathbf{P}}(\tilde{\mathbf{q}})$ is a modified potential function of $\tilde{\mathbf{q}}$. To find $\bar{\mathbf{P}}(\tilde{\mathbf{q}})$, compute the inner product of eq. 5.4.1 (with the appropriate control law) and $\dot{\mathbf{q}}$.

Next, use $\frac{1}{2}\dot{\mathbf{q}}^{\mathbf{T}}\mathbf{H}(\mathbf{q})\dot{\mathbf{q}} + \bar{\mathbf{P}}(\tilde{\mathbf{q}})$ as a Lyapunov function and choose $\mathbf{K_p}$ so that $\bar{\mathbf{P}}(\tilde{\mathbf{q}})$ is positive definite. As long as $\mathbf{K_d} + \mathbf{C}(\mathbf{q},\dot{\mathbf{q}})$ is positive definite, then Lyapunov's second theorem can successfully be applied and convergence of $\tilde{\mathbf{q}} \to 0$ and $\dot{\mathbf{q}} \to 0$ is asymptotically ensured.

■

If the control objective is in some other co-ordinate system (say $\mathbf{x}$) other than the model co-ordinates (say $\mathbf{q}$) where $\mathbf{x} = \mathbf{f}(\mathbf{q})$ then eq (5.4.3) becomes

$$\tau = -\kappa_p \frac{\partial \mathbf{x}^{\mathrm{T}}}{\partial \mathbf{q}}(\mathbf{x} - \mathbf{x}^*) - \mathbf{K_d}\dot{\mathbf{q}} + \mathbf{g}(\mathbf{q}) \tag{5.4.5}$$

with κ_p some positive constant [14]. This control law will guarantee asymptotic convergence to the target co-ordinates, provided that $\mathbf{x}$ is of the same dimension as $\mathbf{q}$; if it is not, then the Jacobian $\partial \mathbf{x}^{\mathrm{T}}/\partial \mathbf{q}$ will be non-square and have multiple solutions for $\mathbf{q}$ at $\mathbf{x}^*$ [14]. This is called the "*ill-posedness of inverse kinematics*" [14]. The stability proof for this controller uses a Lyapunov function

$$E = \frac{1}{2}\dot{\mathbf{q}}\mathbf{H}(\mathbf{q})\dot{\mathbf{q}} + \frac{\kappa}{2}||\tilde{\mathbf{x}}||^2$$

with

$$\frac{\mathrm{d}}{\mathrm{d}t}E = -\dot{\mathbf{q}}^{\mathrm{T}}\mathbf{K_d}\dot{\mathbf{q}}$$

which is clearly an energy argument for stability [14].

Constraint Considerations

The following is a modification of [14]:

given constraints that the system needs to honour during operation, of the form,

$$\phi(\mathbf{x}) = 0$$

where the dimension of $\mathbf{x}$ is equal to the dimension of $\mathbf{q}$ related by $\mathbf{x} = \mathbf{f}(\mathbf{q})$, then the control law

$$\tau = \mathbf{g}(\mathbf{q}) - \mathbf{K_d}\dot{\mathbf{q}} - \frac{\partial \mathbf{x}^{\mathrm{T}}}{\partial \mathbf{q}}\left\{\kappa_p(\mathbf{x} - \mathbf{x}^*) + \lambda_d \frac{\partial \phi(\mathbf{x})}{\partial \mathbf{x}}\right\}$$

causes the system to asymptotically approach $\mathbf{x}^*$ with the Lagrange multiplier $\lambda \to \lambda_d$ as time $t \to \infty$ [14]. The Lagrange multiplier is interpreted as the normal force of the system on the constraint surface in the robot context [14].

Trajectory Tracking Control

The issue of trajectory tracking for Robotics is addressed very simply in [15, Ch. 9.1.2] and [42]. The essential idea follows the Controller Complexity principle in that, the controller has the same mathematical structure as the plant with a feedback term for stability.

Perfect Tracking

If there is no plant-model mismatch then trajectory tracking is trivial and involves clever use of the equality in eq (3.1.1), the idea has been adapted for the prototypical model from [39, Ch. 13]. One first *specifies* a desired trajectory, $\mathbf{x_d} \in \mathbb{R}^N$, that is at least twice differentiable [39, Ch. 13]. Once this trajectory has been specified, simply substitute it into the model equations and the resulting input forces will be the forces that must be applied to the system to achieve that trajectory [39, Ch. 13]. The fundamental requirement for this concept to work is that the initial conditions are the same, $\mathbf{x_d}(0) = \mathbf{x}(0)$ and that, in modern control terms, the system is fully-actuated [39, Ch. 13]. This technique is actually *plant inversion* and provides exact tracking, assuming no disturbance and no plant-model mismatch.

Proof

Given the model eq (3.1.1), the input for a desired trajectory $\mathbf{x_d}$ is

$$\mathbf{G}(\mathbf{x})^{-1}\left(\mathbf{M}(\mathbf{x_d},t)\ddot{\mathbf{x}}_\mathbf{d}+\mathbf{D}(\mathbf{x_d},\mathbf{v_d})\mathbf{v_d}+\mathbf{K}(\mathbf{x_d})\right) \quad = \quad \mathbf{u}$$

which when substituted into the model results in

$$\mathbf{M}(\mathbf{x},t)\ddot{\mathbf{x}}+\mathbf{D}(\mathbf{x},\mathbf{v})\mathbf{v}+\mathbf{K}(\mathbf{x}) \quad = \quad \mathbf{G}(\mathbf{x})\mathbf{G}(\mathbf{x})^{-1}\left(\mathbf{M}(\mathbf{x_d},t)\ddot{\mathbf{x}}_\mathbf{d}+\mathbf{D}(\mathbf{x_d},\mathbf{v_d})\mathbf{v_d}+\mathbf{K}(\mathbf{x_d})\right).$$

Given that $\mathbf{x_d}(0)=\mathbf{x}(0)$ at time $t=0$ and exact equality of all vector functions (i.e. no plant-model mismatch) the above equality is valid.

Hence, by induction the equality is valid for all subsequent times.

Hence $\mathbf{x}=\mathbf{x_d}$ for all time $t\geq 0$.

■

The fact that plant inversion is taking place is easy to see in a scalar linear analogy to the prototypical model i.e.

$$M\ddot{x}+D\dot{x}+Kx \quad = \quad Gu$$

which has the Laplace transform

$$\left(Ms^2+Ds+K\right)X(s) \quad = \quad GU(s)$$

with transfer function from u to x of

$$\frac{X(s)}{U(s)} \quad = \quad \frac{G}{(Ms^2+Ds+K)}.$$

Now, using the technique of specifying the trajectory x_d and solving for u results in

$$M\ddot{x}_d+D\dot{x}_d+Kx_d \quad = \quad Gu$$

and has transfer function from x_d to u of

$$\frac{U(s)}{X_d(s)} \quad = \quad \frac{\left(Ms^2+Ds+K\right)}{G}$$

which is clearly the inverse of the plant transfer function.

Furthermore, the transfer function from x_d to x is then

$$\begin{aligned}\frac{X(s)}{X_d(s)} &= 1\\ X(s) &= X_d(s)\end{aligned}$$

which is perfect tracking. This scalar linear analogy is consistent with the results from the non-linear prototypical framework and hence the term *plant inversion* is used.

Exponential Tracking

The plant inversion result should be juxtaposed with the observer and controller results in Chapter 3.3, which had the identical structure but included a feedback term, which allowed for exponential tracking. Hence the result can be modified to include this term, from which the same conclusions can be drawn i.e. the virtual system

$$\mathbf{M}(\mathbf{x},t)\dot{\nu} + \mathbf{D}(\mathbf{x},\mathbf{v})\nu + \mathbf{K}(\mathbf{x}) \quad = \quad \mathbf{G}(\mathbf{x})\mathbf{u} - \mathbf{K_d}(\nu - \mathbf{v}) \tag{5.4.6}$$

with virtual state $\chi \in \mathbb{R}^N$, virtual velocity $\nu = \dot{\chi}$ contains the system for $\chi = \mathbf{x}$, $\nu = \mathbf{v}$ and a controller for $\chi = \mathbf{x_r}$, $\nu = \mathbf{v_r}$. All that remains is to prove contraction with the virtual system and the controller, implicitly defined by eq (5.4.6), will exponentially track a desired reference trajectory $\mathbf{x_r}$ according to contraction theory[12]. This example is very similar to what was done in the robot manipulator control design in [42].

Proof of Contraction (adapted from [42])

Taking the time derivative of the general metric $\frac{1}{2}\delta\nu^{\mathrm{T}}\mathbf{M}(\mathbf{x},t)\delta\nu$ leads to

$$\frac{\mathrm{d}}{\mathrm{d}t}\left(\frac{1}{2}\delta\nu^{\mathrm{T}}\mathbf{M}(\mathbf{x},t)\delta\nu\right) \quad = \quad -\delta\nu^{\mathbf{T}}\mathbf{R}(\mathbf{x},\mathbf{v})\delta\nu - \delta\nu^{\mathbf{T}}\mathbf{K_d}\delta\nu$$

since $\mathbf{J}(\mathbf{x},\mathbf{v})$ is skew-symmetric and the $\frac{1}{2}\dot{\mathbf{M}}(\mathbf{x},t)$ cancels on both sides. Hence the system contracts for $\delta\nu$.

■

Given that the system contracts for $\delta\nu$ implies that $\mathbf{v} \to \mathbf{v_r}$ exponentially. The trick then is to choose

$$\mathbf{v_r} \quad = \quad \mathbf{v_d} - \Lambda(\mathbf{x} - \mathbf{x_d})$$

with Λ a Hurwitz matrix to ensure exponential tracking of $\mathbf{x} \to \mathbf{x_d}$ [42].

This implies that the control law,

$$\mathbf{u} \quad = \quad \mathbf{G}(\mathbf{x})^{-1}\left(\mathbf{M}(\mathbf{x},t)\dot{\mathbf{v}}_\mathbf{r} + \mathbf{D}(\mathbf{x},\mathbf{v})\mathbf{v_r} + \mathbf{K}(\mathbf{x})\right) + \mathbf{K_d}(\mathbf{v_r} - \mathbf{v}),$$

will exponentially track a given reference trajectory $\mathbf{x_d}$ for some $\mathbf{K_d} > 0$, Hurwitz matrix Λ and $\mathbf{v_r} = \mathbf{v_d} - \Lambda(\mathbf{x} - \mathbf{x_d})$.

[12] See Chapter 3.3

Tracking: Feedback Linearisation

This idea is known as the computed torque method in robotics and involves feedback linearisation with

$$\tau \;=\; \mathbf{H}(\mathbf{q})\mathbf{r}+\mathbf{C}(\mathbf{q},\dot{\mathbf{q}})\dot{\mathbf{q}}+\mathbf{g}(\mathbf{q})$$

which leads to the closed loop dynamics

$$\ddot{\mathbf{q}} \;=\; \mathbf{r}$$

[15, Ch. 9.1.2]. What remains is to choose $\mathbf{r}$, the new input, as

$$\mathbf{r} \;=\; \ddot{\mathbf{q}}_\mathbf{d}-2\mathbf{A}\dot{\tilde{\mathbf{q}}}-\mathbf{A}^2\tilde{\mathbf{q}}$$

with $N\times N$ matrix $\mathbf{A}>0$ and the closed loop dynamics become

$$\ddot{\tilde{\mathbf{q}}}+2\mathbf{A}\dot{\tilde{\mathbf{q}}}+\mathbf{A}^2\tilde{\mathbf{q}} \;=\; 0 \tag{5.4.7}$$

where $\tilde{\mathbf{q}}=\mathbf{q}-\mathbf{q}_\mathbf{d}$ [15, Ch. 9.1.2]. Now eq (5.4.7) appears as a critically damped second order system with time constant $\mathbf{A}$. Recall that eq (5.4.7) is an $N\times 1$ vector differential equation so it is not automatically critically damped along every co-ordinate $\mathbf{q}$. To make this the case the constant matrix $\mathbf{A}$ should be chosen as $\alpha\mathbb{I}$, where α is a positive constant and $\mathbb{I}$ is the $N\times N$ identity matrix, then eq (5.4.7) becomes a system of N independent second order differential equations, each critically damped with time constant α.

Of course it is possible to tease out what is being done here in terms of energy, since it has already been established that feedback linearisation is a special form of energy-balancing in Chapter 5.1. What remains is to observe the effect of $\mathbf{r}$ in terms of energy and the energy analysis will be complete.

Recall that Energy Balancing a desired energy $E_d=\frac{1}{2}\mathbf{v}^\mathrm{T}\mathbf{v}$ with desired power $\dot{E}_d=\mathbf{v}^\mathrm{T}\mathbf{r}$ leads to feedback linearisation of the prototypical model eq (3.1.1). Substitution of the dynamics

$$\mathbf{r} \;=\; \ddot{\mathbf{x}}_\mathbf{d}-2\mathbf{A}\tilde{\mathbf{v}}-\mathbf{A}^2\tilde{\mathbf{x}}$$

into the desired power will result in a closed loop prototypical system

$$\ddot{\tilde{\mathbf{x}}} \;+2\mathbf{A}\tilde{\mathbf{v}}+A^2\tilde{\mathbf{x}}= \;0$$

where $\tilde{\mathbf{x}}=\mathbf{x}-\mathbf{x}_\mathbf{d}$ and $\tilde{\mathbf{v}}=\dot{\tilde{\mathbf{x}}}$. To observe what has been done in terms of energy, it is necessary to use the definition of $\mathbf{r}$ and substitute it into $\dot{E}_d$ resulting in

$$\begin{aligned}\dot{E}_d &= \mathbf{v}^T\ddot{\mathbf{x}}_\mathbf{d}-\mathbf{v}^\mathrm{T}2\mathbf{A}\tilde{\mathbf{v}}-\mathbf{v}^\mathrm{T}\mathbf{A}^2\tilde{\mathbf{x}} \\ &= \mathbf{v}^\mathrm{T}\ddot{\mathbf{x}}_\mathbf{d}-\mathbf{v}^\mathrm{T}2\mathbf{A}\mathbf{v}-\mathbf{v}^\mathrm{T}\mathbf{A}^2\mathbf{x}+\mathbf{v}^\mathrm{T}2\mathbf{A}\mathbf{v}_\mathbf{d}+\mathbf{v}^\mathrm{T}\mathbf{A}^2\mathbf{x}_\mathbf{d}.\end{aligned} \tag{5.4.8}$$

There are cross terms in eq (5.4.8) and it appears that dimensional consistency has been lost with the term $\mathbf{v}^\mathrm{T}\ddot{\mathbf{x}}_\mathbf{d}$. However, it must be remembered that there are unit masses due to the desired energy $E_d=\frac{1}{2}\mathbf{v}^\mathrm{T}\mathbf{v}$ and hence the term does indeed have units of $\frac{J}{s}$. When $\tilde{\mathbf{x}}$ and $\tilde{\mathbf{v}}$ have been multiplied out, it is clear that power is added into the system if a twice differentiable desired trajectory x_d is not zero and the power is zero only when $\mathbf{v}=\mathbf{v}_\mathbf{d}$,

$\mathbf{x} = \mathbf{x_d}$ and $\ddot{\mathbf{x}}_\mathbf{d} = 0$. An intuitive explanation of this desired power function can be put in terms of a mass spring damper system, with a spring that exerts zero force only when $\mathbf{x} = \mathbf{x_d}$, a linear viscous damper that only stops extracting energy from the system when $\mathbf{v} = \mathbf{v_d}$ and a unit mass that moves on its own according to some desired acceleration $\ddot{\mathbf{x}}_\mathbf{d}$. Hence the control philosophy was to have equality between the system and this mythical mass-spring-damper.

The drawback of this method is again, that no plant-model mismatch is allowed [15, Ch. 9].

Robust Tracking: Sliding Mode

It is well known that sliding mode control is a robust, high performance control methodology [15, Ch. 7]. The basic idea involves designing a switching surface $\sigma(\chi)$ which is a function of all of the states $\chi \in \mathbb{R}^N$ and a control law that causes all system trajectories to approach the surface and stay on it [15, Ch. 7.1]. The dynamics on the switching surface then dictate the system performance i.e. the closed loop system behaves as $\sigma = \mathbb{O}$ [15, Ch. 7.1].

Mathematically the goal is to have

$$\frac{1}{2}\frac{\mathrm{d}}{\mathrm{d}t}\sigma^\mathrm{T}\sigma \quad \leq \quad -\eta\mathbb{I}(\sigma^\mathrm{T}\sigma)^{\frac{1}{2}} \tag{5.4.9}$$

where η is a positive constant which implies a finite time convergence (smaller than $\frac{1}{\eta}\sigma_{t=0}$) to the switching surface σ and is clearly a Lyapunov argument for stability [15, Ch. 7.1, Ch. 9.1.2].

Now the switching surface is chosen as

$$\sigma \quad = \quad \dot{\tilde{\mathbf{q}}} + \Lambda\tilde{\mathbf{q}}$$

where Λ is a *Hurwitz* matrix, essentially its eigenvalues are all stable [15, Ch. 9.1.2].

This approach can be simplified and be physically justified with a few alterations by considering the time derivative of $\sigma^\mathrm{T}\mathbf{H}\sigma$ and interpreting the switching surface as a velocity error via

$$\begin{aligned} \sigma &= \dot{\mathbf{q}} - \dot{\mathbf{q}}_\mathbf{r} \\ \dot{\mathbf{q}}_\mathbf{r} &= \dot{\mathbf{q}}_\mathbf{d} - \Lambda\tilde{\mathbf{q}}, \end{aligned}$$

which is an artifice that allows reasoning about the energy related properties to conspire with trajectory following [15, Ch. 9.1.2].

The derivation in [15, Ch. 9.1.2] is modified to suit the prototypical model next.

Consider a switching surface $\sigma(\mathbf{x}, \mathbf{v})$

$$\sigma(\mathbf{x}, \mathbf{v}) \quad = \quad \tilde{\mathbf{v}} + \Lambda\tilde{\mathbf{x}},$$

which is given for a general second order scalar system in [15, Ch. 7.1.1]. Recall that $\tilde{\mathbf{x}} = \mathbf{x} - \mathbf{x_d}$ and $\tilde{\mathbf{v}} = \mathbf{v} - \mathbf{v_d}$. Now use the artifice mentioned previously by letting $\mathbf{v_r} = \mathbf{v_d} - \Lambda\tilde{\mathbf{x}}$ and the sliding surface can be rewritten as

$$\sigma \quad = \quad \mathbf{v} - \mathbf{v_r}$$

which is a general weighted velocity error in the spirit of [15, Ch. 9.1.2].

Now construct the Lyapunov function

$$E = \frac{1}{2}\sigma^{\mathrm{T}}\mathbf{M}(\mathbf{x},t)\sigma$$

which is clearly positive definite for all $\mathbf{x}$ and $\mathbf{v}$. The time derivative of the Lyapunov function,

$$\frac{\mathrm{d}}{\mathrm{d}t}E = \sigma^{\mathrm{T}}\mathbf{M}(\mathbf{x},t)\dot{\sigma} + \frac{1}{2}\sigma^{\mathrm{T}}\dot{\mathbf{M}}(\mathbf{x},t)\sigma,$$

with the prototypical model eq (3.1.1),

$$\mathbf{M}(\mathbf{x},t)\dot{v} = -\mathbf{D}(\mathbf{x},\mathbf{v})\mathbf{v} - \mathbf{K}(\mathbf{x}) + \mathbf{G}(\mathbf{x})\mathbf{u}$$

and clever use of the switching surface definition as in [15, pp. 402] leads to

$$\mathbf{M}(\mathbf{x},t)\left(\dot{\sigma} + \dot{\mathbf{v}}_{\mathbf{r}}\right) = -\mathbf{D}(\mathbf{x},\mathbf{v})\left(\sigma + \mathbf{v}_{\mathbf{r}}\right) - \mathbf{K}(\mathbf{x}) + \mathbf{G}(\mathbf{x})\mathbf{u}$$

and finally

$$\frac{\mathrm{d}}{\mathrm{d}t}E = \sigma^{\mathrm{T}}\left(\mathbf{G}(\mathbf{x})\mathbf{u} - \mathbf{D}(\mathbf{x},\mathbf{v})\mathbf{v}_{\mathbf{r}} - \left[\mathbf{R}(\mathbf{x},\mathbf{v}) + \mathbf{J}(\mathbf{x},\mathbf{v})\right]\sigma - \mathbf{K}(\mathbf{x}) - \mathbf{M}(\mathbf{x},t)\dot{\mathbf{v}}_{\mathbf{r}}\right).$$

Now using the skew-symmetry of $\mathbf{J}(\mathbf{x},\mathbf{v})$ and symmetric positive definiteness of $\mathbf{R}(\mathbf{x},\mathbf{v})$ yields

$$\frac{\mathrm{d}}{\mathrm{d}t}E = \sigma^{\mathrm{T}}\left(\mathbf{G}(\mathbf{x})\mathbf{u} - \mathbf{D}(\mathbf{x},\mathbf{v})\mathbf{v}_{\mathbf{r}} - \mathbf{K}(\mathbf{x}) - \mathbf{M}(\mathbf{x},t)\dot{\mathbf{v}}_{\mathbf{r}}\right) - \sigma^{\mathrm{T}}\mathbf{R}(\mathbf{x},\mathbf{v})\sigma \quad (5.4.10)$$

To design a robust control strategy let the model have bounded modelling errors,

$$\begin{aligned}\bar{\mathbf{M}} &= \hat{\mathbf{M}} - \mathbf{M}\\ \bar{\mathbf{D}} &= \hat{\mathbf{D}} - \mathbf{D}\\ \bar{\mathbf{K}} &= \hat{\mathbf{K}} - \mathbf{K},\end{aligned}$$

where $\bar{\mathbf{M}}$ denotes the error, $\hat{\mathbf{M}}$ denotes the "best guess" and $\mathbf{M}$ is the "true value" [15, pp. 403]. For ease of reading, the arguments to the matrices have been dropped. Let $\mathbf{G}(\mathbf{x})$ be bounded by

$$0 < \mathbf{G}_{min}(\mathbf{x}) \leq \mathbf{G}(\mathbf{x}) \leq \mathbf{G}_{max}(\mathbf{x})$$

where $\mathbf{G}_{max}(\mathbf{x})$ and $\mathbf{G}_{min}(\mathbf{x})$ are the known upper and lower bounds respectively [15, pp. 287-288]. Now $\mathbf{G}(\mathbf{x})$ is a multiplicative uncertainty and hence it is a natural choice that the best approximation is the geometric mean of the limits

$$\hat{\mathbf{G}}(\mathbf{x}) = \left(\mathbf{G}_{min}(\mathbf{x})\mathbf{G}_{max}(\mathbf{x})\right)^{\frac{1}{2}}$$

which is a vectorised version of [15, pp. 287-288].

Define now

$$\bar{\mathbf{G}}(\mathbf{x}) \quad = \quad \mathbf{G}(\mathbf{x})\hat{\mathbf{G}}(\mathbf{x})^{-1}$$

which will be the identity matrix for no mismatch between $\mathbf{G}(\mathbf{x})$ and $\hat{\mathbf{G}}(\mathbf{x})$.

Choose the control law

$$\mathbf{u} \quad = \quad \hat{\mathbf{G}}(\mathbf{x})^{-1}\left(\hat{\mathbf{M}}(\mathbf{x},t)\dot{\mathbf{v}}_\mathbf{r} + \hat{\mathbf{D}}(\mathbf{x},\mathbf{v})\mathbf{v}_\mathbf{r} + \hat{\mathbf{K}}(\mathbf{x}) - \kappa(\mathbf{x},\mathbf{v})sgn(\sigma)\right)$$

where $\kappa(\mathbf{x},\mathbf{v})$ is an $N \times N$ matrix of gains and $sgn()$ is the sign function mathematically defined for scalars as

$$sgn(y) \quad = \quad \begin{cases} +1 & y > 0 \\ 0 & y = 0 \\ -1 & y < 0, \end{cases}$$

that has the property that $y\,sgn(y) = |y|$ i.e. the absolute value of y [15, 402].

Now with the control law substituted into eq (5.4.10),

$$\frac{\mathrm{d}}{\mathrm{d}t}E \quad = \quad \sigma^{\mathrm{T}}\bar{\mathbf{G}}\left(\bar{\mathbf{M}}\dot{\mathbf{v}}_\mathbf{r} + \bar{\mathbf{D}}\mathbf{v}_\mathbf{r} + \bar{\mathbf{K}}\right) - \sigma^{\mathrm{T}}\mathbf{R}\sigma - \sigma^{\mathrm{T}}\bar{\mathbf{G}}\kappa(\mathbf{x},\mathbf{v})sgn(\sigma)$$

the sliding condition, eq (5.4.9), can be verified using

$$\kappa(\mathbf{x},\mathbf{v}) \quad \geq \quad \left|\bar{\mathbf{G}}^{-1}\left(\bar{\mathbf{M}}\dot{\mathbf{v}}_\mathbf{r} + \bar{\mathbf{D}}\mathbf{v}_\mathbf{r} + \bar{\mathbf{K}}\right)\right| + \eta$$

which is an adaptation and extension of [15, Ch. 7.1, pp. 40-403]. The problem with this control law is the sharp switching around $\sigma = 0$ due to the $sgn()$ function [15, Ch. 7.1]. There is a way to make the control law continuous in a boundary around the switching surface and this is addressed next [15, Ch. 7.2]. The fix is to use a saturation function $sat()$ defined as

$$sat(y) \quad = \quad \begin{cases} y & |y| < 1 \\ sgn(y) & \text{otherwise,} \end{cases}$$

and hence use the control law

$$\mathbf{u} \quad = \quad \text{best guess} - \hat{\mathbf{G}}(\mathbf{x})^{-1}\kappa(\mathbf{x},\mathbf{v})sat(\frac{\sigma}{B})$$

where B is the boundary width around the switching surface [15, Ch. 9.2, pp. 294]. The Controller Complexity principle is again at work where the control algorithm is at least as complicated as the plant and further that the feedback term $\kappa(\mathbf{x},\mathbf{v})$ has to be larger than the known uncertainty in the model.

Table 5.3: Robotic Control Laws Adapted to the Prototypical System

Name	Control Law
Position Regulation	
PD Plus Gravity	$\mathbf{G}(\mathbf{x})\mathbf{u} = -\mathbf{K_p}(\mathbf{x}-\mathbf{x}^*) - \mathbf{K_d}\mathbf{v} + \mathbf{K}(\mathbf{x})$
PD Target Torque	$\mathbf{G}(\mathbf{x})\mathbf{u} = -\mathbf{K_p}(\mathbf{x}-\mathbf{x}^*) - \mathbf{K_d}\mathbf{v} + \mathbf{K}(\mathbf{x}^*)$
Task Space Position Regulation	$\mathbf{G}(\mathbf{x})\mathbf{u} = -\kappa_p \frac{\partial \mathbf{x}}{\partial \gamma}(\gamma-\gamma^*) - \mathbf{K_d}\mathbf{v} + \mathbf{K}(\mathbf{x})$
Task Space with Constraints	$\mathbf{G}(\mathbf{x})\mathbf{u} = -\frac{\partial \mathbf{x}}{\partial \gamma}\left\{\kappa_p(\gamma-\gamma^*) + \lambda_d \frac{\partial \phi(\gamma)}{\partial \gamma}\right\} - \mathbf{K_d}\mathbf{v} + \mathbf{K}(\mathbf{x})$ $\phi(\gamma) = 0$
Trajectory Tracking	
Plant Inversion	$\mathbf{G}(\mathbf{x_d})\mathbf{u} = \mathbf{M}(\mathbf{x_d},t)\ddot{\mathbf{x}}_\mathbf{d} + \mathbf{D}(\mathbf{x_d},\mathbf{v_d})\mathbf{v_d} + \mathbf{K}(\mathbf{x_d})$
Feedback Linearisation	$\mathbf{G}(\mathbf{x})\mathbf{u} = \mathbf{M}(\mathbf{x},t)\mathbf{r} + \mathbf{D}(\mathbf{x},\mathbf{v})\mathbf{v} + \mathbf{K}(\mathbf{x})$ $\mathbf{r} = \ddot{\mathbf{x}}_\mathbf{d} + 2\mathbf{A}(\mathbf{v}-\mathbf{v_d}) + \mathbf{A}^2(\mathbf{x}-\mathbf{x_d})$
Exponential Tracking	$\mathbf{G}(\mathbf{x})\mathbf{u} = \mathbf{M}(\mathbf{x},t)\dot{\mathbf{v}}_\mathbf{r} + \mathbf{D}(\mathbf{x},\mathbf{v})\mathbf{v_r} + \mathbf{K}(\mathbf{x}) + \mathbf{K_d}(\mathbf{v_r}-\mathbf{v})$ $\mathbf{v_r} = \mathbf{v_d} - \Lambda(\mathbf{x}-\mathbf{x_d})$
Robust Tracking	$\mathbf{u} = \hat{\mathbf{G}}(\mathbf{x})^{-1}\left(\hat{\mathbf{M}}(\mathbf{x},t)\dot{\mathbf{v}}_\mathbf{r} + \hat{\mathbf{D}}(\mathbf{x},\mathbf{v})\mathbf{v_r} + \hat{\mathbf{K}}(\mathbf{x})\right)$ $-\hat{\mathbf{G}}(\mathbf{x})^{-1}\left(\kappa(\mathbf{x},\mathbf{v})sat(\frac{\sigma}{B})\right)$ $\kappa(\mathbf{x},\mathbf{v}) \geq \left\lvert\bar{\mathbf{G}}^{-1}\left(\bar{\mathbf{M}}\dot{\mathbf{v}}_\mathbf{r} + \bar{\mathbf{D}}\mathbf{v_r} + \bar{\mathbf{K}}\right)\right\rvert + \eta$

Applications to the Prototypical System

The beauty of the results from Robot control is that the control laws are directly applicable to the prototypical model, with a few minor modifications on the stability proofs. The handful of control laws on position regulation, trajectory tracking and control under constraints are therefore directly available for design purposes. All that is required is a change of variables namely $\mathbf{q} \to \mathbf{x}$, $\dot{\mathbf{q}} \to \mathbf{v}$, $\mathbf{H}(\mathbf{q}) \to \mathbf{M}(\mathbf{x},t)$ and finally $\tau \to \mathbf{G}(\mathbf{x})\mathbf{u}$ and all of the rich control laws from robotics are available for use with the prototypical system. It should be clear that in order for the results to be applicable, $\mathbf{G}(\mathbf{x})$ must have an inverse and the system should be fully actuated as it is in eq (5.4.1). All of the control laws presented in this Chapter are presented in Table 5.3. Note that the task space co-ordinates are given as γ, the switching surface is $\sigma = \tilde{\mathbf{v}} + \Lambda\tilde{\mathbf{x}}$ and the system to be controlled is the prototypical model eq (3.1.1).

Design of Energy-Shaping Robot Controllers

There is no design work needed in applying the control laws from Table 5.3. All that is required is to have the system model in the prototypical framework, since these control laws were adapted to fit it. One simply chooses the control law that best fits the control problem at hand.

The recommended control law for position regulation is the PD Target Torque method due to its simplicity and low computational cost, as compared with some of the other position regulation controllers.

The recommended control laws for tracking are the Exponential Tracking control law, if the model used is accurate and the Robust Tracking control law if the model is a simplification and/or disturbances are expected. The Robust Tracking control law also reaches the trajectory in finite time and therefore is a better performing controller.

Application of Energy-Shaping Robot Control to the Simple Pendulum

The position regulation control laws (PD plus gravity, PD Target Torque) have already been applied in Chapter 5.1. Due to the pendulum system being scalar, the task space control laws are not appropriate in this application. Hence the trajectory tracking control laws will be examined. It should be remembered that, the Power-Shaping control law of Chapter 5.2 is also appropriate for solving trajectory tracking problems. A few important sliding-mode control concepts are introduced next before getting to the tracking algorithms.

Sliding-Mode Control Concepts

As previously stated, the goal of the sliding mode algorithm is to cause the system trajectory to approach the switching surface, σ, in finite time [15, Ch. 7.1]. This is the heart of the Robust Tracking algorithm. Once on the switching surface, the dynamics of the system are determined by $\sigma = 0$ [15, Ch. 7.1].

Consider, for example, the switching surface,

$$\sigma(\theta, \omega) \quad = \quad \tilde{\omega} + \lambda \tilde{\theta},$$

with λ a positive constant. Choosing $\lambda = 0.5$ yields a stable switching surface, as per Figure 5.4.1.

To demonstrate the principle of sliding-mode control, the reference trajectory $\theta_d = 1$ is chosen. By doing this, the tracking problem has become a regulation problem. Figure 5.4.1, adapted from [15, Ch. 7.2, pp. 291], depicts the switching surface for $\lambda = 0.5$ and $\theta_d = 1$. A boundary around the switching surface, included as a visual aid for later addressing, is represented by the region B. For a constant θ_d, the velocity error becomes $\tilde{\omega} = \omega$. The dynamics on the switching surface are therefore,

$$\begin{aligned} \sigma &= 0 \\ \omega + \lambda(\theta - 1) &= 0 \\ \implies \dot{\theta} &= -\lambda(\theta - 1). \end{aligned}$$

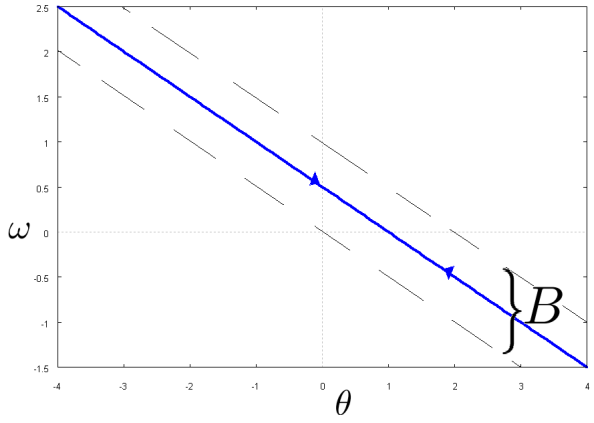

Figure 5.4.1: Switching Surface, with Boundary layer B.

This is a stable, linear, first order, ordinary differential equation. A fact made clear in Figure 5.4.1. The stationary point is, $\theta = 1$, as desired. The exponential tracking algorithm is presented next, followed by the robust tracking algorithm.

Exponentially Convergent Tracking of a Sinusoidal Wave

The control law for exponentially convergent tracking (from Table 5.3) of a sinusoidal wave is:

$$\tau = I\dot{v}_r + mgl\sin(\theta) + \kappa_d(\omega - v_r), \tag{5.4.11}$$

and

$$v_r = \omega_d - \lambda(\theta - \theta_d).$$

Note, the feedback term is,

$$\begin{aligned} \kappa_d(\omega - v_r) &= \kappa_d\left(\tilde{\omega} + \lambda\tilde{\theta}\right) \\ &= \kappa_d\,\sigma, \end{aligned}$$

which is very similar to the sliding-mode controller. The differences are: $\kappa_d = const$ and does not change with state; the switching surface, σ, is not an argument to a function. In fact, this can be shown to be a limiting case of the robust tracking algorithm. This is accomplished by using the $sat()$ function and making the boundary around the switching surface, $B = \infty$, whilst describing the modelling error with a constant.

The sinusoidal reference wave, with frequency $f = 0.25$ Hz, is $\theta_d = \sin(2\pi ft)$. This implies that $\omega_d = (2\pi f)\cos(2\pi ft)$ and furthermore that

$$\dot{v}_r = -(2\pi f)^2\sin(2\pi ft) - \lambda\left(\omega - (2\pi f)\cos(2\pi ft)\right).$$

For brevity's sake these are not substituted into eq (5.4.11).

In terms of visually representing the performance, a plot of σ against time is extremely useful for this purpose [15, Ch. 7, pp. 296]. The phase portrait is messy due to trajectories

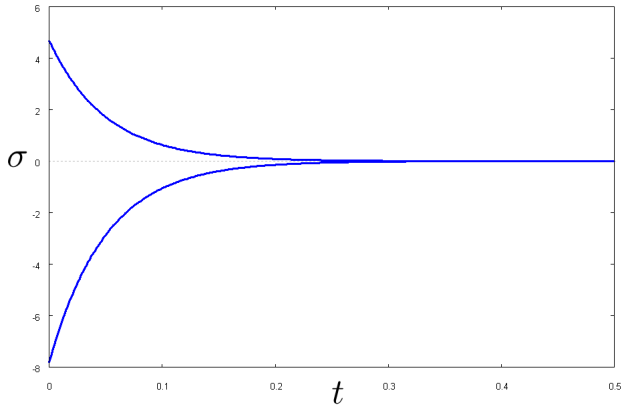

Figure 5.4.2: Switching surface plot of Exponentially Convergent Tracking algorithm

crossing one another, since the system is time varying. Furthermore, there is little insight in terms of rate of convergence on a phase portrait, due to time being an *implicit* variable.

Recall that when $\sigma = 0$, then perfect tracking is achieved. The exponential nature of the control algorithm is clear from Figure 5.4.2. Two (arbitrary) initial conditions are used, namely $(\theta, \omega) = (2.5, 5)$ and $(\theta, \omega) = (-2.5, -5)$. The gain, κ_d is chosen as 10. Note that the switching surface, σ is a linear combination of angle and angular velocity errors. Hence, these initial σ values are not *unique*.

Robust Tracking of a Sinusoidal Wave

The sliding-mode control algorithm (Robust Tracking in Table 5.3), given a varying m is,

$$\tau \quad = \quad \hat{I}\dot{v}_r + \hat{m}gl\,\sin(\theta) - \kappa(\theta,\omega)sat(\frac{\sigma}{B}),$$

where $\hat{m}$ is the best guess of the mass, and $\bar{m}$ is the maximum expected error. The requirement for the sliding condition to hold, is that $\kappa(\theta,\omega) \geq |\bar{I}\dot{v}_r + \bar{m}glsin(\theta)| + \eta$[13]. For comparison's sake, the robust tracking algorithm assumes exact knowledge of the plant initially. The free parameter, η is experimentally chosen to be 20, such that both controllers have similar settling times. The same reference signal, $\theta_d = \sin(2\pi ft)$ is to be tracked. The boundary layer, B, is chosen to be 0.1, which experimentally removes chattering. The switching surface plot against time, for the same previous initial conditions, is depicted in Figure 5.4.3. It should be clear that there is a finite time to reach the surface ($\sigma = 0$) and when the system is on the surface, it remains on it ($\sigma = 0$ from then on). Whereas in Figure 5.4.2, the convergence to $\sigma = 0$ is exponential, as its name implies.

To assess the robustness, $\hat{m}$ is again chosen to be 0.5 kg and $\bar{m} = \pm 0.25$ kg. This means that the maximum expected deviation of the best approximated mass, $\hat{m}$ and the true mass is between 0.75 kg and 0.25 kg. To further test the algorithm, the true mass is defined according to,

$$m \quad = \quad 0.5 + 0.22\,\sin(\theta),$$

[13]Take note, if there is no plant-model mismatch (m is exactly known), then, for a constant $\theta_d = 0$, this control law is feedback linearisation with a feedback term. The expanded feedback term is $-\eta\, sgn(\omega + \lambda\tilde{\theta})$ i.e. a bang-bang controller with PD input and $\pm\eta$ as output. For the control law that includes the $sat()$ function and the boundary B, the control law inside the boundary is a PD controller, $-\eta\omega - \eta\lambda\tilde{x}$ and a bang-bang controller outside of the boundary.

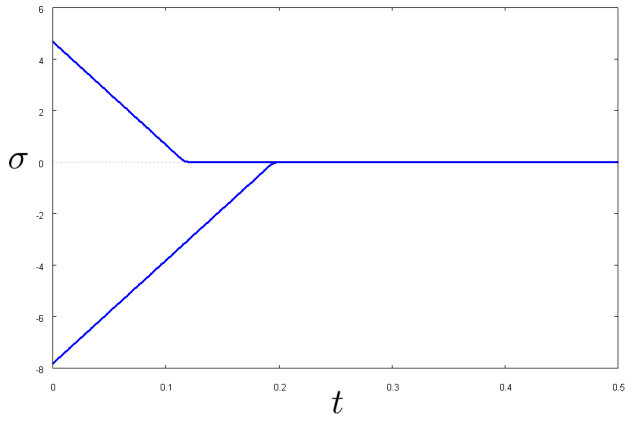

Figure 5.4.3: Switching surface plot of Robust Tracking algorithm

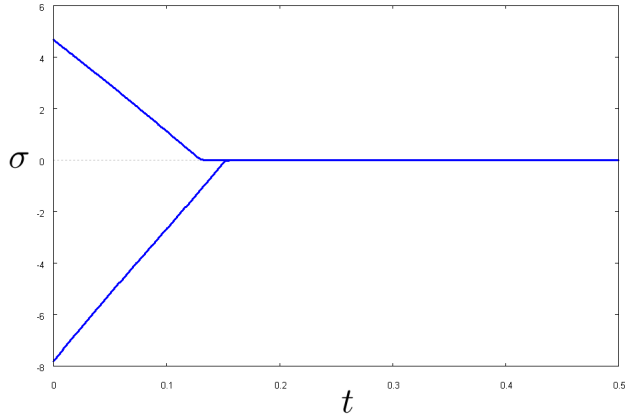

Figure 5.4.4: Switching surface plot of Robust Tracking algorithm under a varying mass

which honours the assumed bounds on the mass.

This is not a realistic description of the system, since the mass of the bob varies with the angle, however it does test the robustness of the technique. The resulting switching surface plot is depicted in Figure 5.4.4. The performance is near identical as the exactly known mass case, with no visible error. This result should be juxtaposed with the exponentially convergent tracking controller previously defined. Figure 5.4.5 depicts the response from the exponentially convergent tracking controller. It is clear that the varying mass causes a visible error in tracking the sinusoidal wave, since σ does not remain zero for any portion of time. Hence the exponentially convergent tracking controller is not robust with respect to parameter variation.

The exponentially convergent tracking controller has a simpler control law and is reliable, provided that the plant is modelled exactly. The robust tracking control law is more computationally complicated but can be made robust with respect to parameter variation. Moreover, it is clear at the design stage the amount of uncertainty in the modelling of the system. Lastly, the robust control algorithm has a finite time to reach the trajectory, whereas the exponentially convergent tracking controller approaches the trajectory exponentially.

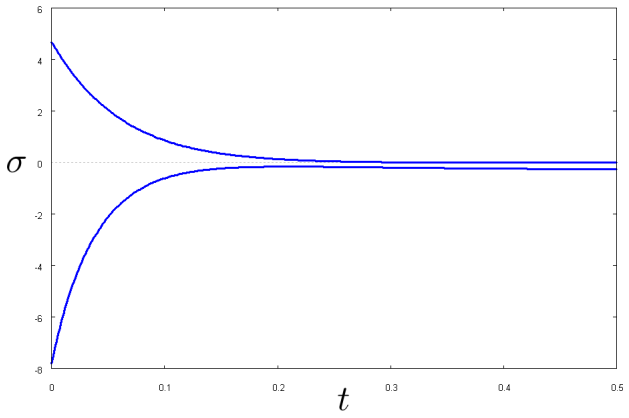

Figure 5.4.5: Switching surface plot of Exponentially Convergent Tracking algorithm under a varying mass

5.5 Interconnection and Damping Assignment (IDAPBC)

The following is a brief summary of the Interconnection and Damping Assignment methodology expounded upon in [6, 16, 17, 18, 19].

Given a state space description in the well known input affine form, where $\mathbf{x} \in \mathbb{R}^N$:

$$\dot{\mathbf{x}} \quad = \quad \mathbf{F}(\mathbf{x}) + \mathbf{G}(\mathbf{x})\mathbf{u}, \tag{5.5.1}$$

interconnection and damping assignment seeks to transform this system into a system that has: a desired *interconnection*, $\mathbf{J_d}(\mathbf{x})$, between states, a desired *damping*, $\mathbf{R_d}(\mathbf{x})$, in the various degrees of freedom as well as a desired potential function, $H_d(\mathbf{x})$[14] [18]. It does this via the the input $\mathbf{u} = \beta(\mathbf{x})$ [18].

The *matching equation* for this problem is then,

$$\mathbf{F}(\mathbf{x}) + \mathbf{G}(\mathbf{x})\beta(\mathbf{x}) \quad = \quad (\mathbf{J_d}(\mathbf{x}) - \mathbf{R_d}(\mathbf{x}))\nabla H_d(\mathbf{x})$$

which is a partial differential equation due to the term $\nabla H_d(\mathbf{x})$ [6].

Differentiating the right hand side along the closed loop trajectories yields,

$$\frac{\mathrm{d}}{\mathrm{d}t}H_d(\mathbf{x}) \quad = \quad -\nabla^T H_d(\mathbf{x})\mathbf{R_d}(\mathbf{x})\nabla H_d(\mathbf{x}),$$

which has desirable stability properties as seen in the Chapter on Lyapunov functions [6].

Now it is possible to split the matching equation into: a fully actuated part using the inverse of $\mathbf{G}(\mathbf{x})$, defined as $\mathbf{G}(\mathbf{x})^{-1}$ which has the property that $\mathbf{G}(\mathbf{x})^{-1}\mathbf{G}(\mathbf{x}) = \mathbb{I}$; and an unactuated part using the left annihilator of $\mathbf{G}(\mathbf{x})$, defined as $\mathbf{G}(\mathbf{x})^{\dagger}$ which has the property that $\mathbf{G}(\mathbf{x})^{\dagger}\mathbf{G}(\mathbf{x}) = \mathbb{O}$ [18, 19].

The fully actuated matching equation is given by,

$$\beta(\mathbf{x}) \quad = \quad \mathbf{G}(\mathbf{x})^{-1}\left\{(\mathbf{J_d}(\mathbf{x}) - \mathbf{R_d}(\mathbf{x}))\nabla H_d(\mathbf{x}) - \mathbf{F}(\mathbf{x})\right\} \tag{5.5.2}$$

and the unactuated matching equation is given by,

$$\mathbf{G}(\mathbf{x})^{\dagger}\mathbf{F}(\mathbf{x}) \quad = \quad \mathbf{G}(\mathbf{x})^{\dagger}(\mathbf{J_d}(\mathbf{x}) - \mathbf{R_d}(\mathbf{x}))\nabla H_d(\mathbf{x}). \tag{5.5.3}$$

Both of these matching equations need to be solved simultaneously, the fully-actuated matching equation solves for the control law directly and the unactuated matching equation makes sure that inputs are not required along co-ordinates in which there is no control authority, for the given Interconnection, Damping and Potential functions [6]. Note that $\mathbf{G}(\mathbf{x})^{-1}$ is the Moore-Penrose pseudo-inverse, which is a well defined for non-square matrices as long as $\mathbf{G}(\mathbf{x})$ has full column rank, which is assumed for IDAPBC's purposes [6].

It should be noted that this technique closely models feedback linearisation in that the plant dynamics are canceled and replaced by the structure the designer wants [15, Ch. 6]. The main difference is that the target dynamics are chosen based on energy, whereas in feedback linearisation, they may be arbitrarily assigned [15, Ch. 6]. Consider the substitution of eq (5.5.2) into (5.5.1), where for readability $(\mathbf{J_d}(\mathbf{x}) - \mathbf{R_d}(\mathbf{x}))\nabla H_d(\mathbf{x}) = \mathbf{F_d}(\mathbf{x})$:

[14] The following properties must be adhered to: $\mathbf{J_d} = -\mathbf{J_d}^{\mathrm{T}}$ and $\mathbf{R_d} = \mathbf{R_d}^{\mathrm{T}} > 0$

$$\dot{\mathbf{x}} = \mathbf{F}(\mathbf{x}) + \mathbf{G}(\mathbf{x})\mathbf{G}(\mathbf{x})^{-1}\left\{\mathbf{F_d}(\mathbf{x}) - \mathbf{F}(\mathbf{x})\right\},$$

which results in

$$\dot{\mathbf{x}} = \mathbf{F_d}(\mathbf{x}),$$

and is identical to feedback linearisation.

Design of Interconnection and Damping Assignment Controllers

The general design technique adapted from [19, 18] is now presented:

1. Choose an H_d which has a unique equilibrium point, x^* at the desired state space.
2. Choose the dissipation $\mathbf{R_d}$ to help convergence to this point.
3. Choose also a $\mathbf{J_d}$, if energy must be exchanged between different states. (Think of the DC motor)
4. Solve the matching equations.

Another, more laborious method, also from [19, 18]:

1. Choose a dissipation structure $\mathbf{R_d}$ and interconnection $\mathbf{J_d}$.
2. Solve the matching equations for all families of $H_a = H - H_d$.
3. Choose the solution which has a minimum at the desired state $\mathbf{x}^*$.

One can further choose which matrices to fix and which to leave free to solve for families of controllers. However, there are only two matching equations and therefore one must fix at least one parameter; either H_d, $\mathbf{R_d}$ or $\mathbf{J_d}$.

Interconnection and Damping Assignment of a Simple Pendulum

First and foremost, the model for the simple pendulum must be modified into the port-controlled Hamiltonian framework. This is done by defining a generalised co-ordinate, q and corresponding "conjugate momentum", p [18]. For the frictionless simple pendulum, these are the angle $q = \theta$ and the angular momentum $p = I\omega$. Now the Hamiltonian (system energy [19]) is:

$$H(q,p) = \frac{1}{2}\frac{p^2}{I} + U_0 - mgl\cos(q).$$

Using Hamiltonian mechanics, [39, Ch. 16], the equations of motion are

$$\begin{pmatrix} \dot{q} \\ \dot{p} \end{pmatrix} = \begin{pmatrix} [H]_p \\ -[H]_q + \tau \end{pmatrix} = \begin{pmatrix} \frac{p}{I} \\ -mgl\sin(q) + \tau \end{pmatrix},$$

which can easily be shown to be identical to the second order model arrived at in other Chapters.

This can be written in port-controlled Hamiltonian form as

$$\dot{\mathbf{x}} = (\mathbf{J}-\mathbf{R})\nabla H + \mathbf{G}u$$

with

$$\mathbf{x} = \begin{pmatrix} q \\ p \end{pmatrix},$$

$$\mathbf{G} = \begin{pmatrix} 0 \\ 1 \end{pmatrix},$$

$$u = \tau,$$

$$\mathbf{J} = \begin{pmatrix} 0 & 1 \\ -1 & 0 \end{pmatrix},$$

$$\mathbf{R} = \begin{pmatrix} 0 & 0 \\ 0 & 0 \end{pmatrix},$$

and

$$\nabla H = \begin{pmatrix} [H]_q \\ [H]_p \end{pmatrix}.$$

Now with the control law, $u = \beta(\mathbf{x})$ the matching condition is, as per eq (5.5.2),

$$(\mathbf{J}-\mathbf{R})\nabla H + \mathbf{G}\beta(\mathbf{x}) = (\mathbf{J_d}-\mathbf{R_d})\nabla H_d,$$

which has solution,

$$\beta(\mathbf{x}) = \mathbf{G}^{-1}\left\{(\mathbf{J_d}-\mathbf{R_d})\nabla H_d - (\mathbf{J}-\mathbf{R})\nabla H\right\},$$

where $\mathbf{G}^{-1}$ is the Moore-Penrose pseudo-inverse,

$$\mathbf{G}^{-1} := (\mathbf{G}^T\mathbf{G})^{-1}\mathbf{G}^{\mathrm{T}},$$

as described in [19].

The other matching equation is eq (5.5.3),

$$\mathbf{G}^{\dagger}(\mathbf{J}-\mathbf{R})\nabla H = \mathbf{G}^{\dagger}(\mathbf{J_d}-\mathbf{R_d})\nabla H_d.$$

Now the left annihilator of $\mathbf{G}$, denoted as $\mathbf{G}^\dagger$ is such that:

$$\mathbf{G}^\dagger\mathbf{G} = \begin{pmatrix} 0 \\ 0 \end{pmatrix};$$

column rank($\mathbf{G}^\dagger$) = column rank($\mathbf{G}$) which implies that

$$\mathbf{G}^\dagger \neq \begin{bmatrix} 0 & 0 \end{bmatrix},$$

as described in [34, pp. 296].

Hence, for the simple pendulum,

$$\begin{aligned} \mathbf{G}^{-1} &= \left(\begin{bmatrix} 0 & 1 \end{bmatrix} \begin{bmatrix} 0 \\ 1 \end{bmatrix} \right)^{-1} \begin{bmatrix} 0 & 1 \end{bmatrix} \\ &= \begin{bmatrix} 0 & 1 \end{bmatrix}, \end{aligned}$$

and

$$\mathbf{G}^\dagger = \begin{bmatrix} 1 & 0 \end{bmatrix}.$$

Desired Dissipation

1,2,3.) If the desire is for the inclusion of dissipation only, then $\mathbf{J_d} = \mathbf{J}$, and $H_d = H$ with

$$\mathbf{R_d} = \begin{pmatrix} 0 & 0 \\ 0 & r \end{pmatrix},$$

which is tantamount to the desired inclusion of viscous damping. Notice that dissipation is only included where it would normally appear. This, incidentally, avoids having to solve the second matching equation, eq (5.5.3), which ensures that the energy is not shaped where there is no control authority to do so.

4.) The control law is

$$\begin{aligned} \beta(\mathbf{x}) &= \begin{bmatrix} 0 & 1 \end{bmatrix} (\mathbf{R} - \mathbf{R_d}) \nabla H \\ &= \begin{bmatrix} 0 & 1 \end{bmatrix} \begin{pmatrix} 0 & 0 \\ 0 & -r \end{pmatrix} \begin{pmatrix} [H]_q \\ [H]_p \end{pmatrix} \\ &= \begin{bmatrix} 0 & -r \end{bmatrix} \begin{pmatrix} [H]_q \\ [H]_p \end{pmatrix}, \end{aligned}$$

which results in,

$$\begin{aligned} \beta(\mathbf{x}) &= -r[H]_p \\ &= -r\frac{p}{I}, \end{aligned}$$

and is clearly $\beta(\mathbf{x}) = -r\omega$ using $p = I\omega$.

1,2,3.) It is possible to solve for *all* controllers for this system which have a general dissipation structure,

$$\mathbf{R_d} = \begin{pmatrix} r_q & r_1 \\ r_1 & r_p \end{pmatrix},$$

with $\mathbf{J} = \mathbf{J_d}$ and H_d a free parameter. This is achieved by defining $H_d = H + H_a$, which is to say that, the desired Hamiltonian is an addition of the original Hamiltonian and another modifying one [18].

4.) The second matching equation is then eq (5.5.3), which is a partial differential equation that solves for *any* modified Hamiltonian with this dissipation structure. Explicitly now,

$$\begin{aligned} \begin{bmatrix} 1 & 0 \end{bmatrix} (\mathbf{R} - \mathbf{R_d}) \nabla H_a &= 0 \\ \begin{bmatrix} 1 & 0 \end{bmatrix} \begin{pmatrix} -r_q & -r_1 \\ -r_1 & -r_p \end{pmatrix} \begin{pmatrix} [H_a]_q \\ [H_a]_p \end{pmatrix} &= 0 \\ \begin{bmatrix} -r_q & -r_1 \end{bmatrix} \begin{pmatrix} [H_a]_q \\ [H_a]_p \end{pmatrix} &= 0, \end{aligned}$$

which is

$$r_q \frac{\partial}{\partial q} H_a + r_1 \frac{\partial}{\partial p} H_a = 0.$$

Solving this equation for H_a allows the engineer to find an entire family of admissible modifications to the natural energy[15] H, and choose one with a suitable equilibrium point. By dividing both sides by r_q this becomes the constant coefficient advection equation,

$$\frac{\partial}{\partial q} H_a + \frac{r_1}{r_q} \frac{\partial}{\partial p} H_a = 0,$$

which has solution

$$H_a = f(p - \frac{r_1}{r_q} q), \tag{5.5.4}$$

with $f()$ an arbitrary differentiable function [50].[16]Equation 5.5.4 is an entire family of admissible solutions. After choosing a specific one, the control law is found by using the first matching equation, eq (5.5.2),

$$\begin{aligned} \beta(\mathbf{x}) &= \begin{bmatrix} 0 & 1 \end{bmatrix} (\mathbf{R} - \mathbf{R_d}) \nabla H_a \\ &= \begin{bmatrix} 0 & 1 \end{bmatrix} \begin{pmatrix} -r_q & -r_1 \\ -r_1 & -r_p \end{pmatrix} \begin{pmatrix} [H_a]_q \\ [H_a]_p \end{pmatrix} \\ &= \begin{bmatrix} -r_1 & -r_p \end{bmatrix} \begin{pmatrix} [H_a]_q \\ [H_a]_p \end{pmatrix}, \end{aligned}$$

which is

$$\beta(\mathbf{x}) = -r_1 \frac{\partial}{\partial q} H_a - r_p \frac{\partial}{\partial p} H_a.$$

[15]Recall that $H_d = H + H_a$.

[16]It should be well noted that with $r_q = r_1 = 0$, this PDE is trivially solved. Originally, the dissipation was only added where it would naturally appear anyway, which circumvented having to solve this PDE. Hence, physical reasoning has allowed the design to skip some of the more advanced mathematical requirements of IDAPBC.

Modification of Potential Function

1,2,3.) With the desire to invert gravity and have the pendulum balance about the upright position implies that, $\mathbf{J_d} = \mathbf{J}$, $\mathbf{R_d} = \mathbf{R}$ and

$$H_d = \frac{1}{2}\frac{p^2}{I} + mgl\cos(q) + U_0.$$

4.) The first matching equation is,

$$\begin{aligned}
\beta(\mathbf{x}) &= \begin{bmatrix} 0 & 1 \end{bmatrix} (\mathbf{J}-\mathbf{R})(\nabla H_d - \nabla H) \\
&= \begin{bmatrix} 0 & 1 \end{bmatrix} \begin{pmatrix} 0 & 1 \\ -1 & 0 \end{pmatrix} (\nabla H_d - \nabla H) \\
&= \begin{bmatrix} -1 & 0 \end{bmatrix} \begin{pmatrix} [H_d]_q - [H]_q \\ [H_d]_p - [H]_p \end{pmatrix} \\
&= \begin{bmatrix} -1 & 0 \end{bmatrix} \begin{pmatrix} [H_d]_q - [H]_q \\ 0 \end{pmatrix} \\
&= [H]_q - [H_d]_q,
\end{aligned}$$

and leads to

$$\beta(\mathbf{x}) = \underbrace{mgl\sin(q)}_{\text{cancels gravity}} + mgl\sin(q).$$

The energy balancing of Chapter 5.1 leads to these exact same controllers (both gravity inversion and desired dissipation) in a more straight forward manner. The second matching equation to be solved is,

$$\begin{aligned}
0 &= \mathbf{G}^{\dagger}(\mathbf{J}-\mathbf{R})(\nabla H_d - \nabla H) \\
0 &= \begin{bmatrix} 1 & 0 \end{bmatrix} \begin{pmatrix} 0 & 1 \\ -1 & 0 \end{pmatrix} (\nabla H_d - \nabla H) \\
0 &= \begin{bmatrix} 0 & 1 \end{bmatrix} \begin{pmatrix} [H_d]_q - [H]_q \\ [H_d]_p - [H]_p \end{pmatrix} \\
0 &= \begin{bmatrix} 0 & 1 \end{bmatrix} \begin{pmatrix} [H_d]_q - [H]_q \\ 0 \end{pmatrix} \\
0 &= 0.
\end{aligned}$$

Hence, the control law is a valid one (as already observed in previous chapters).

It interesting to note that for a very general modification of H_d into,

$$H_d = \frac{1}{2}\frac{p^2}{I} + U(q),$$

the resulting control law is

$$\beta(\mathbf{x}) = mgl\sin(q) - \frac{\partial}{\partial q}U(q).$$

This is feedback linearisation with a potential derived force $-\frac{\partial}{\partial q}U(q)$. Again, a result more easily achieved in Chapter 5.1.

Remarks about Kinetic Energy Shaping

1,2,3.) Consider that the desired kinetic energy is not identical to the original kinetic energy i.e. $[H_d]_p - [H]_p \neq 0$, but $J_d = J$ and $R_d = R$, then the second matching equation, eq (5.5.3), is

$$\begin{aligned} \frac{\partial}{\partial p} H_d \quad - \tfrac{\partial}{\partial p} H = \quad & 0 \\ \Longrightarrow \frac{\partial}{\partial p} H_a \qquad = \qquad & 0. \end{aligned}$$

4.) This is trivial to solve and has solution,

$$H_a \;=\; U(q),$$

essentially stating that the kinetic energy may not be modified if $\mathbf{J}$ and $\mathbf{R}$ are not modified. This is completely expected since the kinetic energy cannot be modified using the states p and q only. It should be remembered from Chapter 5.1and Chapter 5.4 that, the kinetic energy requires acceleration terms in order to alter it.

Concomitant Shaping of Potential and Dissipation

1,2,3.) Given the desire for gravity inversion and the inclusion of dissipation i.e. H_d and $\mathbf{R_d}$ are as previously defined with $\mathbf{J_d} = \mathbf{J}$.

4.) The resulting matching equations are:

$$\begin{aligned} \beta(\mathbf{x}) &= \begin{bmatrix} 0 & 1 \end{bmatrix} ((\mathbf{J}-\mathbf{R_d})\nabla H_d - (J-R)\nabla H) \\ &= \begin{bmatrix} 0 & 1 \end{bmatrix} ((\mathbf{J}-\mathbf{R_d})\nabla H_d - J\nabla H) \\ &= \begin{bmatrix} 0 & 1 \end{bmatrix} \begin{pmatrix} 0 & 1 \\ -1 & -r \end{pmatrix} \begin{pmatrix} [H_d]_q \\ [H_d]_p \end{pmatrix} - \begin{bmatrix} 0 & 1 \end{bmatrix} \begin{pmatrix} 0 & 1 \\ -1 & 0 \end{pmatrix} \begin{pmatrix} [H_d]_q \\ [H_d]_p \end{pmatrix} \\ &= \begin{bmatrix} -1 & -r \end{bmatrix} \begin{pmatrix} [H_d]_q \\ [H_d]_p \end{pmatrix} - \begin{bmatrix} -1 & 0 \end{bmatrix} \begin{pmatrix} [H]_q \\ [H]_p \end{pmatrix}; \end{aligned}$$

and,

$$\begin{aligned} 0 &= \mathbf{G}^{\dagger} ((\mathbf{J}-\mathbf{R_d})\nabla H_d - \mathbf{J}\nabla H) \\ &= \begin{bmatrix} 1 & 0 \end{bmatrix} \begin{pmatrix} 0 & 1 \\ -1 & -r \end{pmatrix} \begin{pmatrix} [H_d]_q \\ [H_d]_p \end{pmatrix} - \begin{bmatrix} 1 & 0 \end{bmatrix} \begin{pmatrix} 0 & 1 \\ -1 & 0 \end{pmatrix} \begin{pmatrix} [H]_q \\ [H]_p \end{pmatrix} \\ &= \begin{bmatrix} 0 & 1 \end{bmatrix} \begin{pmatrix} [H_a]_q \\ [H_a]_p \end{pmatrix}. \end{aligned}$$

The second matching equation implies that the kinetic energy may not be modified.

The first matching equation is,

$$-\frac{\partial}{\partial q} H_a - r \frac{\partial}{\partial p} H_d \;=\; \beta(\mathbf{x}),$$

with $H_a = H_d - H = 2mgl\cos(q)$, $H_d = \frac{1}{2}\frac{p^2}{I} + mgl\cos(q) + U_0$, and therefore

$$\beta(x) \quad = \quad 2mgl\sin(q) - r\frac{p}{I}.$$

This is a linear combination of the gravity inversion control law and the dissipation control law previously derived. Furthermore, it is identical to the gravity inversion and damping of Chapter 5.1, with $q = \theta$ and $p = I\omega$. The effects of these controllers have already been demonstrated in previous Chapters.

The beauty of IDAPBC is that *all* controllers that honor some interconnection and damping structure can be solved for at once. Unfortunately, it requires the solution of, at worst case, coupled non-linear PDE's. Energy-balancing, in the prototypical model framework is much more easily applied than the IDAPBC framework. However, the ground-work already accomplished in the IDAPBC framework can easily be incorporated into the prototypical model framework. The first improvement would be, the extension to the under-actuated case. It should be possible to use a similarly defined matching equation, involving the left annihilator of $\mathbf{G}(\mathbf{x})$ in the prototypical model, to accomplish this.

5.6 Summary of Energy Shaping Control Methods

All of the control techniques involve a matching process, whereby the system energy is matched to a desired energy via the input. The usefulness of designing controllers in the energy domain is sure to be appreciated at this stage.

A summary of the different control strategies and when to apply them follows.

Energy-Balancing is a technique that is useful for state regulation and can, indirectly, change the possible trajectories of the system via energy-shaping. Furthermore, the solutions leading to the control law are algebraic and no difficult partial differential equations need to be solved, unlike the IDAPBC methodology.

Power-Shaping is a technique that is useful for causing a system to attain a particular energy level, and maintain it. It has been extended via the inclusion of a non-linear integrator and an impulse at zero speed and can now actively compensate for a non-linear dissipation function, without feedback linearisation. The beauty of the Power-Shaping control law is that is causes the system to exponentially reach a natural trajectory i.e. a trajectory that the system is already capable of via the energy function. The control law is computationally complex though.

A number of constructive techniques for assigning a closed loop energy have been reported on.

The Controller Interpolation via a Common Lyapunov technique has shown the usefulness of being able to smoothly interpolate between different controllers. Moreover, the framework guarantees stability in a constructive manner, using a common Lyapunov function. If controllers have already been designed, which stabilise a system in different operating regions, then they may be smoothly interpolated using this technique. It is possible, therefore, to compensate for a control law's deficiencies with another, seamlessly.

The Robot control laws are already well established in that industry. A list of controllers for both position regulation and tracking were presented. The recommended control law for position regulation is the PD Target Torque method due to its simplicity and low computational cost, as compared with some of the other position regulation controllers. There are two recommended control laws for tracking: the Exponential Tracking control law and the Robust Tracking control law. If the model used is accurate, then the exponential tracking control law should be used. The Robust Tracking control law should be used if the model is a simplification and/or disturbances are expected. The Robust Tracking control law also reaches the trajectory in finite time and therefore is a better performing controller.

Finally, the Interconnection and Damping Assignment Passivity Based Control (IDAPBC) has a great deal to offer, at the cost of being mathematically difficult. The beauty of IDAPBC is that *all* controllers that honour some interconnection and damping structure can be solved for at once. Energy-balancing, in the prototypical model framework is much more easily applied than the IDAPBC framework and leads to the same controllers. However, IDAPBC has already solved the problem of controlling under-actuated systems and is well established in the field of Energy-Shaping control.

To extend the energy-balancing framework, ideas from IDAPBC can be adapted to suit the prototypical model. The first improvement would be, the extension to the under-actuated case. It should be possible to use a similarly defined matching equation, involving the left annihilator of $\mathbf{G}(\mathbf{x})$ in the prototypical model, to accomplish this.

6 Further Insight into Other Control Methods

"*Available energy is energy which we can direct into any desired channel. Dissipated energy is energy which we cannot lay hold of and direct at pleasure, such as the energy of the confused agitation of molecules which we call heat.*"

- James Clerk Maxwell, 'Diffusion', Encyclopaedia Britannica (1878)

6.1 On the Similarity of Controller and Plant

Feedback Linearisation removes the plant dynamics and leaves behind a chain of integrators [15, Ch. 6]. In Chapter 5.1, it was shown that energy balancing is a form of feedback linearisation[1].

In Chapter 3.3, the ideas from [41, 40, 42] were presented and the idea of a *virtual system* was explained. The *virtual system* idea allows the control engineer to design an exponentially stable tracking controller or observer in the same framework.

In linear state feedback, if one wants to fully assign the closed loop eigenvalues, then the controller must be of the same order as the plant.

All of these ideas are linked. The controller in all of these cases has at least the same mathematical structure as the plant, in order to fully control the system. This increases the computational complexity of the control law.

In fact, throughout this dissertation, the control laws kept appearing as: a mathematical expression functionally similar to the plant plus a number of feedback terms. This pattern sparked the idea that, perhaps, in order to fully control a plant, the control algorithm needs to be at least as computationally complicated as the plant.

An excellent example, further demonstrating this idea, is *Maxwell's Demon* described in the context of an air traffic controller in [24]. Maxwell's Demon was described in approximately 1870 as a thought experiment that considers an imaginary creature (a "Demon") who is in control of a frictionless door between two partitions of a gas [24]. The demon has the ability to measure the speed of the particles in the gas and selectively let particles through (by way of opening and shutting the frictionless door) from one compartment into the other compartment [24]. This allows the demon to effectively "reverse" the second law of thermodynamics by making one compartment's temperature increase (increasing the average velocity of the particles by selectively letting through faster molecules) and the other compartment's temperature decrease [24].

[1] Plant inversion as a worst case.

Now Szilard reasoned that if entropy was changing in the gas system, and the demon was part of the system, then the demon must be taken into account in the entropy balance [24]. Hence the controller (Demon) has to bear a computational burden ("negentropy", information) equal to the degree that entropy needs to be reduced [24]. For want of a better name, this phenomenon is referred to as the Controller Complexity principle.

A formal proof of this idea is a recommended research direction.

6.2 PID Control of a Mass Spring Damper System

Before the effect of PID on a mass spring damper system is shown, the effect of a constant input force must be explored. Once this is understood, because of linearity, the resulting phase portrait will be a linear combination of the phase portraits, due to constant input forces, viscous damping and proportional feedback respectively. Given that second order models are typically used in the design of PID loops, the results presented here are directly applicable to practice [5, pp. 298-302].

A model of a mass spring damper system takes the form,

$$m\ddot{x} = -kx - b\dot{x} + F, \tag{6.2.1}$$

where m is the mass, k is the spring stiffness constant, b is the viscous damping constant and F is the input force.

Firstly, as was already mentioned in Chapter 3.4, viscous damping causes the trajectories of the mass spring system to asymptotically approach the origin. (This is depicted in Figure 3.4.6).

Next, consider the application of a constant force, $F = 1$ N with no dissipation, $b = 0$ Ns/m. The phase portrait of this system is depicted in Figure 6.2.1. It should be noted that the trajectories now orbit around a new point, $x = \frac{1}{2}$ m whereas in the unforced case, the trajectories all orbit around the point $x = 0$ m. These two values are called the *singular values* of the system and may be found using a number of techniques [15, pp. 20]. The two easiest methods are using the state space description and using energy directly. Putting equation (6.2.1) into state space form yields,

$$\begin{aligned} \dot{x} &= v \\ \dot{v} &= -kx - bv + F, \end{aligned}$$

which has the form,

$$\dot{\chi} = S(\chi),$$

with $\chi = \begin{bmatrix} x & v \end{bmatrix}^T$.

The singular points are found by setting $\dot{\chi} = \mathbb{O}$ [15, pp. 20].

This implies that, assuming F constant,

$$\begin{aligned} 0 &= v \\ 0 &= -kx - bv + F, \end{aligned}$$

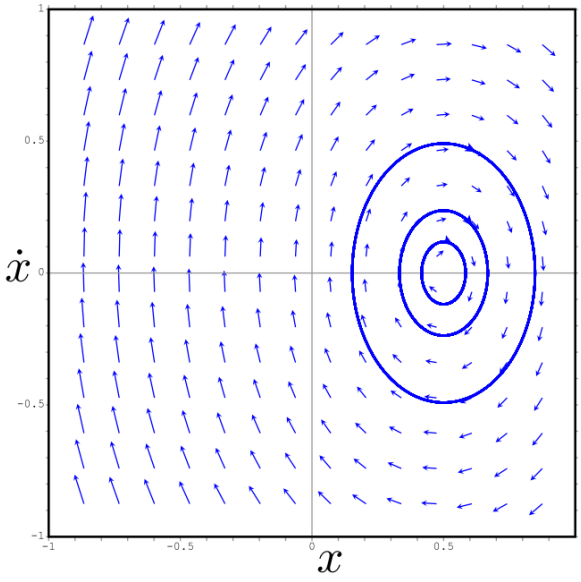

Figure 6.2.1: Mass Spring Damper with constant force, $F = 1$ N, $m = 1$ kg, $b = 0$ Ns/m, $k = 2$ N/m.

which when simplified leads to

$$\begin{aligned} v &= 0 \\ x &= \frac{F}{k}. \end{aligned}$$

For $k = 2$ N/m and $F = 1$ N then the singular point is found to be $x = \frac{1}{2}$ which is clear from Figure 6.2.1.

Using the energy directly requires finding the energy of equation (6.2.1), which can be found using a variety of well known methods.

The energy is, assuming constant F,

$$\frac{1}{2}m\dot{x}^2 + \frac{1}{2}kx^2 \quad -Fx = \quad E_0 - \int bv^2 \mathrm{d}t.$$

Let the energy of the system, $E_s = \frac{1}{2}m\dot{x}^2 + \frac{1}{2}kx^2 - Fx$. Now taking the gradient of $\nabla E = (kx - F, \dot{x})$ and setting it equal to $\mathbb{O}$ gives exactly the same singular point values

$$\begin{aligned} x &= \frac{F}{k} \\ \dot{x} &= 0. \end{aligned}$$

It should be clear that a change of k will change the curvature of the paraboloid that is the energy of the system, since it affects the potential function. Furthermore, a change in the value of b will affect the tightness of the spiral in the phase plane due to the more rapidly lowering of the plane in Figure 3.4.5. This is as a result of dissipating energy.

Now a special form of PID control, with set-point weighting [5, pp. 294], chosen to simplify the analysis, is

$$\begin{aligned} F &= -\kappa_p x - \kappa_d v + \zeta \\ \dot{\zeta} &= \kappa_i (x^* - x). \end{aligned}$$

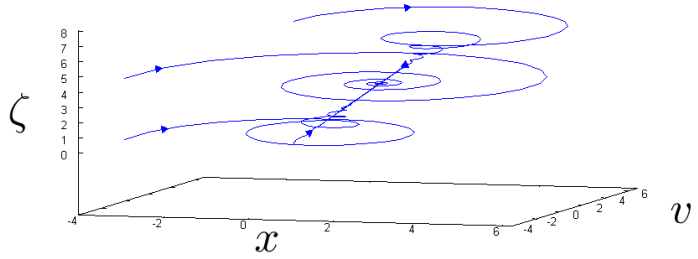

Figure 6.2.2: Phase portrait of PID action on a mass spring damper, $m = 1$ kg, $b = 0.5$ Ns/m, $k = 2$ N/m, $\kappa_p = 0$ N/m, $\kappa_d = 0$ Ns/m, $\kappa_i = 0.1$ N/ms

κ_p and κ_d can be seen to affect k and b respectively which has the effects already explained.

Hence the proportional term of PID affects the potential function, the derivative term affects the dissipation of the system and the integral term is discussed next.

ζ has the affect that it instantaneously offsets the *singular point* of the mass spring damper system by raising and lowering the plane of intersection in Figure 3.4.5, depending on whether the state, x is equal to x^*or not. The closed loop dynamics are,

$$\begin{aligned} \dot{x} &= v \\ \dot{v} &= -(k+\kappa_p)x-(b+\kappa_d)v+\zeta \\ \dot{\zeta} &= \kappa_i(x^*-x), \end{aligned}$$

which has the stationary point,

$$\begin{aligned} v &= 0 \\ \zeta &= (k+\kappa_p)x^* \\ x &= x^*. \end{aligned}$$

One cannot tell whether this stationary point is stable or not, but at the very least the state x is at the desired point x^*. It should be noted that, the force due to the integrator, has cancelled out the effects of the spring k and the proportional control action, due to κ_p [2]. A three-dimensional phase portrait with various initial conditions $(x,v,\zeta) = (0,0,0), (-4,0,0), (-4,0,4), (0,0,8)$ is depicted in Figure 6.2.2. Given that κ_p and κ_d affect k and b respectively, only k and b need to be altered in this simulation, with $\kappa_p = \kappa_d = 0$. The desired position is arbitrarily set to $x^* = 2$. This means that the force of the spring at the stationary point is $kx^* = k2 = 4$ N. It is clear in the phase portrait that all of the trajectories converge to the plane $\zeta = 4$ i.e. the integrator has cancelled out the effect of the spring at the new equilibrium point. All the while, the spring and damper cause the asymptotic spiraling into the desired state $(x,v) = (2,0)$.

[2] In fact, this ability of integral action to change the stationary point of a system does not depend on linearity [5, pp. 295]. This is probably the reason for PID control being employed so successfully across all engineering disciplines.

Insights into PID gained from Energy-Shaping

Forces dependent on x and v affect the potential and dissipation functions respectively. The effect of time varying forces is to raise and lower the plane of intersection of the energy function, depicted in Figure 3.4.5.

The rate at which the plane of intersection of the energy function is moving up or down, the power, is dependent on $v\,\kappa_i \int (x^* - x)\mathrm{d}t$ and the dissipation $(b+\kappa_d)\,v^2$. The spring and damper naturally cause the system to spiral towards zero, while the integrator (instantaneously) affects the stationary point and therefore the point that the spring and damper approach. This also explains why if κ_i is too large, the system can become unstable. Essentially, the natural dynamics are not allowed to settle towards the new stationary point and power is continuously added by the integrator, which compounds the issue. In other words, the plane of $\zeta = (k+\kappa_p)\,x^*$ is "missed" due to the energy being added to the system too quickly. The exact value of κ_i for marginal stability is given by,

$$\kappa_i \quad = \quad \frac{(k+\kappa_p)(b+\kappa_d)}{m},$$

which is dimensionally correct and can be found analytically using standard linear techniques.

Hence the effect of PID is one of energy shaping itself, the proportional term affects the curvature of the paraboloid (by altering the potential function/spring term), the derivative term affects the rate at which the plane of intersection of the energy function decreases to the equilibrium point i.e. the 'tightness' of the spiral (by altering the dissipation function) and the integrator affects the equilibrium point of the system.

6.3 PI Control of a First-Order System

In the process control sector of industry, coupled first order systems (with or without delay) are the types of models typically used for control design [34, pp. 40-45].

Consider, for simplicity's sake, the single input, single output, first-order system,

$$r\frac{\mathrm{d}y}{\mathrm{d}t} \quad = \quad -k\,y + u,$$

where y is the output of interest and u is the input and r and k are model parameters. A good deal of insight is gained by putting this into the prototypical form,

$$m\frac{\mathrm{d}^2\mathrm{y}}{\mathrm{d}t^2} + r\frac{\mathrm{dy}}{\mathrm{d}t} + k\,y \quad = \quad u,$$

with $m = 0$. This means that the system behaves as a "mass-less mass-spring-damper". Hence there is no inertia to overcome and the system will return to the "springs" natural equilibrium ($y = 0$) at a rate limited by how strong the damper is. The theory of differential equations has the same result (for real parameters r and k) since the natural response to the differential equation,

$$r\frac{\mathrm{d}y}{\mathrm{d}t} + k\,y \quad = \quad 0,$$

has the solution, with y_0 given by initial conditions,

$$y = y_0 e^{-\frac{k}{r}t}.$$

This solution has all of the properties reasoned about previously by intuition.

Now consider the PI control law (with set-point weighting),

$$u = -\kappa_p y + \kappa_i \int (y^* - y)\,\mathrm{d}t,$$

which results in,

$$r\frac{\mathrm{d}y}{\mathrm{d}t} + ky = -\kappa_p y + \kappa_i \int (y^* - y)\,\mathrm{d}t, \tag{6.3.1}$$

when applied to the system. By differentiating both sides of eq (6.3.1) with respect to time and factoring, the closed-loop system becomes,

$$r\frac{\mathrm{d}^2 y}{\mathrm{d}t^2} + (k + \kappa_p)\frac{\mathrm{d}y}{\mathrm{d}t} + \kappa_i (y - y^*) = 0. \tag{6.3.2}$$

By inspection, the first-order system under PI control behaves now as a mass-spring-damper system with "mass" r, linear "damper" constant $(k+\kappa_p)$ and "spring" $\kappa_i (y - y^*)$. The "spring" term is interesting as it has a natural equilibrium at y^* and re-iterates the point of the integrator reducing steady-state error to zero. Another interesting feature brought about by this representation is that the proportional term actually acts like a damper under closed-loop conditions. Hence if the closed-loop system is too oscillatory, the proportional term should be increased to dampen out the oscillations.

By analysing the PI control of a first-order system, in terms of the prototypical model and the energy domain, new insight into the closed-loop behaviour of the system has been gained.

6.4 State Feedback shapes the Potential and Dissipation functions

State feedback is a well known linear control methodology and typically has a control law of the form,

$$\mathbf{u} = -\mathbf{K}\chi,$$

subject to the model

$$\dot{\chi} = \mathbf{A}\chi + \mathbf{B}\mathbf{u},$$

where $\chi \in \mathbb{R}^N$ and $\mathbf{u} \in \mathbb{R}^M$ [51, pp. 249].

The non-linear analog of this method has a control law of the form,

$$\mathbf{u} = -\mathbf{K}(\chi),$$

subject to the 'input affine' model,

$$\dot{\chi} \quad = \quad \mathbf{F}(\chi) + \mathbf{G}(\chi)\mathbf{u} \tag{6.4.1}$$

where again $\chi \in \mathbb{R}^N$ and $\mathrm{u} \in \mathbb{R}^M$ [52, pp. 239-241]. If the model is derived from physical considerations using Lagrangian or Hamiltonian mechanics, it is clear that the states χ, will consist of generalised co-ordinates (distance, charge, angle etc.) and generalised velocities (velocity, current, angular velocity etc.) or some scalar multiple of these [36][25, Appendix B]. Hence the states may be partitioned as $\chi = \begin{bmatrix} \mathbf{x} & \mathbf{v} \end{bmatrix}^T$ where $\mathbf{x} \in \mathbb{R}^N$ are the generalised co-ordinates and $\mathbf{v} \in \mathbb{R}^N$ are the generalised velocities. Given this, the control law

$$\mathbf{u} \quad = \quad -\mathbf{K}(\chi)$$

can be decomposed into a part containing the generalised co-ordinate $\mathbf{x}$, a part linear in the generalised velocity, $\mathbf{v}$, and a 'mixed' part with

$$-\mathbf{K}(\chi) \quad = \quad -\mathbf{K_p}(\mathbf{x}) - \mathbf{K_d}(\mathbf{x},\mathbf{v})\mathbf{v} - \mathbf{K_m}(\mathbf{x},\mathbf{v}). \tag{6.4.2}$$

Before continuing, it is pertinent to mention that the input affine model can be generated from the prototypical model eq (3.1.1) as long as $\mathbf{M}(\mathbf{x},t)$ has an inverse. $\mathbf{M}(\mathbf{x},t)$ will realistically always have an inverse since it is always positive definite, and it is always positive definite, because, if it weren't, then a negative kinetic energy could be possible, and this is disallowed [10]. Hence from,

$$\mathbf{M}(\mathbf{x},t)\ddot{\mathbf{x}} + \mathbf{D}(\mathbf{x},\mathbf{v})\mathbf{v} + \mathbf{K}(\mathbf{x}) \quad = \quad \mathbf{G}(\mathbf{x})\mathbf{u}$$

the following is arrived at

$$\begin{aligned} \dot{\mathbf{x}} &= \mathbf{v} \\ \dot{\mathbf{v}} &= -\mathbf{M}(\mathbf{x},t)^{-1}\left(\mathbf{D}(\mathbf{x},\mathbf{v})\mathbf{v} + \mathbf{K}(\mathbf{x})\right) + \mathbf{M}(\mathbf{x},t)^{-1}\mathbf{G}(\mathbf{x})\mathbf{u} \end{aligned}$$

which is exactly equal to the input affine model, eq (6.4.1) with $\chi = \begin{bmatrix} \mathbf{x} & \mathbf{v} \end{bmatrix}^{\mathrm{T}}$,

$$\mathbf{F}(\chi) \quad = \quad \begin{pmatrix} \mathbf{v} \\ -\mathbf{M}(\mathbf{x},t)^{-1}\left(\mathbf{D}(\mathbf{x},\mathbf{v})\mathbf{v} + \mathbf{K}(\mathbf{x})\right) \end{pmatrix}$$

and

$$\mathbf{G}(\chi) \quad = \quad \mathbf{M}(\mathbf{x},t)^{-1}\mathbf{G}(\mathbf{x}).$$

So it has been shown that the input affine model can be derived from the prototypical model and furthermore that the general non-linear state feedback can be decomposed in eq (6.4.2). Hence when the general state feedback is applied to the prototypical model one finds

$$\mathbf{M}(\mathbf{x},t)\ddot{\mathbf{x}} + \mathbf{D}(\mathbf{x},\mathbf{v})\mathbf{v} + \mathbf{K}(\mathbf{x}) \quad = \quad -\mathbf{G}(\mathbf{x})\left(\mathbf{K_p}(\mathbf{x}) + \mathbf{K_d}(\mathbf{x},\mathbf{v})\mathbf{v} + \mathbf{K_m}(\mathbf{x},\mathbf{v})\right)$$

which results in

$$\mathbf{M}(\mathbf{x},t)\ddot{\mathbf{x}} + \Big(\underbrace{\mathbf{D}(\mathbf{x},\mathbf{v}) + \mathbf{G}(\mathbf{x})\mathbf{K_d}(\mathbf{x},\mathbf{v})}_{\text{new } \mathbf{D}(\mathbf{x},\mathbf{v})}\Big)\mathbf{v} + \Big(\underbrace{\mathbf{K}(\mathbf{x}) + \mathbf{G}(\mathbf{x})\mathbf{K_p}(\mathbf{x})}_{\text{new } \mathbf{K}(\mathbf{x})}\Big) \quad = \quad -\underbrace{\mathbf{G}(\mathbf{x})\mathbf{K_m}(\mathbf{x},\mathbf{v})}_{\text{forcing function}}$$

and each of the terms in the control law can clearly be seen to affect the dissipation, potential and input force.

The linear case follows the exact same derivation with $\mathbf{K_p}(\mathbf{x}) = \mathbf{K_p}\,\mathbf{x}$, $\mathbf{K_d}(\mathbf{x},\mathbf{v})\mathbf{v} = \mathbf{K_d}\,\mathbf{v}$ and $\mathbf{K_m}(\mathbf{x},\mathbf{v}) = 0$ where $\mathbf{K_p}$, $\mathbf{K_d}$ are suitably defined constant matrices[3].

Hence both linear and non-linear state feedback shape the potential and dissipation functions, with the general non-linear state feedback introducing a forcing function dependent on $\mathbf{x}$ and $\mathbf{v}$. It should be noted that there is a clear physical interpretation of what has happened to the prototypical system when applying the control law[4]. This insight is lost in the input affine case and suggests, that it is perhaps best to leave the model equations as coupled second order differential equations.

6.5 Feedback Linearisation is a natural result of Energy Balancing

The goal of Feedback Linearisation is to transform the model equations into the control of a number of integrators [15, Ch. 6].

For example consider the input affine model from eq (6.4.1) again,

$$\dot{\chi} \;=\; \mathbf{F}(\chi) + \mathbf{G}(\chi)\mathbf{u}.$$

A control of the form

$$\mathbf{u} \;=\; \mathbf{G}(\chi)^{-\mathbf{1}}\{\mathbf{r} - \mathbf{F}(\chi)\}$$

results in

$$\dot{\chi} \;=\; \mathbf{r}$$

and achieves Feedback Linearisation. All that remains is to design $\mathbf{r}$ according to some control objective and the control problem is solved [15, Ch. 6]. There are restrictions that must be kept in mind when applying this technique, the interested reader is referred to [15, Ch. 6] and [52, Chapter 5.3] for a detailed exposition on the method and restrictions.

Given the prototypical model eq (3.1.1), the energy of the system E_s is given by

$$E_s \;=\; \frac{1}{2}\mathbf{v}^{\mathrm{T}}\mathbf{M}(\mathbf{x},t)\mathbf{v} + \int \mathbf{K}(\mathbf{x})^{\mathrm{T}}\mathrm{d}\mathbf{x}$$

and is derived in Chapter 4. An energy balancing controller essentially makes the controller supply the difference between the stored and the desired energy E_d, which is described in detail in Chapter 5.1.

[3] It should be clear here that state feedback is actually a generalised PD controller

[4] For systems which have negligible inertia, such as chemical systems, $\mathbf{M}(\mathbf{x},t) = 0$ and the control law will affect the model as follows:

$$\Big(\underbrace{\mathbf{D}(\mathbf{x},\mathbf{v}) + \mathbf{G}(\mathbf{x})\mathbf{K_d}(\mathbf{x},\mathbf{v})}_{\text{new}\,\mathbf{D}(\mathbf{x},\mathbf{v})}\Big)\mathbf{v} + \Big(\underbrace{\mathbf{K}(\mathbf{x}) + \mathbf{G}(\mathbf{x})\mathbf{K_p}(\mathbf{x})}_{\text{new}\,\mathbf{K}(\mathbf{x})}\Big) \;=\; -\underbrace{\mathbf{G}(\mathbf{x})\mathbf{K_m}(\mathbf{x},\mathbf{v})}_{\text{forcing function}}.$$

It requires that

$$\frac{\mathrm{d}}{\mathrm{d}t}(E_s - E_d) \quad = \quad 0,$$

which results in

$$\mathbf{v}^{\mathrm{T}}(\mathbf{M}(\mathbf{x},t)\ddot{\mathbf{x}} + \mathbf{D}(\mathbf{x},\mathbf{v})\mathbf{v} + \mathbf{K}(\mathbf{x}) - \mathbf{G}(\mathbf{x})\mathbf{u}) \quad = \quad \mathbf{v}^{\mathrm{T}}(\mathbf{y_d} + \Phi(\mathbf{x},\mathbf{v})) \tag{6.5.1}$$

where $\mathbf{y_d}$ are the target dynamics as a result of choosing E_d and $\Phi(\mathbf{x},\mathbf{v})$ are the desired dissipation, loss-less power transformations, Coriolis/Centripetal forces lumped together. Notice that for a solution to exist $\frac{\mathrm{d}}{\mathrm{d}t}E_d$ must equal $\mathbf{v}^{\mathrm{T}}$ times some function. Now the solution of eq (6.5.1) results in a control law of the form,

$$\begin{aligned} \mathbf{u} &= \mathbf{G}(\mathbf{x})^{-1}\left(\underbrace{\mathbf{K}(\mathbf{x}) + \mathbf{D}(\mathbf{x},\mathbf{v})\mathbf{v} + \mathbf{M}(\mathbf{x},t)\ddot{\mathbf{x}}}_{\text{cancel dynamics}} - \mathbf{u}^*\right) \\ \mathbf{u}^* &= \mathbf{y_d} + \Phi(\mathbf{x},\mathbf{v}), \end{aligned}$$

which is clearly of the same form as the feedback linearisation control law[5]. It should be noted that if $E_d = E_s$, then the control law results in $\mathbf{u} = \mathbb{O}$. This is intuitive since there is no control problem if the system already behaves in the desired manner. Interconnection and Damping Assignment Passivity Based Control (IDAPBC) is also shown to be feedback linearisation in Chapter 5.5. The key point in both energy-balancing and IDAPBC is that the target dynamics, $\mathbf{r}$, are chosen, bearing the influence on the system energy in mind. It is worth mentioning that a desired energy of $E_d = \frac{1}{2}\mathbf{v}^{\mathrm{T}}\mathbf{v}$ which is the kinetic energy of N uncoupled unit masses and $\dot{E}_d = \mathbf{v}^{\mathrm{T}}\mathbf{r}$ where $\mathbf{r}$ is some new input force leads to exactly the control of a N dimensional double integrator i.e. $\ddot{\mathbf{x}} = \mathbf{r}$ as is expounded upon in Chapter 5.1.

6.6 Controlled Lyapunov related to Power Shaping

The controlled Lyapunov technique involves choosing a Lyapunov function[6] (which is positive definite), $V(\mathbf{x})$ for the system

$$\dot{\mathbf{x}} \quad = \quad \mathbf{F}(\mathbf{x},\mathbf{u})$$

with state $\mathbf{x} \in \mathbb{R}^N$ and input $\mathbf{u} \in \mathbb{R}^M$ [5, pp. 124]. Taking the time derivative of the Lyapunov function leads to

$$\begin{aligned} \frac{\mathrm{d}}{\mathrm{d}t}V(\mathbf{x}) &= \frac{\partial V}{\partial \mathbf{x}}\dot{\mathbf{x}} \\ &= \frac{\partial V}{\partial \mathbf{x}}\mathbf{F}(\mathbf{x},\mathbf{u}), \end{aligned}$$

where the system model $\dot{\mathbf{x}} = \mathbf{F}(\mathbf{x},\mathbf{u})$ has been used [5, pp. 124].

[5] There is a subtlety here in that this is actually plant inversion; this is addressed in full in Chapter 5.1

[6] The Lyapunov function is a *scalar* which takes a vector input.

All that remains is for the designer to create a control law $\mathbf{u} = \beta(\mathbf{x})$ that stabilises the system by ensuring that $\frac{\partial V}{\partial \mathbf{x}} \mathbf{F}(\mathbf{x}, \beta(\mathbf{x})) < 0$ for the desired region in the state space [5, pp. 124]. This is not a trivial task in general.

Now if $V(\mathbf{x})$ is chosen to be the actual energy of the system, E_s, then it follows that $\dot{V}(\mathbf{x}) = \dot{E}_s$ which is the power flow of the system . This will include the input, as shown in Chapter 4. Hence, designing a control law with this $\dot{V}(\mathbf{x})$ in mind is tantamount to power shaping.

6.7 Contraction Analysis is an Energy Argument for a Suitably Chosen Metric

Contraction analysis is a technique which offers an alternative to Lyapunov based proofs of stability [41]. It is stronger than Lyapunov stability in that conclusions can be drawn about rate of convergence, region of convergence as well as whether any two trajectories converge to a point or some nominal trajectory [41]. If a region in the state space of a system is *contracting* then it enjoys this strong form of stability, which is to say that any two trajectories in the contracting region exponentially approach each other [41]. The method is described in full in Chapter 3.3. With the introduction of a *virtual system*, contraction analysis is significantly easier to use to prove stability as compared to Lyapunov stability.

Now the most general form of Contraction analysis involves looking at the time derivative of the differential form,

$$\delta\chi^{\mathrm{T}}\mathbf{M}_{\mathbf{e}}(\chi,t)\delta\chi$$

where $\delta\chi$ is the virtual displacement (the separation between any two neighbouring trajectories in the state space at the *same* time), $\mathbf{M}_{\mathbf{e}}(\chi,t)$ is the metric chosen for the state space and $\chi \in \mathbb{R}^N$ [41]. Now if the metric $\mathbf{M}_{\mathbf{e}}(\chi,t)$ is chosen such that the differential form has the units of energy, then contraction analysis becomes an argument about the "incremental" energy i.e. the difference in energy between neighbouring trajectories in the state space.

Let the state $\chi = \begin{bmatrix} \mathbf{x} & \mathbf{v} \end{bmatrix}^{\mathrm{T}}$ with the differential form $\delta\chi^{\mathrm{T}}\mathbf{M}_{\mathbf{e}}(\chi,t)\delta\chi$ given by

$$\begin{bmatrix} \delta\mathbf{x} & \delta\mathbf{v} \end{bmatrix} \begin{bmatrix} 0 & 0 \\ 0 & \mathbf{M}(\mathbf{x},t) \end{bmatrix} \begin{bmatrix} \delta\mathbf{x} \\ \delta\mathbf{v} \end{bmatrix}$$

where $\mathbf{M}(\mathbf{x},t)$ is as defined in the prototypical model eq (3.1.1). If the time derivative of the differential form is always decreasing for any virtual displacement $\delta\chi = \begin{bmatrix} \delta\mathbf{x} & \delta\mathbf{v} \end{bmatrix}^{\mathrm{T}}$, then the system eq (3.1.1) is said to be *contracting* [41]. Taking the time derivative of the differential form defined in terms of energy leads to

$$\frac{\mathrm{d}}{\mathrm{d}t}\left(\delta\chi^{\mathrm{T}}\mathbf{M}_{\mathbf{e}}(\chi,t)\delta\chi\right) = \delta\mathbf{v}^{\mathrm{T}}\mathbf{M}(\mathbf{x},t)\delta\dot{\mathbf{v}} + \frac{1}{2}\delta\mathbf{v}^{\mathrm{T}}\dot{\mathbf{M}}(\mathbf{x},t)\delta\mathbf{v}. \tag{6.7.1}$$

Now by calculating the virtual displacement and velocities of the prototypical model eq (3.1.1)

$$\mathbf{M}(\mathbf{x},t)\delta\dot{\mathbf{v}} + [\mathbf{D}(\mathbf{x},\mathbf{v})\mathbf{v}]_{\mathbf{v}}\delta\mathbf{v} + [\mathbf{D}(\mathbf{x},\mathbf{v})\mathbf{v}]_{\mathbf{x}}\delta\mathbf{x} + \mathbf{D}(\mathbf{x},\mathbf{v})\delta\mathbf{v} + \mathbf{K}(\mathbf{x})_{\mathbf{x}}\delta\mathbf{x} = \mathbf{G}(\mathbf{x})\delta\mathbf{u} + [\mathbf{G}(\mathbf{x})\mathbf{u}]_{\mathbf{x}}\delta\mathbf{x}$$

and solving for

$$\begin{aligned} \mathbf{M}(\mathbf{x},t)\delta\dot{\mathbf{v}} = {} & \mathbf{G}(\mathbf{x})\delta\mathbf{u} + [\mathbf{G}(\mathbf{x})\mathbf{u}]_{\mathbf{x}}\delta\mathbf{x} - [\mathbf{D}(\mathbf{x},\mathbf{v})\mathbf{v}]_{\mathbf{v}}\delta\mathbf{v} \\ & - [\mathbf{D}(\mathbf{x},\mathbf{v})\mathbf{v}]_{\mathbf{x}}\delta\mathbf{x} - \mathbf{D}(\mathbf{x},\mathbf{v})\delta\mathbf{v} - \mathbf{K}(\mathbf{x})_{\mathbf{x}}\delta\mathbf{x} \end{aligned} \tag{6.7.2}$$

yields the dynamics of the system due to an arbitrary virtual displacement in the state space $\delta\chi$[7].

Substitution of eq (6.7.2) into (6.7.1) and remembering that $\mathbf{D}(\mathbf{x},\mathbf{v}) = \mathbf{R}(\mathbf{x},\mathbf{v}) + \mathbf{J}(\mathbf{x},\mathbf{v}) + \frac{1}{2}\dot{\mathbf{M}}(\mathbf{x},t)$, leads to

$$\begin{aligned}
\frac{\mathrm{d}}{\mathrm{d}t}\left(\delta\chi\mathbf{M}_{\mathbf{e}}(\chi,t)\delta\chi\right) &= \delta\mathbf{v}\left(\mathbf{G}(\mathbf{x})\delta\mathbf{u} + [\mathbf{G}(\mathbf{x})\mathbf{u}]_{\mathbf{x}}\,\delta\mathbf{x} - [\mathbf{D}(\mathbf{x},\mathbf{v})\mathbf{v}]_{\mathbf{v}}\,\delta\mathbf{v}\right) \\
&\quad + \delta\mathbf{v}\left(-[\mathbf{D}(\mathbf{x},\mathbf{v})\mathbf{v}]_{\mathbf{x}}\,\delta\mathbf{x} - \mathbf{R}(\mathbf{x},\mathbf{v})\delta\mathbf{v} - [\mathbf{K}(\mathbf{x})]_{\mathbf{x}}\,\delta\mathbf{x}\right) \\
&= -\delta\mathbf{v}\left(\mathbf{R}(\mathbf{x},\mathbf{v}) + [\mathbf{D}(\mathbf{x},\mathbf{v})\mathbf{v}]_{\mathbf{v}}\right)\delta\mathbf{v} \\
&\quad - \delta\mathbf{v}\left([\mathbf{K}(\mathbf{x})]_{\mathbf{x}} + [\mathbf{D}(\mathbf{x},\mathbf{v})\mathbf{v}]_{\mathbf{x}} - [\mathbf{G}(\mathbf{x})\mathbf{u}]_{\mathbf{x}}\right)\delta\mathbf{x} + \delta\mathbf{v}\mathbf{G}(\mathbf{x})\delta\mathbf{u}
\end{aligned}$$

which is the incremental power equation for the prototypical system. This needs to be less than $\beta\mathbf{M}_{\mathbf{e}}(\chi,t)$ for all $\delta\mathbf{v}$, $\delta\mathbf{x}$ and $\delta\mathbf{u}$ in order for contraction to occur [41, 40, 42]. This should be juxtaposed with the typical approach used in contraction analysis i.e. choose a controller structure $\mathbf{u} = \mathbf{F}(\chi)$ and then analyse the system for contraction in terms of $\delta\chi$ and the free parameters of $\mathbf{F}(\chi)$ [41, 40, 42].

It is very interesting to note that if

$$\mathbf{G}(\mathbf{x})\delta\mathbf{u} = \left([\mathbf{K}(\mathbf{x})]_{\mathbf{x}} + [\mathbf{D}(\mathbf{x},\mathbf{v})\mathbf{v}]_{\mathbf{x}} - [\mathbf{G}(\mathbf{x})\mathbf{u}]_{\mathbf{x}}\right)\delta\mathbf{x}$$

then $\frac{\mathrm{d}}{\mathrm{d}t}\left(\delta\chi\mathbf{M}_{\mathbf{e}}(\chi,t)\delta\chi\right)$ is negative definite for all $\delta\mathbf{v}$ as long as $[\mathbf{D}(\mathbf{x},\mathbf{v})\mathbf{v}]_{\mathbf{x}}$ is positive definite. The controller $\mathbf{u}$ is then found by integration of

$$\int \mathbf{G}(\mathbf{x})\delta\mathbf{u} = \int_{\mathbf{x_d}}^{\mathbf{x}} \left([\mathbf{K}(\mathbf{x})]_{\mathbf{x}} + [\mathbf{D}(\mathbf{x},\mathbf{v})\mathbf{v}]_{\mathbf{x}} - [\mathbf{G}(\mathbf{x})\mathbf{u}]_{\mathbf{x}}\right)\delta\mathbf{x}$$

and solving for $\mathbf{u}$, assuming such a solution exists. The inspiration for this idea of constructing an incremental control input and solving for u via integration is found in [40]. Hence, contraction analysis is an energy argument for a suitably chosen metric.

[7] Note: $[h]_y$ is the partial derivative of h with respect to y

7 Recommendations and Conclusions

7.1 Conclusion

The principles related to energy have been shown to be an invaluable tool in both modelling and control algorithm design. The main techniques for energy-shaping control are energy balancing and power shaping. Three constructive energy-shaping techniques were expounded upon: controller interpolation using a common Lyapunov function, energy-shaping controllers from robotics and IDAPBC. The generalisation of *The Energy Method* has offered a viable alternative to Lagrangian and Hamiltonian mechanics. Furthermore, since it is founded on the conservation of energy, it adds insight into the understanding of systems that can be put into prototypical form. All physical systems can be put into this prototypical framework since it is founded on the first law of thermodynamics.

Power-shaping has been extended to account for dissipation. Since dissipation was shown to act as a constant disturbance in the power equation, it could be compensated for using a non-linear energy integrator. Power-shaping has further been extended to handle multi-dimensional systems as well as non-constant desired energies, E_d.

The Heuristic Fuzzy Logic controller was shown to be an interpolation between controllers that make a common Lyapunov function negative definite.

A number of energy shaping robot control laws have been adapted for the prototypical system.

Thus, by considering the effects of a control algorithm on the energy of a system, additional insight into the action of the controller on the system is gained.

The link between phase portraits and the energy of a system was established. Hence, shaping the energy of a system shapes the phase portrait and shaping the phase portrait shapes the time domain performance. Phase portraits therefore represent the link between energy and time. Phase portraits also provide global information at a glance, information that is not available in time plots such as step responses, initial condition plots and their ilk.

Contraction analysis is an invaluable tool for stability proofs. This is achieved by only using the terms that directly affect stability of the system. Furthermore, the trick of defining an appropriate virtual system, allows the control engineer to design observers or controllers in a single framework. Conclusions about stability follow in a very simple, straightforward manner

Energy Shaping controllers have far richer control structures and allow for greater performance (even in the presence of non-linearity and modelling errors) than linear PID techniques. Furthermore, the energy-shaping controllers are synthesised in a framework with which every engineer is familiar, namely energy. There is a tremendous advantage to using physical insight into control algorithm development, rather than the abstract mathematical techniques that appear to have dominated the control engineering field of late and which seem to lose track of both engineering insight and reality.

7.2 Recommendations for Further Research

Given the basics of IDAPBC in Chapter 5.5 and the similarity in the matching conditions of Chapter 5.1 and 5.2, it should be possible to extend the energy-shaping techniques presented in this dissertation into the under-actuated case. It is conjectured that by solving the same equations, but with an additional *left annihilator* equation, the under-actuated case can be taken care of.

A formal proof of the Controller Complexity principle and its links to entropy in the spirit of Maxwell's Demon would add a valuable tool to non-linear control.

The extension of the prototypical model to include distributed systems (eg. flexible links and boundary value problems) should allow for the energy shaping insight to extend to these sorts of systems.

The extension of the phase portrait insights into more than three dimensions would be an invaluable tool for non-linear control system analysis and design.

It would be extremely interesting to see the effect of other well known control structures, such as the Linear Quadratic Regulator (LQR) , on the energy of the system. Of course, if the algorithm is a general state feedback strategy, then its exact effect on the energy of the prototypical system was shown in Chapter 6. It is therefore a reasonable prediction that LQR is a time-varying dissipation and potential shaping controller, when applied to the prototypical system.

A related topic that would yield some interesting results would be the optimal control problem cast in terms of the system's physical energy.

References

[1] J C Maxwell. On Governors. *Proceedings of the Royal Society*, 100:1–12, 1868.

[2] M Takegaki and S Arimoto. A New Feedback Method for Dynamic Control of Manipulators. *Journal of Dynamic Systems and Control*, 103:119 (7 pages), 1981.

[3] H Takatsu and T Itoh. Future Needs for Control Theory in Industry - Report of the Control Technology Survey in Japanese Industry. *IEEE Transactions on Control Systems Technology*, 7:298–305, 1999.

[4] L Desbourough and R Miller. Increasing Customer Value of Industrial Control Performance Monitoring - Honeywell's Experience. volume 98 of *AIChE Symposium*, 2002.

[5] K J Astrom and R M Murray. Feedback Systems: An Introduction for Scientists and Engineers. Princeton University Press, February 2009.

[6] D Jeltsema, R Ortega, and J Sherpen. An Energy-Balancing Perspective of Interconnection and Damping Assignment Control of Nonlinear Systems. *Automatica*, 40:1643–1646, 2004.

[7] A M Bloch, N E Leonard, and J E Marsden. Controlled Lagrangians and the Stabilization of Mechanical Systems I: The First Matching Theorem. *IEEE Transactions on Automatic Control*, VOL. 45, NO. 12:2253–2270, December, 2000.

[8] A M Bloch, D E Chang, N E Leonard, and J E Marsden. Controlled Lagrangians and the Stabilization of Mechanical Systems II: Potential Shaping. *IEEE Transactions on Automatic Control*, VOL. 46:1556–1571, October, 2001.

[9] D V Zenkov, A M Bloch, and J E Marsdon. Controlled Lagrangian Methods and Tracking of Accelerated Motions, 2003.

[10] Russell Tedrake. 6.832 Underactuated Robotics. Online, Spring 2009. Massachusetts Institute of Technology: MIT OpenCouseWare (Accessed 09 September 2011), License: Creative Commons BY-NC-SA.

[11] M Spong. The Swing-Up Control Problem of the Acrobot. *Control Systems, IEEE*, 15:49–55, 1995.

[12] A Favache and D Dochain. Power-Shaping Control of an Exothermic Continuous Stirred Tank Reactor (CSTR). In *Proceedings of the 48th IEEE Conference on Decision and Control, 2009 held jointly with the 2009 28th Chinese Control Conference. CDC/CCC 2009.*, pages 1866–1871. Strong Point Center in Process Systems Engineering, Trondheim, Norway, 2009.

[13] L K Wong, F H F Leung, and P I S Tam. Lyapunov Function Based Design of Heuristic Fuzzy Logic Controllers. In *Proceedings of the Sixth IEEE International Conference on Fuzzy Systems*, 1997.

[14] S Arimoto. Control of Mechanical Systems. *Scholarpedia*, 4:6520, 2009. Revision 91168.

[15] J E Slotine and W Li. *Applied Nonlinear Control*. Prentice Hall, 1991.

[16] H Hoang, F Couenne, C Jallut, and Y Le Gorrec. Hamiltonian Formulation and IDA-PBC Control of Non-isothermal Continuous Stirred Tank Reactors. *Proceedings of the 9th International Symposium on Dynamics and Control of Process Systems (DYCOPS 2010),*, 9:707–712, July 5-7, 2010.

[17] A van der Schaft and D Jeltsema. Port-Hamiltonian Systems: from Geometric Network Modeling to Control. In *EECI*, April, 2009.

[18] R Ortega, A van der Schaft, I Mareels, and B Maschke. Putting Energy Back In Control. *IEEE Control Systems Magazine*, 21:18–33, 2001.

[19] R Ortega, A van der Schaft, B Maschke, and G Escobar. Interconnection and Damping Assignment Passivity-based Control of Port Controlled Hamiltonian Systems. *Automatica*, 38:585–596, 2002.

[20] D Basic, F Malrait, and P Rouchon. Euler-Lagrange Models with Complex Currents of Three-Phase Electrical Machines. arXiv, June 24 2008.

[21] J M A Scherpen, D Jeltsema, and J B Klaassens. Lagrangian Modelling of Switching Electrical Networks. *Systems & Control Letters*, 48:365–374, 2003.

[22] P. Cominos and N. Munro. PID Controllers: Recent Tuning Methods and Design to Specification. *IEE Process Control, Theory and Applications*, 149:46–53, January 2002.

[23] R Serway and J Jewett. *Physics for Scientists and Engineers*. Brooks Cole, 6th edition, 2004.

[24] S.R Sporn. The Air Traffic Controller and Maxwell's Demon. In *Proceedings of the 1994 IEEE National Aerospace and Electronics Conference*, pages 1309–1316, 1994.

[25] R Ortega, A Loria, P J Nicklasson, and H Sira-Ramirez. *Passivity-based Control of Euler-Lagrange Systems*. Springer, 1998.

[26] A M Bloch, N E Leonard, and J E Marsden. Stabilization of Mechanical Systems using Controlled Lagrangians, 1997.

[27] D E Chang, A M Bloch, N E Leonard, J E Marsden, and C A Woolsey. The Equivalence of Controlled Lagrangian and Controlled Hamiltonian Systems for Simple Mechanical Systems. *ESAIM: Control,Optimisation, and Calculus of Variations*, 8:393–422, 2002.

[28] K Reddy Chevva. *Practical Challenges in the Method of Controlled Lagrangians*. PhD thesis, Faculty of the Virginia Polytechnic Institute and State University, School of Engineering Science and Mechanics, August 2005.

[29] S Boyd. Lecture 14: Lyapunov Theory with Inputs and Outputs. Stanford Website, Winter 2008.

[30] S Boyd. Lecture 12: Basic Lyapunov Theory. Stanford Website, Winter 2008.

[31] S Boyd. Lecture 16: Analysis of Systems with Sector Non-linearities. Stanford Website, Winter 2008.

[32] LK Wong, P I S Tam, and F H F Leung. Lyapunov Function Based Design of Fuzzy Logic Controllers and its Application on Combining Controllers. *IEEE Transactions on Industrial Electronics*, 45:502–509, 1998.

[33] A Behal, W Dixon, D Dawson, and B Xian. *Lyapunov-Based Control of Robotic Systems*. CRC Press, 2010.

[34] K M Hangos, J Bokor, and G Szederkenyi. *Analysis and Control of Nonlinear Process Systems*. Springer, 2004.

[35] A Bogdanov. Optimal Control of a Double Inverted Pendulum on a Cart. Technical report, Department of Computer Science & Electrical Engineering, OGI School of Science & Engineering, OHSU, December 2004.

[36] C G Gray. Principle of Least Action. *Scholarpedia*, 4(12):8291, 2009.

[37] F Tisseur and K Meerbergen. The Quadratic Eigenvalue Problem. *Society for Industrial and Applied Mathematics*, 43(2):235–286, May 2001.

[38] J C M van der Burg, R Ortega, J M A Scherpen, J A Acostaand, and H B Siguerdidjane. An Experimental Application of Total Energy Shaping Control: Stabilization of the Inverted Pendulum on a Cart in the Presence of Friction. In *Proceedings of the European Control Conference*, pages 1990–1996. European Control Conference in 2007, 2007.

[39] D A Wells. *Schaum's Outlines: Lagrangian Mechanics*. McGraw Hill, 1967.

[40] W Lohmiller and J E Slotine. Contraction Analysis: A Practical Approach to Nonlinear Control Applications. In *Proceedings of the 1998 IEEE International Conference on Control Applications*. IEEE, September 1998.

[41] W Lohmiller and J E Slotine. On Contraction Analysis for Nonlinear Systems. *Automatica*, 34:683–696, 1998.

[42] J E Slotine and J Jouffroy. Methodological Remarks on Contraction Theory. In *43rd IEEE Conference on Decision and Control*, pages 2537–2543. Centre for Ships & Ocean Structures, Norwegian University of Science and Technology, December 2004.

[43] G. Williams. *Chaos Theory Tamed*. Joseph Henry Press, 1997.

[44] Roger Penrose. *The Road to Reality*. Vintage, 2005.

[45] M S de Queiroz, D M Dawson, S P Nagarkatti, and F Zhang. *Lyapunov Based Control of Mechanical Systems*. Birkhauser Boston, 2000.

[46] K M Passino and S Yurkovich. *Fuzzy Control*. Addison-Wesley Longman Inc., 1998.

[47] R A Nelson and M G Olsson. The Pendulum - Rich Physics from a Simple System. *American Journal of Physics*, 54 (2):112–121, 1986.

[48] W Zhong and H Rock. Energy and Passivity-based Control of the Double Inverted Pendulum on a Cart. In *Proceedings of the 2001 IEEE International Conference on Control Applications*, pages 896–901, 2001.

[49] S Muhammed and A Doria-Cerezo. Output Feedback Based Controllers for Dynamic Positioning of Ships. In *Dynamic Positioning Conference*, 2010.

[50] S A Sarra. The Method of Characteristics with applications to Conservation Laws. Website, October 17 2002.

[51] R S Burns. *Advanced Control Engineer*. Butterworth Heinemann, 2001.

[52] E Sontag. *Mathematical Control Theory: Deterministic Finite Dimensional Systems*. Springer, New York, 1998.